

**Functional Studies of *STK31*:
A Cell Fate Determinant in Spermatogonia
and Cancer Development**

FOK, Kin Lam Ellis

**A Thesis Submitted in Partial Fulfillment
of the Requirement for the Degree of
Doctor of Philosophy
in
Physiology**

The Chinese University of Hong Kong

December 2009

UMI Number: 3436629

All rights reserved

INFORMATION TO ALL USERS

The quality of this reproduction is dependent upon the quality of the copy submitted.

In the unlikely event that the author did not send a complete manuscript and there are missing pages, these will be noted. Also, if material had to be removed, a note will indicate the deletion.



UMI 3436629

Copyright 2010 by ProQuest LLC.

All rights reserved. This edition of the work is protected against unauthorized copying under Title 17, United States Code.



ProQuest LLC
789 East Eisenhower Parkway
P.O. Box 1346
Ann Arbor, MI 48106-1346

Thesis/Assessment Committee

Professor Yung W.H. (Chair)

Professor Chan H.C. (Supervisor)

Professor Yu S.B. (Committee Member)

Professor Lee W.M. (External Examiner)

Content

Abstract	i
中文摘要.....	iii
Declaration	v
Acknowledgements	vii
List of tables	viii
List of figures	ix
List of abbreviations	xi
List of publications	xiii
List of conference abstracts	xv
Chapter 1 Overview	1
1.1 Post genomic era.....	1
1.2 Spermatogenesis.....	1
1.2.1 Testis structure.....	1
1.2.2 Cells involved in spermatogenesis.....	2
1.2.3 Three phases in spermatogenesis.....	4
1.3 Cancer development.....	7
1.4 Similarities between cancer development and spermatogenesis.....	8
1.5 Identification and characteristics of <i>NYD-SPK/STK31</i>	8
1.6 Hypotheses and aims of study.....	20
Chapter 2 Expression profile and cellular localization of <i>STK31</i>	23
2.1 Introduction.....	23
2.1.1 Tudor domain.....	23
2.1.2 Serine/Threonine Kinase domain.....	23
2.1.3 Classification of germline stem cells.....	24
2.1.4 Asymmetric division.....	27
2.1.5 Cancer/Testis antigen (CT antigen).....	28
2.1.6 Aim.....	29
2.2 Materials and Methods.....	29

2.2.1 Animals.....	30
2.2.2 Clustalx alignment.....	30
2.2.3 RT-PCR.....	30
2.2.4 Western blot.....	30
2.2.5 Testis hyperthermia model	31
2.2.6 Histology and immunofluorescent study	31
2.2.7 Cloning of <i>STK31</i>	32
2.2.8 Cell culture and transfection	32
2.3 Results	33
2.3.1 <i>STK31</i> is highly conserved	33
2.3.2 <i>STK31</i> contains two highly conserved domains	33
2.3.3 Testis-specific expression of <i>STK31</i>	37
2.3.4 <i>Stk31</i> is expressed in transition-state spermatogonia.....	38
2.3.5 <i>STK31</i> is reactivated in multiple cancer cell lines	40
2.3.6 <i>STK31</i> forms granular structures in HEK293 cells.....	44
2.3.7 Aggregated granules formed by <i>STK31</i> distributed asymmetrically during mitosis	47
2.4 Discussion	47
2.4.1 Spermatogonia specific expression of <i>Stk31</i>	47
2.4.2 <i>Stk31</i> as a marker for transitional state between undifferentiated and differentiated spermatogonia.....	48
2.4.3 Tudor domain and the intracellular localization of <i>STK31</i>	49
2.4.4 Asymmetric distribution of aggregated granules during mitosis	50
2.4.5 Reactivation of <i>STK31</i> in multiple cancers.....	51
2.4.6 Possible role of <i>STK31</i> in spermatogenesis and cancer	51
2.5 Conclusion.....	52
Chapter 3 Functional studies of <i>Stk31</i> in mouse spermatogonia	53
3.1 Introduction	53
3.1.1 Male germline stem cells (GSCs).....	53
3.1.2 Niche of male GSC.....	53
3.1.3 Asymmetric division of GSCs.....	56

3.1.4 Self renewal of male GSCs.....	58
3.1.5 Differentiation of GSC	61
3.1.6 Aim.....	62
3.2 Materials and Methods	62
3.2.1 Animals.....	62
3.2.2 Purification of GSCs	62
3.2.3 Establishment of GSC cultures.....	63
3.2.4 Long-term GSC cultures on STO feeder layer	64
3.2.5 Serum free and feeder free culture.....	65
3.2.6 Time Lapse Imaging of GSCs culture	65
3.2.7 Collection of GSCs for molecular analysis.....	65
3.2.8 RT-PCR.....	65
3.2.9 Recipient mice	66
3.2.10 Germ cell transplantation.....	66
3.2.11 Retinoic acid treatment of GSCs	67
3.2.12 Immunofluorescent studies	67
3.2.13 Cloning of <i>Stk31</i>	68
3.2.14 Retrovirus production	68
3.2.15 Transduction.....	69
3.2.16 Selection of transduced GSCs.....	69
3.3 Results	69
3.3.1 Establishment of GSCs culture on STO feeder cells	69
3.3.2 Molecular characterization of GSCs culture	72
3.3.3 GSC cultures maintain spermatogonial stem cell activity	74
3.3.4 Retinoic acid induce differentiation in GSCs	76
3.3.5 Induction of <i>Stk31</i> expression upon RA-induced differentiation.....	78
3.3.6 Asymmetrical distribution of induced <i>Stk31</i> protein during GSCs mitotic division.....	81
3.3.7 <i>Stk31</i> induce differentiation phenotype in GSCs.....	81
3.4 Discussion.....	83
3.4.1 GSCs on STO layers enhance flexibility of genetic manipulation.....	83

3.4.2 Cultures on STO layers shows primitive GSCs signatures	85
3.4.3 Induction of <i>Stk31</i> during GSCs differentiation	86
3.4.4 Mechanisms for <i>Stk31</i> asymmetry in GSCs.....	87
3.4.5 <i>Stk31</i> is a cell fate determinant in GSCs.....	88
3.5 Conclusion	89
Chapter 4 Functional studies of <i>STK31</i> in human colon cancer	90
4.1 Introduction	90
4.1.1 Cancer stem cells	90
4.1.2 Properties of cancer stem cells.....	95
4.1.3 Signaling involved in cancer stem cells	96
4.1.4 Colon cancer stem cell.....	97
4.1.5 Aim	101
4.2 Materials and Methods	101
4.2.1 miR RNAi against <i>STK31</i>	101
4.2.2 Cell culture and transfection	101
4.2.3 Western blot.....	102
4.2.4 Contact inhibition assay.....	102
4.2.5 Proliferation assay	103
4.2.6 Migration assay.....	103
4.2.7 Attachment assay	104
4.2.8 Enterocytic differentiation assay	104
4.2.9 Colony formation assay	104
4.2.10 Human whole genome microarray.....	105
4.2.11 Real-time PCR.....	105
4.2.12 Tumorigenicity assay.....	105
4.2.13 Statistical analysis.....	106
4.3 Results	106
4.3.1 Generation of <i>STK31</i> stable knock-down Caco2 cells.....	106
4.3.2 Knock-down of <i>STK31</i> decreases proliferation in confluent culture	108

4.3.3 Knock-down of <i>STK31</i> reactivates contact inhibition	109
4.3.4 Knock-down of <i>STK31</i> causes G1/S arrest upon confluence.....	111
4.3.5 Knock-down of <i>STK31</i> enhances binding to ECM.....	113
4.3.6 Knock-down of <i>STK31</i> decreases cell migration.....	115
4.3.7 Knock-down of <i>STK31</i> induces enterocytic differentiation.....	118
4.3.8 Knock-down of <i>STK31</i> decreases tumorigenicity <i>in vitro</i> and <i>in vivo</i>	120
4.3.9 Signaling pathways involved in CSCs properties alteration in <i>STK31</i> knock-down cells.	123
4.4 Discussion.....	129
4.4.1 Regulators of “stemness” in colon cancer stem cell	129
4.4.2 Signaling pathways regulating “stemness”	130
4.4.3 Acquisition of “stemness”	132
4.4.4 Cell fate specification in CSCs	133
4.4.5 <i>STK31</i> as a novel diagnostic and therapeutic target.....	134
4.5 Conclusion.....	135
Chapter 5 General Discussion.....	136
5.1 <i>STK31</i> , presence and future.....	136
5.2 Differentiation in GSCs versus de-differentiation in CSCs	138
5.3 Concluding remarks.....	141
Reference list.....	143
Appendix	170
I. Primer list.....	170
II. PCR reaction	172
III. Cloning PCR reaction.....	172
IV. Real-time PCR reaction.....	172
V. Buffer recipe	172

Abstract

Spermatogenesis is a complicated process involving mitosis, meiosis and post-meiotic differentiation. Due to the lack of *in vitro* models, genes that are involved in mammalian spermatogenesis are largely unknown. Spermatogenesis and tumorigenesis share important biological similarities. This co-relation can be signified by a special group of genes called cancer/testis (CT) antigens, which are only expressed in the testes and cancer. Although cancer biology has been extensively studied for decades, promising therapeutic methods are not available for every type of cancer. Recent discovery of cancer stem cells and functional genomics studies have shed light on the development of new diagnostic and therapeutic approaches. This thesis describes the expression, cellular localization and function of a novel CT gene, *STK31*, in spermatogonia and cancer development.

In the first part of the experiment, the expression and cellular localization of *STK31* were investigated. RT-PCR results showed that *STK31* was reactivated in 47 – 86% of multiple cancers. Immunofluorescent study and GFP tagging experiment showed that *STK31* was localized in the cytoplasm and formed aggregated granules that divide asymmetrically during mitosis. Further study by co-staining with E-cadherin demonstrated that the mouse homolog, *Stk31*, was expressed in the transition state between undifferentiated and differentiated spermatogonia. These data suggest the possible involvement of *STK31* in mouse spermatogonia and cancer development.

In the second part of the experiment, the function of *Stk31* in mouse spermatogonia was investigated. A GSC culture on an STO feeder layer was established. Studies on growing properties, expression of molecular markers and germ cell transplantation showed that GSC culture maintained spermatogonial stem cell activity. Retinoic acid was then used to induce differentiation of GSC. The

differentiation status was confirmed by monitoring the expression of molecular markers. RT-PCR and immunofluorescent study showed that the expression of *Stk31* was induced in RA-induced differentiation and *Stk31* proteins were asymmetrically distributed during GSC division. Overexpression of *Stk31* in GSCs using retroviral transduction induced the differentiation phenotypes. These data indicate the involvement of *Stk31* in mouse spermatogonia cell fate determination.

In the third part of the experiment, the function of *STK31* in human colon cancer was investigated. A stable *STK31* knock-down Caco2 cells were established by stably transfecting two miR RNAi designs with different efficiency into Caco2 cells. Flow cytometry analysis showed that knock-down of *STK31* resulted in G1 phase arrest. Cell counts and MTS assays suggested that knock-down of *STK31* decreased cell proliferation in confluent cultures. Knock-down of *STK31* also enhanced cell attachment to several ECM proteins and decreases cell migration as suggested by attachment assays and migration assays. Moreover, knock-down of *STK31* enhanced enterocytic differentiation and inhibited tumorigenicity both *in vitro* and *in vivo* as indicated by colony formation assays and xenograft assays. Data obtained from whole genome microarray studies indicate that *STK31* regulates these “stemness” properties through altering the expression of key players in various pathways including KIT, SMAD1 and Cyclin D2. These results suggest the involvement of *STK31* in colon cancer as a regulator of “stemness”.

Further studies of *Stk31* in spermatogenesis *in vivo* would allow the identification of the asymmetry machinery of GSCs and the signaling mechanism underlying cell fate determination. Further studies of *STK31* in cancer stem cells would allow the development of new diagnostic and therapeutic approaches.

中文摘要

精子發生是一個複雜的過程，包括有絲分裂，減數分裂和減數分裂後的分化。由于缺乏體外模型，參與哺乳類動物的精子發生過程中的基因大部分仍然是未知的。精子發生與腫瘤發生有很多相似之處。這種相關性體現在一組只在睪丸和癌組織中表達，稱為 CT 抗原的基因。雖然對於癌症生物學的深入研究已經進行了幾十年，但是並非每一種腫瘤都有有效的治療方法。最近發現的腫瘤干細胞及其功能基因組學的研究可以為新的診斷和治療方法帶來新的突破。本論文對一個新發現的 CT 抗原基因 *STK31* 在精子發生與腫瘤發生過程中的表達，細胞定位和功能進行了研究。

實驗的第一部分對 *STK31* 的表達和細胞定位進行了研究。RT-PCR 的結果顯示 *STK31* 的表達在 47 - 86% 的多種癌症中被重新激活。免疫熒光及 GFP 融合蛋白實驗顯示了 *STK31* 表達在細胞漿中，並形成在有絲分裂中分佈不均等的聚合顆粒。進一步的研究利用 E-Cadherin 作為標記的雙染實驗證明小鼠的 *Stk31* 在分化中的精原細胞中表達。以上證據提示了 *STK31* 可能參與了小鼠精原細胞及癌症發生的過程。

實驗的第二部分對 *Stk31* 在小鼠精原細胞中的功能進行研究。我們建立了精原干細胞 (GSC) 的原代培養。研究顯示它們的生長特性，分子標記表達，以及生殖細胞移植的實驗都表明了該培養系統保留了精原干細胞的活性。之後用 Retinoic acid 誘導精原干細胞的分化。分子標記的表達確定了它的分化狀態。RT-PCR 與免疫熒光都顯示了 *Stk31* 的表達在 RA 誘導的分化過程中被激活，並且 *Stk31* 在 GSC 的有絲分裂中不均等分佈。進一步的試驗利用逆轉錄病毒轉導將 *Stk31* 在 GSC 中過表達，並引起了分化表型。以上結果提示了 *Stk31* 在小鼠精原細胞中起了決定細胞的命運的作用。

實驗的第三部分對 *STK31* 在結腸癌中的功能進行了研究。我們利用兩個不同效率的 miR RNAi 設計建立了兩個 *STK31* 穩定敲低的 Caco2 細胞株。流式細胞

儀的分析顯示了敲低了 *STK31* 會造成細胞停止在 G1 期。細胞計數和 MTS 實驗顯示了敲低 *STK31* 會降低細胞在長滿後的細胞增殖。細胞貼壁實驗和細胞遷移實驗顯示了敲低 *STK31* 會增強細胞貼附在細胞外基質蛋白的能力，並減低細胞遷移。而且，敲低 *STK31* 會增加腸粘膜細胞的分化。通過細胞群形成實驗及異源細胞移植試驗證明敲低 *STK31* 可以抑制細胞在體外和體內形成腫瘤的能力。全基因組芯片的研究顯示 *STK31* 是通過調控一些信號通路中的重要分子，例如 KIT，SMAD1 及 CyclinD2，來進行對“干性”的調節。這些結果顯示了 *STK31* 是結腸癌“干性”的調節器。

進一步關於 *Stk31* 在小鼠體內生精過程的研究可望找出 GSC 不平等分裂的機器，及決定細胞命運的通路機制。進一步關於 *STK31* 在腫瘤干細胞的研究渴望找出新的癌症診斷和治療方法。

Declaration

I hereby declare that this thesis represents my own work, except where due acknowledgement is made, and that it has not been previously included in a thesis, dissertation or report submitted to this University or to any other institution for a degree, diploma or other qualification.

Signature

Fok Kin Lam Ellis

This thesis is dedicated to my parents.

Acknowledgements

I would like to express my sincere thanks to Prof. Hsiao Chang Chan for her patient guidance and unlimited support throughout my course of study.

I would like to thank my family for their encouragement.

I would also like to thank every member in ECBRC and my friends for all their support during these years.

I would like to give special thanks to Ms. Hilda Chung. Thanks for her great love and care, no matter whether it is happy, sad, succeed or fail, she is always by my side.

List of tables

Table 2.1 – A comparisons of markers of human and mouse spermatogonia

Table 3.1 – Regeneration of spermatogenesis and restoring fertility of recipient mice after germ cell transplantation

Table 4.1 – CSC marker used in various cancer

Table 4.2 – Differentially expressed genes in *STK31* knock down cells

List of figures

- Figure 1.1** – The structure of the testis
- Figure 1.2** – Cells involved in spermatogenesis
- Figure 1.3** – Three phases of spermatogenesis
- Figure 1.4** – Similarities between spermatogenesis and tumorigenesis
- Figure 1.5** – Representative images showing differentiation hybridization from adult and fetal testis
- Figure 1.6** – Clustalx alignment of nucleotide sequence of *NYD-SPK* and transcript variants of *STK31*
- Figure 1.7** – Clustalx alignment of protein sequence of *NYD-SPK* and transcript variants of *STK31*
- Figure 1.8** – Northern blot analysis showing the testis specific expression of *STK31*
- Figure 1.9** – RT-PCR showing the testis specific expression of *STK31*
- Figure 1.10** – Northern blot analysis showing the developmental dependent expression of *Stk31* during spermatogenesis
- Figure 1.11** – *In situ* hybridization analysis showing the expression of *Stk31* in spermatogonia
- Figure 2.1** – Two classification schemes in mouse spermatogonia
- Figure 2.2** – Clustalx alignment of *STK31* protein sequence from human, mouse, rat, horse, cattle and chimpanzee
- Figure 2.3** – Schematic diagram showing the conserved domains in *STK31*
- Figure 2.4** – Western blot analysis of *Stk31* in mouse multiple tissues
- Figure 2.5** – Western blot analysis of mouse hyperthermia testis
- Figure 2.6** – Immunofluorescence study of *Stk31* in mouse testis
- Figure 2.7** – Co-immunofluorescence study of E-cadherin and *Stk31* in mouse testis
- Figure 2.8** – RT-PCR showing the reactivation of *STK31* in various cancer and cell lines
- Figure 2.9** – Immunofluorescence study of *STK31* in Caco2 cells
- Figure 2.10** – Western blot for STK31-GFP fusion proteins
- Figure 2.11** – Live cell images of STK31-GFP fusion protein
- Figure 2.12** – Immunofluorescence study of STK31-GFP fusion proteins during mitosis
- Figure 3.1** – Niche of mouse male GSCs
- Figure 3.2** – Regulations of GSCs self-renewal and differentiation in *Drosophila* and mouse testis
- Figure 3.3** – Culturing properties of GSCs on STO feeder layer
- Figure 3.4** – Culturing properties of GSCs on laminin
- Figure 3.5** – Culturing properties of GSCs on STO feeder under serum-free

condition

Figure 3.6 – Expressions of stage specific germ cell markers in GSCs cultured on STO feeder layer

Figure 3.7 – Morphology of testis after germ cell transplantation

Figure 3.8 – Induction of GSCs differentiation by retinoic acid

Figure 3.9 – Expressions of stage specific germ cell markers in GSCs after RA induced differentiation

Figure 3.10 Immunofluorescence study of *Stk31* in differentiating GSCs

Figure 3.11 – Asymmetry of *Stk31* in GSCs division

Figure 3.12 – Induction of differentiation phenotypes by *Stk31*

Figure 4.1 – “Cancer stem cell” and “Clonal evolution” model for cancer heterogeneity

Figure 4.2 – Comparison between conventional cancer therapy and CSCs targeted therapy

Figure 4.3 – Cell hierarchy in colon stem cells

Figure 4.4 – Overexpression and knock down of *STK31* in HEK293 cells and Caco2 cells

Figure 4.5 – Proliferation studies of *STK31* knock-down Caco2 cells

Figure 4.6 – Morphologies of *STK31* knock-down cells under different confluence

Figure 4.7 – Cell cycle profile of *STK31* knock-down cells under different confluence

Figure 4.8 – Attachment assay of *STK31* knock-down cells

Figure 4.9 – Migration assay of *STK31* knock-down cells

Figure 4.10 – Enterocytic differentiation of *STK31* knock-down cells

Figure 4.11 Colony formation assay of *STK31* knock-down cells

Figure 4.12 – Tumorigenicity of *STK31* knock-down cells *in vivo*

Figure 4.13 – Real-time PCR for selected differential expressed genes in *STK31* knock-down cells

Figure 5.1 - Schematic diagram of the role of *STK31* in germline stem cells and cancer stem cells

List of abbreviations

a.a.	amino acid
ATCC	American Type Culture Collection
BDF1	F1 generation of C57/BL6 x DBA
bp	base pair
BTB	blood testis barrier
cDNA	complementary DNA
CMV	cytomegalovirus
CSC	cancer stem cell
CSF-1	colony stimulating factor-1
CT antigen	Cancer/Testis antigen
DIV	days in vitro
DMEM	Dulbecco's modified Eagle medium
DNA	deoxyribonucleic acid
DNaseI	deoxyribonuclease I
dNTPs	deoxynucleoside triphosphate
dpp	days postpartum
ECM	extracellular matrix
EG	embryonic germ
EGF	epidermal growth factor
EGFR	epidermal growth factor receptor
EmGFP	Enhanced modified green fluorescent protein
ES	embryonic stem
FBS	fetal bovine serum
FGF	fibroblast growth factor
FSH	Follicle Stimulating Hormone
GB	gonialblast
GDNF	glial cell line-derived neurotrophic factor
GFP	green fluorescent protein
GnRH	gonadotropin releasing hormone
GSC	germline stem cell
HBSS	Hank's balanced salt solution
HRP	horse-radish peroxidase
IGF	Insulin-like growth factor
IgG	immunoglobulin isotype G
iPS	induced pluripotent stem cell
kb	kilo base pair
kDa	kilo delton

KO	knock out
LASEC	Laboratory animal service centre
Lgl	Lethal giant larvae
LH	Luteinizing Hormone
LIF	Leukaemia inhibitory factor
MAb	monoclonal antibody
MEF	mouse embryonic fibroblast
miR	microRNA
MMLV	Moloney Murine Leukemia Virus
MOI	multiplicity of infection
mRNA	messenger RNA
NYD-SPK	Na Yi Da-Sperm Protein Kinase
ORF	open reading frame
P/S	penicillin streptomycin mix
PAb	polyclonal antibody
PAGE	polyacrylamide gel electrophoresis
PBS	phosphate buffered saline
PCR	Polymerase Chain Reaction
PFA	paraformaldehyde
PKC	Protein kinase C
PSA	prostate-specific antigen
RA	retinoic acid
RIPA	radio-immunoprecipitation assay
RNA	ribonucleic acid
RNAi	RNA interference
RT-PCR	Reverse Transcription - Polymerase Chain Reaction
S.D.	standard deviation
S.E.M.	standard error mean
SCC	somatic cyst cell
SCF	stem cell factor
SSC	spermatogonial stem cell
STK	Serine/Threonine Kinase
TA	transit amplifying
TBST	Tris-buffered saline plus Tween 20
TGF	Transforming growth factor
TU	transducing unit
UTR	untranslated region

List of Publications

1. *Stk31* is a cell fate determinant in mouse germline stem cell
Fok KL, Chung CM, Chen YC, Kung HF, Li K, Zhang XH, Chung YW, Chan HC
In preparation
2. *STK31* regulates “Stemness” in colon cancer cells.
Fok KL, Chung CM, Yi SQ, Zhang XH, Jiang XH, Chung YW, Chan HC.
In preparation
3. A sperm GPI-anchored protein elicits sperm-cumulus cross-talk leading to the acrosome reaction.
Yin L, Chung CM, Huo R, Liu H, Zhou C, Xu W, Zhu H, Zhang J, Shi Q, Wong HY, Chen J, Lu Y, Bi Y, Zhao C, Du Y, Ma M, Cai Y, Chen WY, **Fok KL**, Tsang LL, Li K, Ni Y, Chung YW, Zhou Z, Sha J, Chan HC.
Cell Mol Life Sci. 2009 Mar;66(5):900-8
4. Immunization with Bin1b decreases sperm motility with compromised fertility in rats.
Xu W, Zhang X, Chen W, **Fok KL**, Rowlands DK, Chui YL, Chan HC.
Fertil Steril. 2009 Jan 7
5. A suppressor of multiple extracellular matrix-degrading proteases and cancer metastasis.
Yin LL, Chung CM, Chen J, **Fok KL**, Ng CP, Jia RR, Ren X, Zhou J, Zhang T, Zhao XH, Lin M, Zhu H, Zhang XH, Tsang LL, Bi Y, Zhou Z, Mo F, Wong N, Chung YW, Sha J, Chan HC.
J Cell Mol Med. 2008 Nov 6
6. A novel member of the Rhomboid family, RHBDD1, regulates BIK-mediated apoptosis.
Wang Y, Guan X, **Fok KL**, Li S, Zhang X, Miao S, Zong S, Koide SS, Chan HC, Wang L.
Cell Mol Life Sci. 2008 Nov;65(23):3822-9
7. Involvement of cystic fibrosis transmembrane conductance regulator in infection-induced edema.

Ajonuma LC, He Q, Sheung Chan PK, Yu Ng EH, **Fok KL**, Yan Wong CH, Tsang LL, Ho LS, Lau MC, Huang HY, Yang DZ, Rowlands DK, Tang XX, Zhang XH, Chung YW, Chan HC.
Cell Biol Int. 2008 Jul;32(7):801-6.

8. YWK-II protein as a novel G(o)-coupled receptor for Müllerian inhibiting substance in cell survival.

Yin X, Ouyang S, Xu W, Zhang X, **Fok KL**, Wong HY, Zhang J, Qiu X, Miao S, Chan HC, Wang L.
J Cell Sci. 2007 May 1;120(Pt 9):1521-8

9. Differentiation of adult rat bone marrow stem cells into epithelial progenitor cells in culture.

Shu C, Li TY, Tsang LL, **Fok KL**, Lo PS, Zhu JX, Ho LS, Chung YW, Chan HC.
Cell Biol Int. 2006 Oct;30(10):823-8.

List of conference abstracts

1. Signaling mechanism of a testis-specific transfection factor.
Ellis Kin Lam Fok, Hu Zhu, Wen Ming Xu, Jiahao Sha, Hsiao Chang Chan.
International Symposium on Frontiers in Life Sciences: molecular basis of disease, prevention and treatment. .
Cell Biol.Int., 30,(8),S38.2006.
2. Expression of two novel genes, NYD-SPK and NYD-SP24, in mouse ovary. Ellis Kin Lam Fok, Hu Zhu, Jiahao Sha, Hsiao Chang Chan.
International Symposium on Cell Biology: from basic research to clinical applications.
Cell Biol.Int., 28,(8-9),S6.2004.

Chapter 1

Overview

1.1 Post-genomic era

Years after the completion of Human Genome Project, we have entered into a new generation of functional genomics, focusing on transcriptomes, proteomes, epigenomes and interactomes. With the development of “state-of-the-art” techniques such as the protoarray, RNAi and deep sequencing, high throughput functional studies have made considerable progress in recent years. However, functional studies in mammalian reproductive systems are still technically challenging due to the lack of *in vitro* models. Recent expansion of toolbox such as GSCs culture and germ cell transplantation technique in both male and female reproductive systems, have opened up new possibilities in the field of reproductive biology^{1,2}. The identification of CT antigen, a special group of genes that have restricted expression in the testis and cancer^{3,4}, has built up the co-relation between spermatogenesis and cancer development. The discovery of cancer stem cells has had great impacts in the field of cancer biology. Functional genomics studies in cancer stem cells would provide not only a great step towards the understanding of tumor origin and progression, but also facilitate the research on cancer diagnosis and therapy⁵⁻⁷. In this thesis, we will describe the study of a novel gene named *NYD-SPK/STK31* in spermatogenesis and cancer development.

1.2 Spermatogenesis

1.2.1 Testis structure

The testis is the organ where spermatogenesis occurs. There are two distinct compartments within the testis, the interstitial tissue and the seminiferous tubules. The seminiferous tubules can be further divided into basal and adluminal

compartments. The interstitium and basal compartment are separated by the basement membrane while the adluminal compartments are defined by tight junctions formed by Sertoli cells named the “blood-testis barrier (BTB)”. The adluminal compartments are connected to a collection area named the rete and the spermatozoa are transferred to the epididymis through the efferent duct for downstream maturation processes (Figure 1.1).

1.2.2 Cells involved in spermatogenesis

1.2.2.1 Leydig cells and peritubular cells

Leydig cells are located in the interstitium (Figure 1.2). It produces steroid hormones known as androgens in response to Luteinizing Hormone (LH) stimulation. Androgens in conjunction with Follicle Stimulating Hormone (FSH) regulate the functions of Sertoli cells.

The peritubular cells are located in the basal compartment (Figure 1.2) and participate in the cell-cell interactions with Sertoli cells. These cells regulate Sertoli cell function through Transforming growth factor- β (TGF- β) and Insulin-like growth factor (IGF) ⁸.

1.2.2.2 Sertoli cells

Sertoli cells, also known as “nurse cells”, are the primary somatic cells types that directly interact with all stages of germ cells. The blood-testis barrier is formed by tight junctions between adjacent Sertoli cells that restrict substance exchange between blood vessels and the lumen of seminiferous tubules, thus defining the microenvironment for paracrine regulation of germ cell differentiation ⁸⁻¹⁰. Apart from this, Sertoli cells also take part in removing dead cells through phagocytosis and pinocytosis.

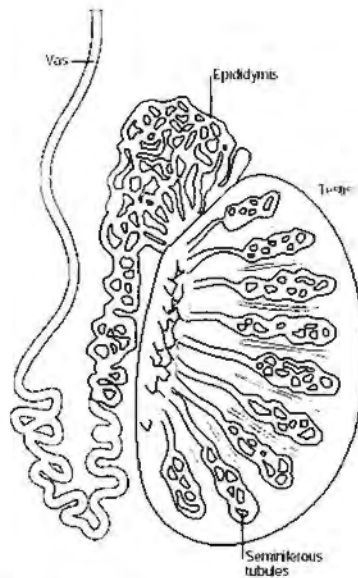


Figure 1.1| The structure of the testis. Spermatogenesis occurs in the seminiferous tubules. The adluminal compartments are connected to the rete testis where spermatozoa are collected. These spermatozoa are transferred to the epididymis for downstream maturation processes. Adapted from ¹¹.

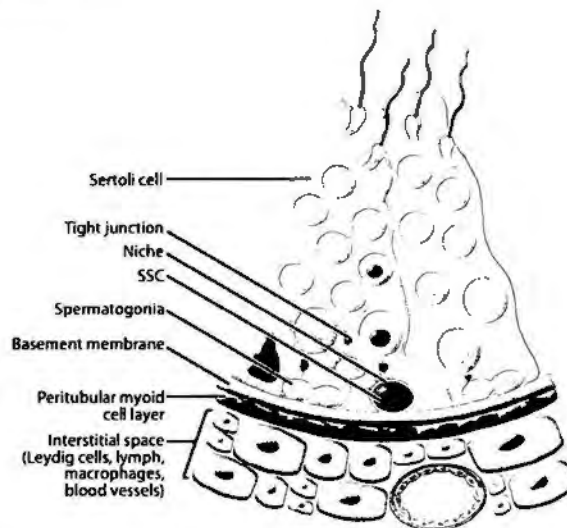


Figure 1.2| Cells involved in spermatogenesis. Leydig cells are located in the interstitium where they produce androgen that regulates Sertoli cell function. The peritubular cells are located in the basal compartment. They interact with Sertoli cells and regulate their function through the paracrine system. Sertoli cells and germ cells are located in the seminiferous tubules. Tight junctions between adjacent Sertoli cells form the “Blood Testis Barrier”. Sertoli cells “nurse” all stages of germ cells through paracrine regulation. Spermatogonia are located on the basal side of the seminiferous tubules. During spermatogenesis, germ cells migrate from the basal to the adluminal compartment. Adapted from ¹².

1.2.2.3 Male germ cells

Male germ cells are the only cell type that undergoes meiosis in postnatal life. However, not all stages of germ cells undergo the meiotic cycle. Stem cell populations known as spermatogonia increase the number of stem cells in the reservoir through mitotic cycle. The differentiation of spermatogonia gives rise to pre-meiotic germ cells termed primary spermatocytes, which are tetraploid. After the first meiotic division, diploid secondary spermatocytes are formed. The appearance of secondary spermatocytes is transient; they undergo a second meiotic division to form haploid gametes called round spermatids. Differentiation of round spermatids gives rise to spermatozoa. These processes require interactions between germ cells and Sertoli cells.

1.2.3 Three phases in spermatogenesis

1.2.3.1 Mitotic phase

Mitotic phase in germ line lineage is restricted to spermatogonia (Figure 1.3). Mitosis of spermatogonia can be symmetric or asymmetric (discussed later in this thesis). Symmetric division can result in two stem cells or two committed progeny while asymmetric division results in one daughter stem cell and one committed progeny¹³. Symmetric division enlarges the stem cell population, which is crucial for regeneration after stimuli such as radiation or hyperthermia. On the other hand, asymmetric division maintains tissue homeostasis by regulating the self-renewal and differentiation of stem cells. Mis-regulation of this homeostatic pathway could result in sterility or lethal disease such as cancer. One specialized feature of the germ line mitotic phase is that committed progeny undergo incomplete cytokinesis resulting in two daughter cells interconnected with an intercellular cytoplasmic bridge¹³.

1.2.3.2 Meiotic phase

Differentiated spermatogonia give rise to primary spermatocytes by entering the preleptotene stage of the meiotic process (Figure 1.3). The primary spermatocytes undergo two divisions of meiosis. During the first division, sister chromatids align at the cell equator where a series of recombinations occur, a process known as cross-over. Cells passing through the prophase of the first meiotic division can be subdivided into preleptotene, leptotene, zygotene, pachytene, and diplotene stages according to their cytological basis. The centromere does not divide in this round of division. However, the centromere does divide in the second meiotic division and round spermatids are formed ¹⁴.

1.2.3.3 Post-meiotic phase

In this process, no cell divisions occur. Instead, numerous restructuring processes in morphology and biochemistry transpire, eventually leading to the formation of functional spermatozoa (Figure 1.3). This phase is also known as spermiogenesis. Restructuring processes include: 1. nuclear condensation by switching chromosome packing proteins from histones to protamine, followed by migration of the condensed nucleus to the periphery of the cell; 2. formation of acrosome, which is surrounded by cell membrane and attached to the anterior end of the nucleus and contains hydrolytic enzymes crucial for penetration through the oolemma during fertilization; 3. flagellum formation, which involves the development of microtubules arising from the centrioles of the round spermatid into elongate spermatid with the connecting piece, the middle piece, the principal piece, and the end piece; and 4. cytoplasm reorganization by shedding a large part of its cytoplasm as residual body, which is phagocytosed by Sertoli cells ¹⁵.

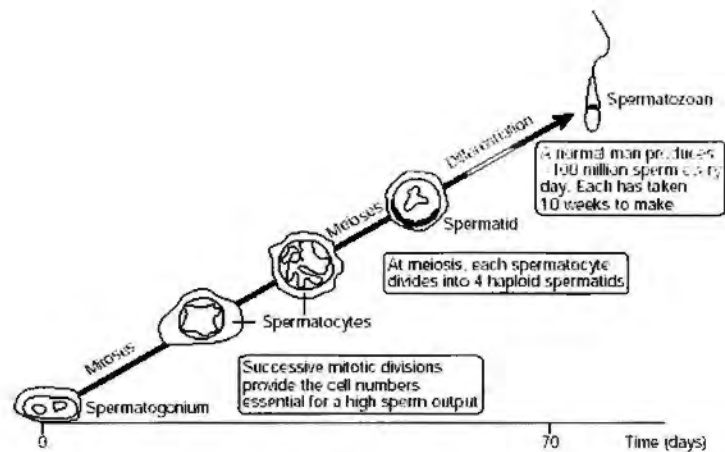


Figure 1.3| Three phase of spermatogenesis. Mitosis phase is restricted to spermatogonia. Mitotic division increases the number of stem cells. Differentiated spermatogonia enter the meiotic phase, giving rise to primary spermatocytes. In the meiotic phase, chromosomes replicate once but divide twice, giving rise to haploid round spermatids. In the post-meiotic phase, a series of morphological and biochemical restructuring processes occur and eventually give rise to functional spermatozoa. Adapted from ¹¹.

1.3 Cancer development

Cancer development is a multistep process. Various genetic alterations including chromosomal alterations, epigenetics changes or mutation at the single gene level might be involved.

Immortalization is considered the initial step of tumorigenesis. It describes a status where cells are able to bypass cellular senescence and divide indefinitely. This status was documented in various stem cells systems where continuous supplies of cells are needed for replacement. However, in normal somatic cells, proliferation is regulated through cell cycle checkpoints and telomerase activity. Cell cycle checkpoints arrest the cells at specific stages of the cell cycle due to the lack of driving force for cell division. The length of the telomere is shortened during each replication and excessive loss of telomere length results in genomic instability followed by cellular senescence ¹⁶.

Growth of immortalized cells is suppressed when they comes into contact with adjacent cells, a phenomenon known as contact inhibition. Cells that are sensitive to contact inhibition grow in a single monolayer while cells that have lost contact inhibition grow into multiple layers. Tumor cells have acquired the ability to escape contact inhibition through a step known as transformation ^{17,18}.

When the microenvironment of the primary site becomes unfavorable because of stress such as hypoxia, lack of nutrients or the accumulation of metabolites, tumor cells migrate to adjacent regions or new sites in order to sustain their growth. During the migration process, cell-cell interactions decrease while cell-matrix interactions increase. Cell-matrix interactions reconstruct the cytoskeleton which acts as the motility machinery. In parallel with migrations, adverse microenvironment would also induce angiogenesis increasing blood supply to the tumor ¹⁹.

Metastasis describes the process by which tumor cells invade and voyage

through circulating systems from the primary site followed by attachment and growth in a secondary site. First, the release of proteolytic enzymes digests the extracellular matrix (ECM) during the invasion; second, the expression of anti-apoptotic proteins facilitate the survival of the cells in circulating system; and third, the expression of adhesion molecules promotes the attachment to the new secondary sites^{20,21}.

1.4 Similarities between cancer development and spermatogenesis

Spermatogenesis and tumor development share important biological similarities (Figure 1.4).

Immortalization – In spermatogenesis, spermatogonial stem cells undergo numerous rounds of cell divisions without abnormal cell cycle checkpoint arrest (first barrier) and senescence caused by telomere shortening (second barrier). The first step by which normal cells bypass these two barriers and undergo tumorigenesis in cancer development is called transformation²².

Migration – During spermatogenesis, spermatogenic cell migrate from the basal lamina towards the lumen of the seminiferous tubule. In later stages of cancer development, tumor cells migrate from the primary site to invade other parts of the body, a process known as metastasis²².

Meiosis – In the meiotic phase of spermatogenesis, a gamete with half chromosome number – a haploid genome, is formed. While in a cancer cell, a stage where chromosome number is not equal to multiple of haploid number is described as aneuploidy. This is usually seen when a particular chromosome is duplicated²².

1.5 Identification and characteristics of *NYD-SPK/STK31*

In our previous studies, cDNA from adult and 6 month old fetal testes were

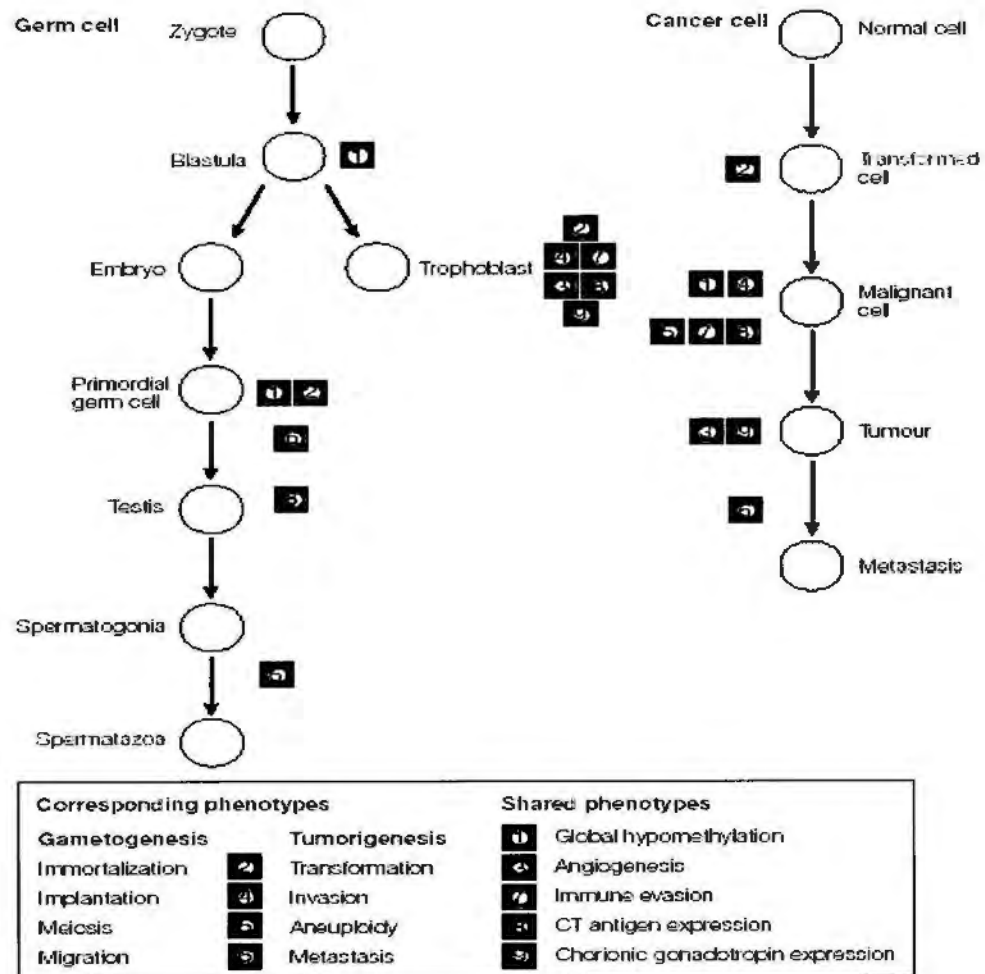


Figure 1.4| Similarities between spermatogenesis and tumorigenesis. Spermatogenesis and tumorigenesis share important biological similarities. Immortalization in spermatogonia stem cells is similar to the transformation in cancer cells. Migration of germ cells is similar to the metastasis in cancer cells. Meiosis in germ cells results in haploid gametes. This situation is similar to the aneuploid state in cancer cells. Adapted from ²².

hybridized to human cDNA microarray containing 9216 cDNA fragments²³. *NYD-SPK* was found to be highly expressed in adult but not fetal testes. Signal intensities were 117.82 and 35.52 in adult testes and fetal testes respectively (Figure 1.5). The nucleotide sequence was deposited to GeneBank (Accession number AF332194).

NYD-SPK was located in human chromosome 7p15.3, which spans 25 exons. The mRNA is comprised of 3617bp. The open reading frame starts at base 468 to 3458. Sequence analysis showed that the nucleotide sequence of *NYD-SPK* was highly similar to transcript variant 2 of *STK31*, but *NYD-SPK* is 56bp longer at the 5' end. The sequence can be aligned with all three transcript variants of *STK31* starting from base 459 to poly A tail at base 3617 (Figure 1.6).

The open reading frame encodes a protein of 997 amino acid residues with a predicted molecular weight of 113.2kDa. Protein sequence analysis showed that *NYD-SPK* can be completely aligned with all three transcript variants of *STK31*. Variant 1 is 22 a.a. longer at the N-terminus possibly resulted from start codon from alternative exon (Figure 1.7). Since the protein sequences are the same in *NYD-SPK* and *STK31*, I used *STK31* to design and report downstream experiments in this thesis.

Northern blot analysis using normal human multiple tissues RNA was used to study the expression profile of *STK31*, and the result showed that the expression was testis specific (Figure 1.8). Then, a more comprehensive array of normal human tissue cDNA was used to study the expression of *STK31* using RT-PCR. The results showed that a specific band at 481bp could be amplified in the testis. This supported our previous data that *STK31* was testis specific (Figure 1.9). No expression of

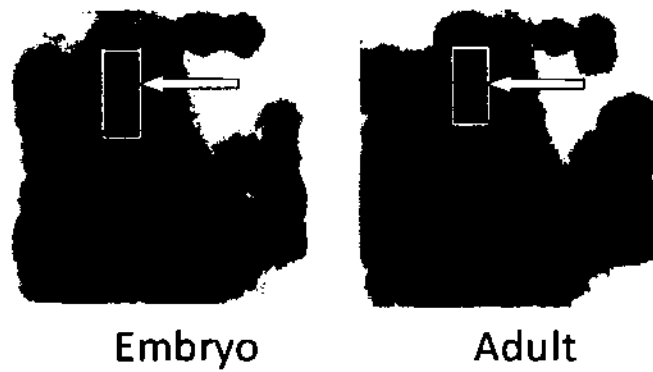


Figure 1.5| Representative images showing differentiation hybridization from adult and fetal testes. cDNA from adult (Right panel) and fetal testis (Left panel) were hybridized to human cDNA microarray. The locations of *NYD-SPK/STK31* spots are marked by the white rectangles. Signal intensities (Arrows) in the adult were 117.82 and 35.53 in adult and fetal testis respectively.

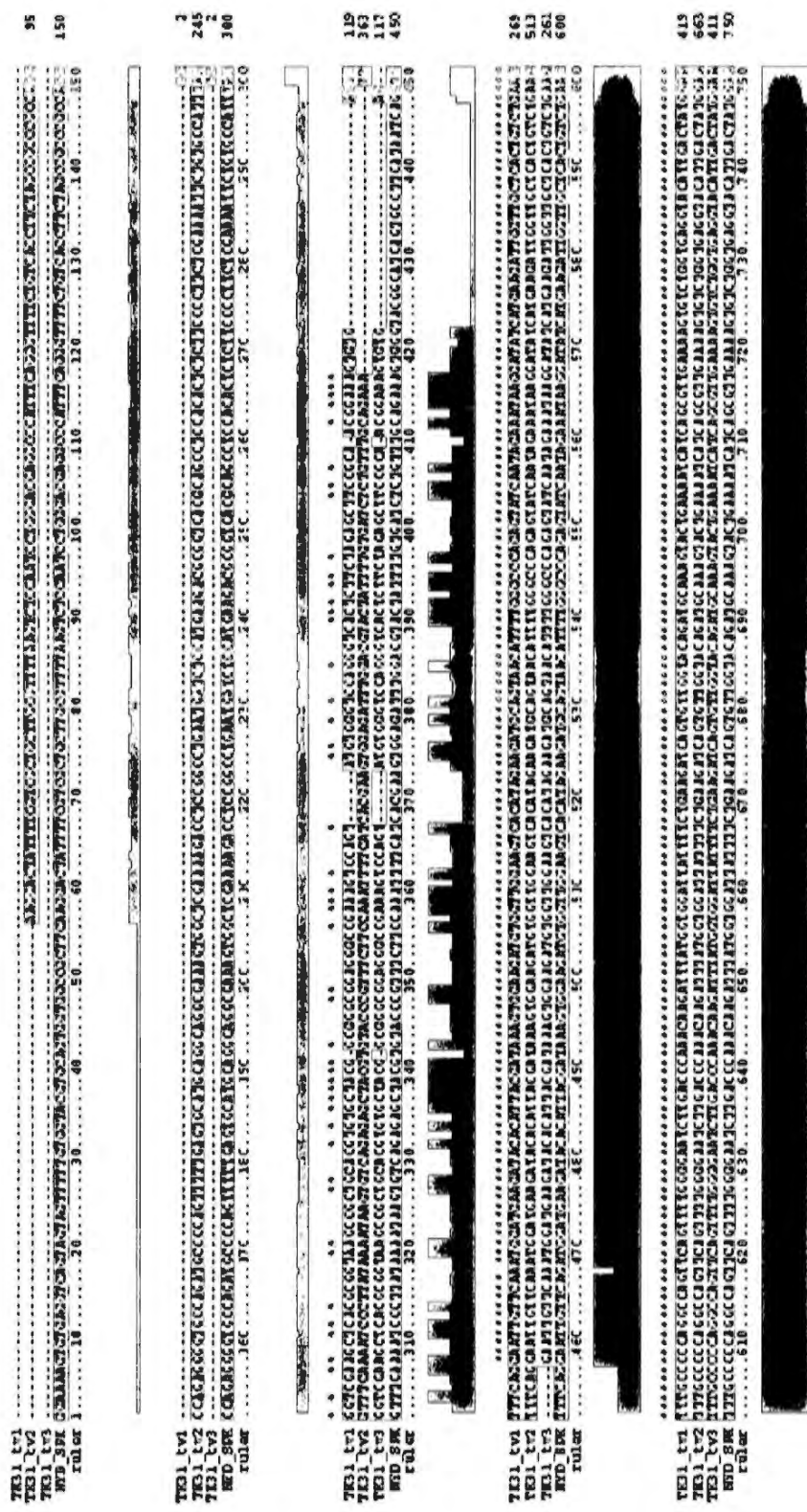


Figure 1.6| Clustalx alignment of nucleotide sequence of NYD-SPK and transcript variants of STK31. mRNA sequences of NYD-SPK were aligned with three transcript variants of STK31. Aligned nucleotides are marked by asterisks. NYD-SPK is highly similar to transcript variant 2 of STK31. The major differences among the four mRNA were found in the 5'UTR region.

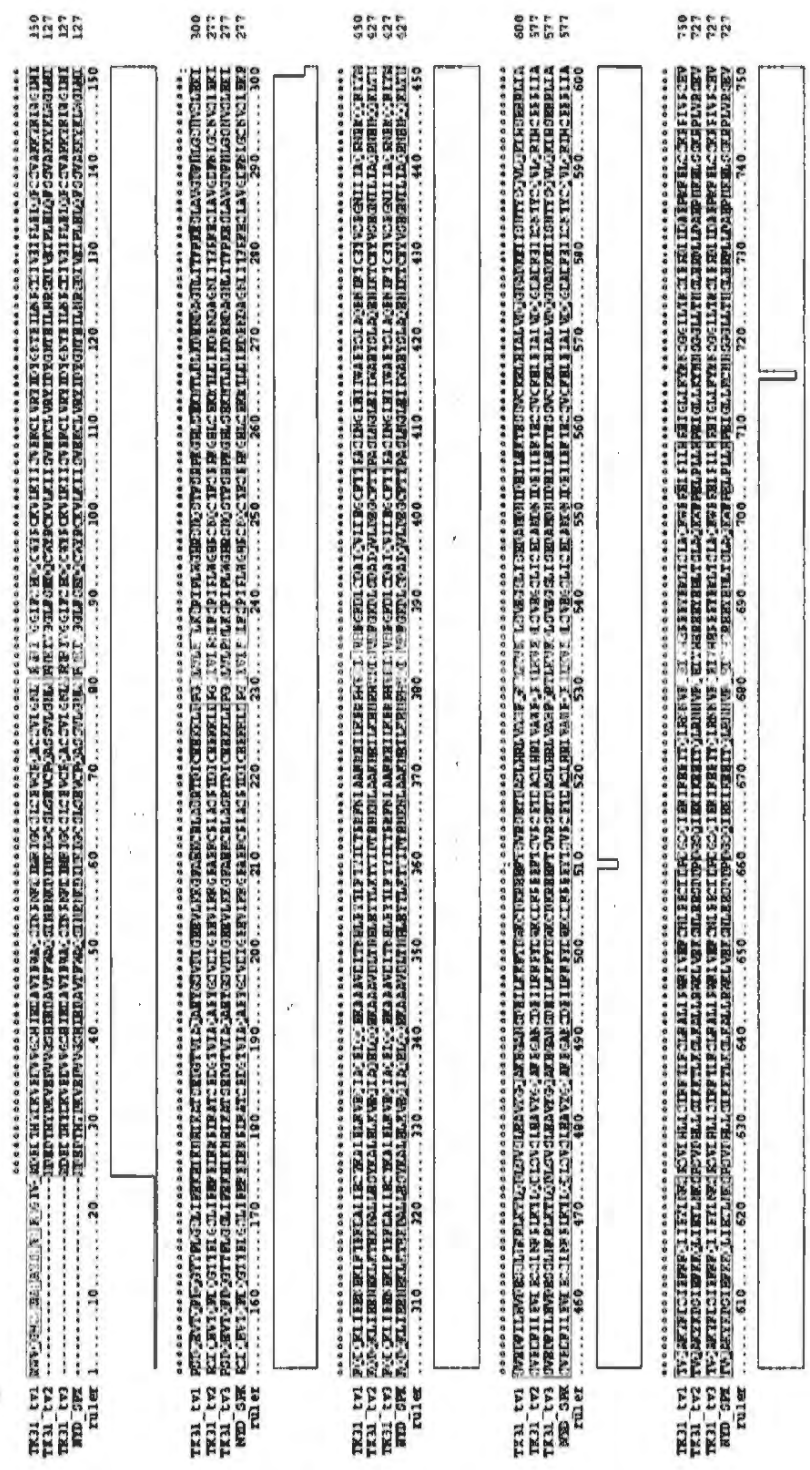


Figure 1.7] ClustalX alignment of protein sequence of NYD-SPK and transcript variants of STK31. Protein sequences of NYD-SPK were aligned with three transcript variants of STK31. Aligned amino acid residues are marked by asterisks. Residues with high score similarities are marked by double dots and similar residues are marked by single dots. The protein sequences encoded from four mRNA were the same except for the N terminus of transcript variant 1 of STK31 which included an alternative exon.

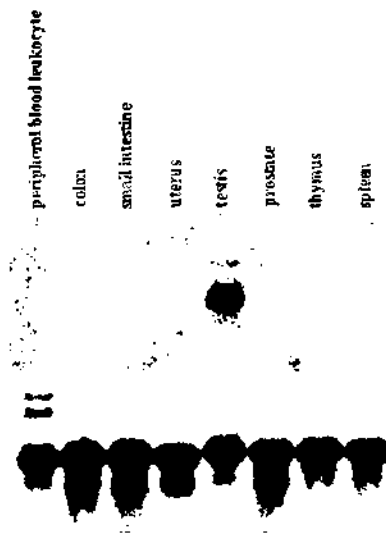


Figure 1.8| Northern blot analysis showing the testis specific expression of *STK31*. A panel of human multiple tissues poly A⁺ RNA (Clontech) including peripheral blood leukocyte, colon, small intestine, uterus, testis, prostate, thymus and spleen were probed with *STK31* (Top panel) and β actin (Bottom panel). A signal at 3.5 kb represents *STK31* mRNA and was found only in testis but not other tissue.

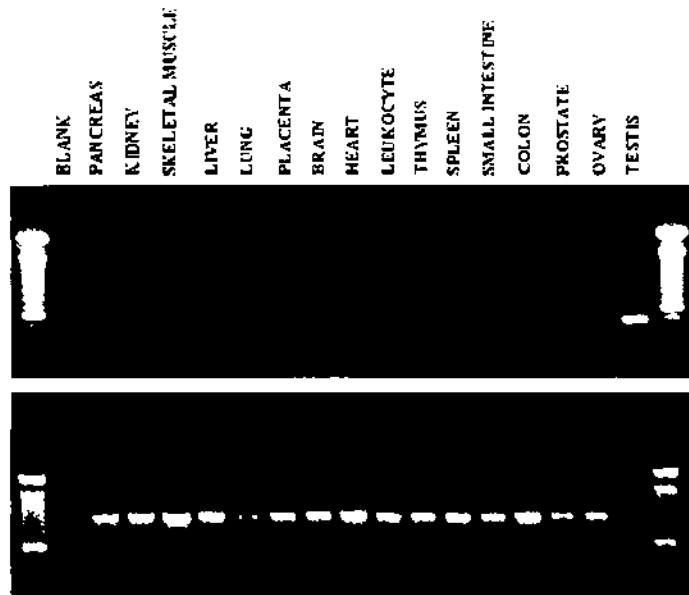


Figure 1.9| RT-PCR showing the testis specific expression of *STK31*. *STK31* was amplified (Top panel) in a panel of human multiple tissue cDNA including (from the left) pancreas, kidney, skeletal muscle, liver, lung, placenta, brain, heart, leukocytes, thymus, spleen, small intestine, colon, prostate, ovary and testis. *GAPDH* was amplified as internal control (Bottom panel). No DNA template control was labeled as blank. Specific amplification of size 481bp was noted in testis. Weak expression was also noted in pancreas.

STK31 was detected in other vital organs including brain, liver, heart, and lung. It is interesting to note that there was no expression in the ovaries suggesting that the function of *STK31* may either be male specific or is expressed in the ovaries during a different time scale from males. A weak expression was also noted in the pancreas.

The expression of mouse homolog gene, *Stk31*, was found to be testis-specific²⁴, and the expression could be detected in all types of germ cells²⁵. To confirm these findings, northern blot analysis using mouse testis RNA of various developmental stages from 6 dpp to 30 dpp was used. The result showed that *Stk31* RNA could be detected at 6 dpp where only primitive type A spermatogonia is present (Figure 1.10)²⁶. The expression increased in a developmental dependent manner and reached the peak at 24dpp. To further characterize which type of cells express *Stk31*, probes for *Stk31* were hybridized *in situ* to mouse testis sections. In contrast to previous reports²⁵, expression of *Stk31* was restricted to spermatogonia; no expression was detected in Sertoli cells, Leydig cells, spermatocytes and more differentiated germ cells (Figure 1.11).

1.6 Hypotheses and aims of study

We had demonstrated that *STK31* was a testis specific gene. It was highly expressed in adult but not fetal testes, and the expression was developmental dependent and restricted to spermatogonia. It was also reported to be reactivated in gastrointestinal cancer²⁷ and there was no expression in normal colon and small intestine tissues. Therefore, two hypotheses were made:

1. *Stk31* may plays a pivotal role in spermatogonia during spermatogenesis
2. *STK31* may be involved in the development of gastrointestinal cancer.

The aims of this thesis were first, to study the expression profile and cellular localization of *STK31*; second, to study its function in spermatogenesis and cancer

development; and third, to determine the underlying mechanisms of *STK31* in spermatogenesis and cancer development.

Chapter 2

Expression and cellular localization of *STK31*

2.1 Introduction

In an evolution point of view, protein sequences that are crucial for functions would be conserved during evolution. Therefore, searching for conserved domain within a novel protein would facilitate the functional studies of that protein.

2.1.1 Tudor domain

The tudor domain is a conserved domain among several RNA associated proteins²⁸. It was originally identified as a region of 50 amino acids found in the tudor protein, which is a posterior gene encoded in *Drosophila*²⁹⁻³¹. It has been demonstrated to mediate RNA binding³² and protein-protein interaction through binding to methylated or di-methylated lysine^{33,34} and di-methylated arginine³⁵. The cellular localization of tudor domain containing protein was unique. The tudor domain has been proposed to take part in the formation of germinal granules in mouse germ cells³⁶⁻³⁸ and stress granules in somatic cells³⁹. Although the exact functions of tudor domains remain largely unknown, they have been postulated to take part in male germ cell differentiation and regulate spermatogenesis^{36-38,40}.

2.1.2 Serine/Threonine Kinase domain

Protein kinases represent a significant portion of proteins involved in signal transduction. Over 500 protein kinases have been identified⁴¹ and tyrosine kinase and serine/threonine kinase are the two main class in the human kinome. They exert specific and reversible control on protein phosphorylation. STK takes part in vital cellular processes through the phosphorylation of a vast array of cytoplasmic and nuclear effectors such as transcription factors and cell cycle regulators⁴². Although

expressions of STKs have been found to be frequently altered in cancer, STKs have drawn less attention than the tyrosine kinase family⁴³. Examples of well known STKs that are misregulated in cancer include mitogen activated protein kinases and aurora and related kinases. These kinases have been demonstrated to take part in various steps in tumorigenesis including tumor growth and metastasis⁴⁴⁻⁴⁶.

2.1.3 Classification of germline stem cells

Spermatogonium is a cell type in seminiferous tubules that initiate spermatogenesis. The term “spermatogonia” includes spermatogonial stem cells and differentiated progenitors. They form one of the most active stem cells systems in postnatal life. Spermatogonia in rodents and humans have common properties including clear cytoplasm, high nucleus to cytoplasm ratio and basal localization⁴⁷. Spermatogonia can be subdivided into different classes and the classification in rodents is more detailed than humans due to the availability of study model.

Early studies divided human spermatogonia into two subtypes A_{dark} and A_{pale} spermatogonia and both are undifferentiated stem cells⁴⁸. In this system, A_{dark} spermatogonia are reserve stem cells that rarely replicate. The limited frequency of proliferation was speculated to minimize genetic mutations during the DNA replication process. Proliferation of A_{dark} spermatogonia would result in A_{dark} or A_{pale} spermatogonia. On the other hand, A_{pale} spermatogonia were considered the renewing stem cell that actively undergoes self-renewal division. The self-renewal division of A_{pale} spermatogonia results in A_{pale} spermatogonia which replace the parental cell and B spermatogonia which are committed to differentiation⁴⁸⁻⁵¹.

In rodents, two classification schemes have been proposed (Figure 2.1). The first scheme is similar to the human system where spermatogonia are divided into reserve and renewing stem cells. The renewing stem cells include four types of cells,

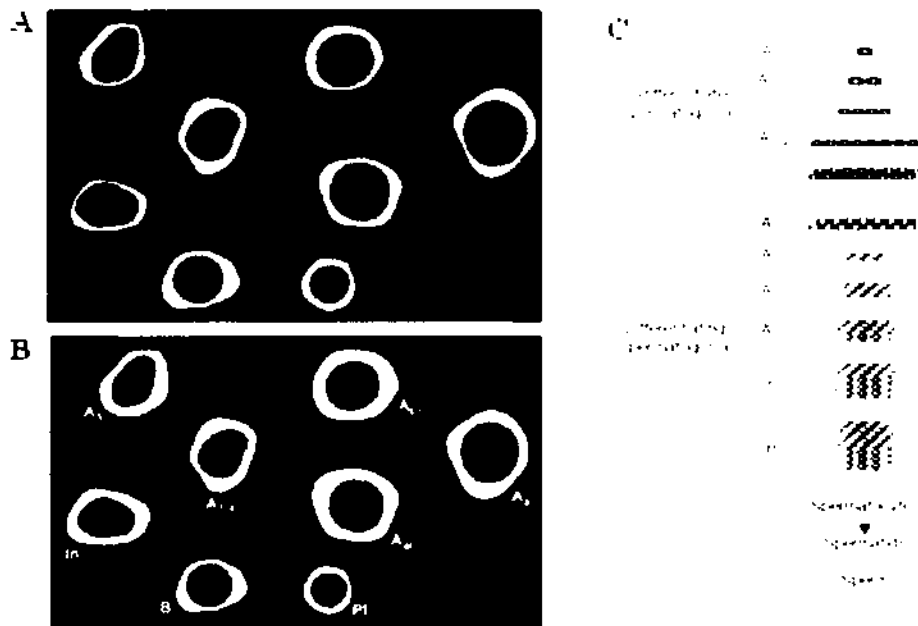


Figure 2.1| Two classification schemes in mouse spermatogonia. In the first scheme, $A_1 - A_4$ spermatogonia act as the renewing stem cells while A_0 spermatogonia act as the reserve stem cells (A). A_4 spermatogonia are able to generate new A_1 spermatogonia. In the second scheme, A_s spermatogonia is the proposed stem cell. Mitotic division of A_s spermatogonia give rise to A_{pr} spermatogonia which are connected with intercellular cytoplasmic bridge. Subsequent mitosis give rise to more differentiated progeny (B). A_s , A_{pr} and A_{1-4} spermatogonia are considered undifferentiated spermatogonia while A_{1-4} , Intermediate and type B spermatogonia were considered as differentiated spermatogonia (C). Adapted from 47,52

Marker	Human	Rodent
$\alpha 6$ -integrin (CD49f)	+	+
$\beta 1$ -integrin (CD29)		+
CD9	?	+
CD133	+	?
CDH1	?	+
CHEK2	+	?
GFRA1	+	+
GPR12S	+	+
KIT		+
MAGE-A4	+	?
Neurogenin3	?	+
NSE	+	?
PLZF	+	+
POUSF1		+
RET	?	+
STRAB	?	+
Thy-1 (CD90)	+	+
TSPY	+	

Table 2.1| A comparisons of markers of human and mouse spermatogonia. Expressed markers are noted by (+); Absence of markers are noted by (-); Markers with unknown expression are noted by (?). Some of the markers are common in human and mouse. However, a significant portion of the markers are only suitable for one species. Adapted from 47,

$A_1 - A_4$ spermatogonia, while the reserve stem cells are named A_0 spermatogonia. In this scheme, A_4 spermatogonia are able to generate new A_1 spermatogonia or more differentiated Intermediate and B spermatogonia ^{53,54}. In the second scheme, the proposed stem cells are named A_{single} (A_s) spermatogonia. A_s spermatogonia divide to form a self-renew daughter A_s spermatogonia or A_{pair} (A_{pr}) spermatogonia. A_{pr} spermatogonia are interconnected by an intercellular cytoplasmic bridge. A_{pr} spermatogonia further proliferate, giving rise to chains of spermatogonia named $A_{aligned}$ (A_{al}) spermatogonia. A_s , A_{pr} and A_{al} spermatogonia are considered undifferentiated spermatogonia (Figure 2.1). The A_{al} spermatogonia then form differentiated spermatogonia named A_{1-4} , Intermediate and type B spermatogonia ⁵⁵⁻⁵⁸. The second scheme is the most widely accepted nowadays, however, a recent report demonstrated that differentiated progeny can de-differentiate into stem cells, raising new discussion regarding this issue ^{52,59}.

The classification of spermatogonia can be characterized by morphological properties or expression of molecular markers. A recent report has described a method to characterize spermatogonia under high resolution microscope ⁶⁰, however, this method requires specialized fixation method and experienced observations and therefore have not been widely used. Characterizations of spermatogonia by determining the expression of molecular markers were relatively easy and have therefore been extensively used. However, there are no unique markers for specific types of spermatogonia, therefore, a combination of markers are often used simultaneously. Table 2.1 summarizes the markers used to characterize spermatogonia in mice and humans. There are a number of markers for spermatogonial stem cells including $\alpha 6$ integrin ⁶¹, $\beta 1$ integrin ⁶¹, CD9 ⁶², E-cadherin ⁶³, GFRA1 ^{64,65}, Plzf ⁶⁶, Oct3/4 ^{67,68}, STRA8 ⁶⁹ and Thy1 ⁷⁰. Known markers for differentiating spermatogonia include DAZL ^{71,72}, DDX4 ^{73,74}, c-kit ^{75,76} and a few

others. However, no unique makers have been identified for A_{pr} or A_{al} spermatogonia. Humans and rodents share a number of spermatogonia markers like *Plzf* and *GFRA1*, however, not all rodent markers are applicable in humans. For example, *c-kit* was reported in mouse differentiating spermatogonia but is undetectable in human spermatogonia ⁷⁷. Therefore, the identification of more markers for differentiating spermatogonia applicable for both rodents and humans would be a huge stepping stone towards the study of differentiating spermatogonia.

2.1.4 Asymmetric division

“Mitosis” is a term describing cell division in which cellular materials including chromosomes, cytoplasm and organelles partition equally in daughter cells ^{78,79}. In both the hierarchal cell system and the stem cell system, mitotic divisions can be asymmetric in regards to cytoplasmic materials and nucleic acids despite the same number of inherited chromosomes. Cytoplasmic materials, which divide asymmetrically, determine the cell fate of daughter cells after segregation and are therefore termed segregating determinants or cell fate determinants ⁸⁰⁻⁸². The result of this asymmetric division is a daughter cell that self-renews to replace the parental cell while another daughter cell commits to differentiate or moves downstream in the cell hierarchy. The segregating determinant has been demonstrated in systems including neural progenitors cells ⁸³, hematopoietic stem and progenitors cells ⁸⁴, muscle satellite cell ⁸⁵ and T cells ⁸⁶. Regarding the nucleic acid, a symmetric division would result in two daughter cells that each inherit one template strand and one newly synthesized strand. However, in asymmetric division, stem cells selectively retain sister chromatids from the old template strand DNA (immortal strand) while the committed cells receive the inheriting newly synthesized strand DNA. The purpose of this nucleic acid asymmetry was postulated to limit the chance

of acquiring mutations in stem cell populations. This phenomenon was described as the “immortal strand hypothesis”^{87,88} and proved in neural stem cells⁸⁹, intestinal stem cells⁹⁰, mammary gland epithelial cells⁹¹ and muscle satellite cells⁹². The asymmetry of cell fate determinants and immortal strands can occur in the same cell type as in muscle satellite cells^{85,92}. On the other hand, independent occurrence was also reported: hematopoietic stem cells showed asymmetry in cell fate determinant⁸⁴ while non-random template strand segregation was not observed⁹³.

Unlike mitotic asymmetry in stem cell systems, mitotic asymmetry in somatic cells received less attention. Recent reports have shown that mitotic asymmetry does occur in somatic cells^{94,95}. In the first report, CDC25B phosphatase was distributed asymmetrically in mother centrosome during interphase. The purpose for asymmetric localization was proposed to synchronize the centrosome duplication and cell cycle progression⁹⁴. In the second report, localization of aggresome, formed by disease based misfolded proteins, was polarized in anaphase and distributed asymmetrically after cytokinesis. This mechanism was speculated to prevent inheritance of misfolded proteins to one of the daughter cells in order to preserve a long lived cell⁹⁵. The function of this somatic cell mitotic asymmetry remains to be determined.

2.1.5 Cancer/Testis Antigen (CT antigen)

As described in chapter 1, gametogenesis and cancer development show significant similarities. Therefore, genes that are functionally active in gametogenesis might recapitulate similar cellular processes during tumor development. The term CT antigen is used to describe genes that have restricted expression in cancer and testis^{3,4}. Expression patterns of CT antigens vary depending on the differentiation stage of gametogenesis. In tumor cells, their expression was also heterogeneous⁹⁶. Depending on the chromosomal location, CT antigens can be further divided into

CT-X antigens (located in X chromosome) and non-X CT antigens ²². Regardless of the chromosomal location, CT antigens are regulated epigenetically through promoter demethylation or hypomethylation and histone acetylation, although other regulations might also be involved. The reactivation of CT antigens showed bias regarding tumor types. Groups of high CT gene expressors (>50% reactivation) include bladder cancer, non-small cell lung cancer and melanoma. Breast and prostate cancer are considered moderate CT gene expressors with an expression frequency >20%. With less than 20% of samples showing reactivation of CT antigen, renal and colon cancer were considered the low CT gene expressor group ³. Another characteristic property of CT antigens are their immunogenic nature. CT antigens may induce immune responses since the normal expression in the testis is protected from the immune system by the blood-testis barrier ⁹⁷. These properties make CT antigens excellent targets as cancer vaccine and immunotherapy ^{4,22,96,97}.

2.1.6 Aim

Previous studies demonstrated that *Stk31* RNA could be detected in spermatogonia (Chapter 1). *STK31* is testis-specific; it is not normally expressed in other healthy organ systems. On the other hand, *STK31* is reactivated in gastrointestinal cancer. Therefore, we hypothesize: 1. *Stk31* is expressed in spermatogonia; 2. *STK31* is reactivated in multiple cancers.

The specific aims of this chapter are: first, to characterize the expression of *Stk31* in the testis; second, to characterize the expression of *STK31* in various cancers.

2.2 Materials and methods

2.2.1 Animals

C57/BL6 mice were purchased from LASEC, CUHK. All procedures were approved by the Animal Ethics Committee, CUHK (AEEC Number: 06/044/MIS)

2.2.2 Clustal alignment

Clustal alignment was performed by Clustalx1.83 software.

2.2.3 RT-PCR

Liver cancer cell lines cDNA were kindly provided by Prof. Guan XY (Department of Clinical Oncology, The University of Hong Kong). Nasopharyngeal cancer cell lines cDNA were kindly provided by Prof. Lo KW (Department of Anatomical and Cellular Pathology, The Chinese University of Hong Kong). Gastrointestinal and ovarian cancer samples were kindly provided by our collaborators in Mainland China.

Primer pairs used in this study were STK31 and GAPDH (Appendix). 1 μ l of cDNA was mixed with PCR mix [1X PCR buffer; 0.25 μ M Forward primer; 0.25 μ M Reverse primer; 0.20 μ M dNTPs; 1U GoTaq polymerase (Promega)] and amplified in thermocycler (Bio-Rad or MJ research) as indicated (Appendix). PCR products were resolved by agarose electrophoresis and analyzed by Gel-Documentation system (Alpha-Innotech).

2.2.4 Western blot

Multiple mouse tissues and various cancer cell lines were collected and homogenized in RIPA buffer (Appendix) followed by lysis on ice for 30 minutes. Tissue debris was removed by centrifugation at 15,000 rpm for 30 minutes at 4°C (Eppendorf). Protein concentrations were determined by Protein Assay Solution (Bio-Rad) and microplate spectrophotometer (BioTek).

Proteins were reduced in Sample Buffer (Appendix) followed by heat denatured at 100°C for 5 minutes. Protein samples were resolved by SDS-PAGE followed by blotting onto Hybond N nitrocellulose membrane (Amersham) using Trans-Blot® SD Semi-Dry Electrophoretic Transfer Cell (Bio-Rad). The membrane was then blocked with 4% non-fat milk in 1X TBST for 30 minutes at room temperature followed by overnight probing with 1:1000 Mouse Anti-STK31 MaxPab (Abnova) and 1:2000 Rabbit Anti- β tubulin (Santa Cruz) at 4°C. Non specific binding of primary antibodies was washed off with 1X TBST and the membrane was probed with 1:10,000 HRP-linked Sheep Anti-mouse IgG (Amersham) for 1 hour at room temperature. Membranes were washed with 1X TBST and signals were developed using ECL reagent (Amersham) and SuperRX-film (Fuji Medical).

2.2.5 Testis hyperthermia model

Adult male mice were anesthetized by Ketamine/Xylezine mix. Their scrotums were exposed to a 43°C water bath for 30 minutes. A 33°C water bath was used as control. Mice were allowed to recover and were humanely terminated at indicated time points for the collection of testes samples.

2.2.6 Histology and immunofluorescent study

For mouse testis staining, adult mice testes were fixed with 4% PFA and embedded in paraffin. Paraffin blocks were sectioned into 5 μ m thick sections and placed on slides. Paraffin sections were rehydrated through a series of ethanol treatment followed by washing in 1X PBS. Antigens were retrieved by boiling in Sodium Citrate buffer for 10 minutes followed by cooling down at room temperature for 30 minutes.

For culture cells staining, Caco2 cells and HEK293 stable transfectants were

seeded on a cover slip two days before study. Cells were fixed with 4% PFA in room temperature for 5 minutes followed by washing in 1X PBS.

Retrieved sections and cells on the cover slip were permeabilized and blocked in 5% normal goat serum in (Invitrogen) 1X PBST for 30 minutes at room temperature. The testes sections and Caco2 cells were then probed with 1:100 Mouse Anti-STK31 MaxPAb (Abnova) and/or 1:50 Rabbit Anti-E-cadherin (Santa Cruz) at 4°C overnight. The HEK293 stable transfectants were probed with 1:200 Mouse Anti β -tubulin MAb (Sigma) at 4°C overnight. Non specific bindings of primary antibodies were washed off with 1X PBST and the sections were probed with Alexa®488 Anti-mouse high cross absorbed Ab and/or Alexa®568 Anti-rabbit high cross absorbed Ab (Molecular Probe) (for testes sections and Caco2 cells) or Texas-Red Anti-mouse Ab (Santa Cruz) (for HEK293 stable transfectant) for 1 hour at room temperature. Sections were washed with 1x PBST and the nucleus was counterstained with 100ng/ml Hoechst 33342 (Invitrogen) for 5 minutes at room temperature. The slides were mounted by Anti Fade Gold mounting media (Invitrogen) and images were taken by Nikon ECLIPSE 80i imaging system (Nikon) and analyzed by SPOT Advanced software (SPOT Diagnostic Inc.).

2.2.7 Cloning of *STK31*

The human homolog *STK31* in pReceiver M-01a vector was purchased from Genecopoeia (Genecopoeia, USA). For GFP tagging experiment, *STK31* were shuttled to pEGFP-N2 and pEGFP-C2 vectors (Clontech) through introducing *EcoRI* and *XhoI* restriction sites. Stop codon in *STK31* was substituted in pEGFP-N2 fusion construct.

2.2.8 Cell culture and transfection

Caco2 and HEK293 cells were purchased from ATCC. Cells were cultured in DMEM medium supplemented with 10% FBS and 1% P/S and maintained in 37°C, 5% CO₂ incubator.

HEK293 cells were transfected with 2.5 ug DNA and 6µl Lipofectamine 2000 reagent (Invitrogen). In order to obtain maximum transfection efficiency, 8x10⁵ HEK293 cells were seed onto 35 mm culture dish with DNA:liposome complex pre-loaded in medium. In GFP tagging experiment, stable transfected cells were selected with 700µg/ml Geneticin[®] (Invitrogen) and maintained in 500µg/ml Geneticin[®] containing medium.

2.3 Results

2.3.1 *STK31* is highly conserved

In an evolution point of view, proteins with pivotal functions are typically highly conserved among species. To determine the degree of homology in *STK31*, clustalx alignment was made to compare amino acid sequences of *STK31* from chimpanzees, horses, cattles, humans, rats and mice (Figure 2.2). The result shows that *STK31* is highly conserved among six mammalian species. Highly conserved regions were observed in the 5' and the 3' end of *STK31* indicating the presence of conserved domains. Conserved segments in the middle of protein indicated the presence of structural motif. Overall, there is over 84% homology within the six species. This result showed that *STK31* might have pivotal functions.

2.3.2 *STK31* contains two highly conserved domains

To determine whether there are conserved domains among the high score residues, the amino acid sequence of *STK31* was subjected to bioinformatics analysis



Figure 2.3| Schematic diagram showing the conserved domains in *STK31*. Protein sequence of *STK31* was used to blast for conserved domains. Two conserved domains were found. Tudor domain (Blue) is located in the N-terminus while Serine/Threonine Kinase Catalytic domain (Red) was located in the C-terminus.

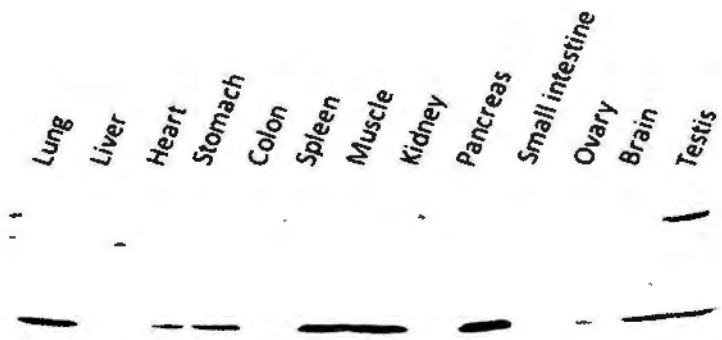


Figure 2.4| Western blot analysis of *Stk31* in mouse multiple tissues. Whole cell lysates from a panel of mouse tissues including lung, liver, heart, stomach, colon, spleen, muscle, kidney, pancreas, small intestine, ovary, brain and testis were separated by SDS-PAGE and probed with antibody against *STK31* (Top panel). β tubulin was used as loading control (Bottom panel). A specific band with a molecular weight of ~113kDa was detected in testis but not in other tissues.

and the results show that there are two conserved domains in *STK31*, the tudor domain and the Serine/Threonine Kinase Catalytic domain (Figure 2.3). The tudor domain is located at the N terminus, this domain is found in many RNA binding proteins, however, its function is still unknown. Recently, this domain has been implicated in protein-protein interactions in which methylated protein substrates bind to this domain³³⁻³⁵. The Serine/Threonine Kinase Catalytic domain is located at the C terminus and confers phosphotransferase activity to serine and/or threonine residues. The enzymatic activities of this domain might be regulated by phosphorylation of specific residues in activation segment of the catalytic domain and/or reversible conformational changes in auto-regulatory tail⁹⁸.

2.3.3 Testis-specific expression of *STK31*

Previous studies demonstrated the expression profile of *STK31* in RNA level (Section 1.5). Here, the protein expression profile of *Stk31* in mouse multiple tissues was determined by western blot using the antibodies against full length *STK31* (Abnova). From the results, a specific band with an estimated molecular weight of 113kDa was observed in testis whole cell lysate (Figure 2.4). The band detected in the colon had a molecular weight >150kDa while the band detected in the liver had a molecular weight <102kDa. Due to these differences in molecular weight, they were therefore considered as non-specific binding. No expression was detected in other tissue lysates including pancreas, which had been previously shown to have low level of *STK31* mRNA. This result suggested that the weak PCR product in the human pancreas, as shown in RT-PCR (Section 1.5), may be an artifact. If the mRNA was present in the pancreas, it was either suppressed at translational level or encoded a protein that could not be recognized by antibodies against *STK31*. These results demonstrated that the protein of *STK31* is testis specific.

2.3.4 *Stk31* is expressed in transition-state spermatogonia

In situ hybridization from our previous study has shown that *Stk31* is expressed in spermatogonia (Figure 1.11). Furthermore, northern blot results showed that *Stk31* is expressed in the testis from 6 dpp mice where only primitive type A spermatogonia is present (Figure 1.10). These results suggested that *Stk31* mRNA may be expressed in specific types of spermatogonia. Since different types of spermatogonia are not well characterized and there are no specific markers for various stages of spermatogonia; in order to study the expression of *Stk31* in spermatogonia at the protein level, two sets of experiments were carried out.

In the first set of experiments, the mice testes were exposed to hyperthermic conditions by soaking the scrotum in a 42°C water bath. This procedure caused apoptosis of all types of germ cells. The only germ cells that survived this stress were spermatogonial stem cells. These cells will repopulate the seminiferous tubules during the early recovery period and regenerate spermatogenesis during recovery period^{99,100}. Testes were collected for western blot analysis at various time points. The results showed that the expression of *Stk31* decreased during the degeneration period (1 hour to 16 hour post treatment). No expression was detected during the early recovery period (7 – 14 days) and the expression appeared in the recovery period (28 – 56 days) and persists to fully regenerated stage at 98 days (Figure 2.5A). The expression did not show a significant difference in the control group, which was kept at 33°C (Figure 2.5B). These results demonstrated that *Stk31* is not expressed in spermatogonial stem cell.

In the second set of experiments, the expression of *Stk31* was studied by immunofluorescent staining. Consistent with previous *in situ* hybridization results, *Stk31* protein was detected in spermatogonia but not in more differentiated germ cells

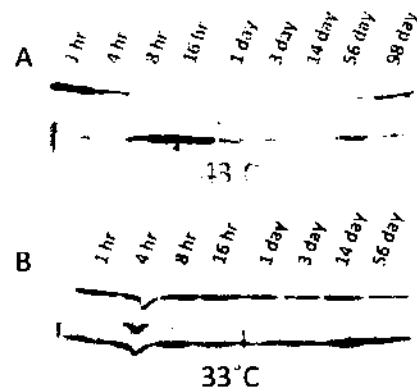


Figure 2.5| Western blot analysis of mouse hyperthermia testis. Whole cell lysates from various time points after hyperthermia treatment (A) or control treatment (B) were analyzed by western blot against *Stk31* (A and B, Top panels). β tubulin was used as loading control (A and B, Bottom panels). Expression of *Stk31* decrease in degeneration period (1 – 16 hours). The expressions become undetectable during the early recovery period (7 – 14 days) and re-appear during the recovery period (28 – 56 days) and persist after regeneration. No change in expression was detected in control treatment group.

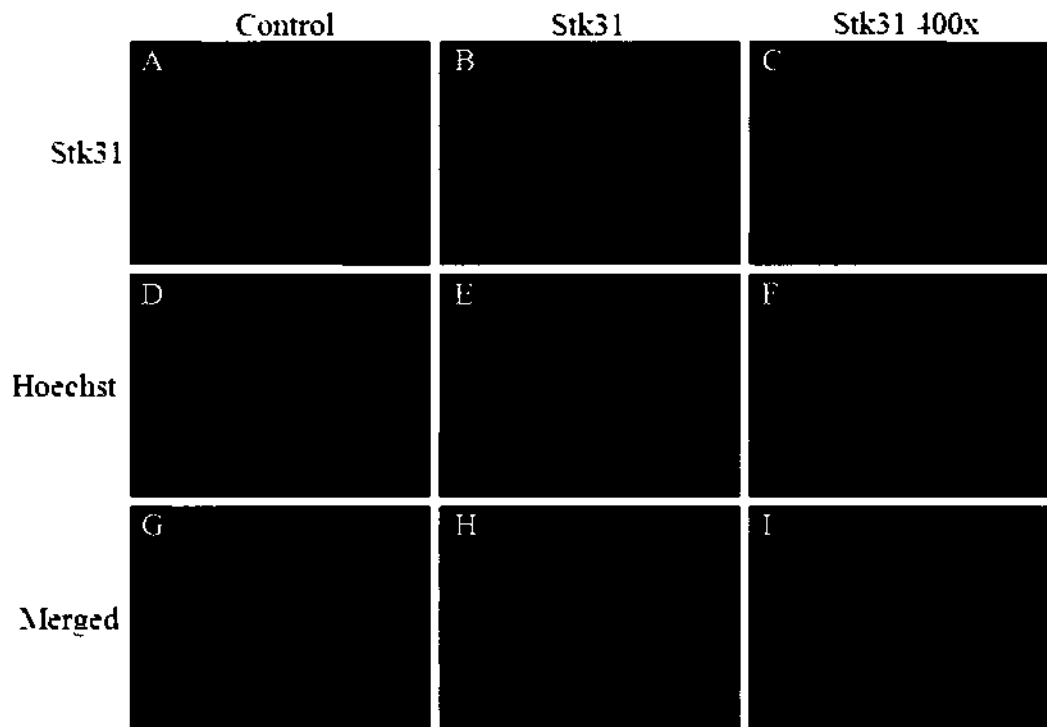


Figure 2.6| Immunofluorescence study of *Stk31* in mouse testis. Adult mouse testis sections were stained with anti-STK31 antibody (B and C) or no antibody control (A). Nuclei were counterstained with Hoechst (D – F). Merged images are shown in the bottom panels (G – I). Signals were detected in spermatogonia but not in more differentiated germ cells, Sertoli cells and Leydig cells. Magnification 100x (A, B, D, E, G, and H), 400x (C, F, and I).

(Figure 2.6). Interestingly, granular signals, which are similar to nuage formed by tudor domain containing protein, were observed in some spermatogonia. To clarify the subtype of spermatogonia that expresses *Stk31*, E-cadherin was used as an indicator for undifferentiated spermatogonia^{63,65}. In this set of co-staining experiments, *Stk31* was co-localized with E-cadherin in the majority of spermatogonia (*E-cad*⁺/*Stk31*⁺) (Figure 2.7). However, it was interesting to note that some spermatogonia were E-cadherin positive only (*E-cad*⁺/*Stk31*⁻) (Figure 2.7 inset), while some spermatogonia were *Stk31* positive only (*E-cad*⁻/*Stk31*⁺) (Figure 2.7 inset). These results suggest that *Stk31* is expressed during the transition stage from undifferentiated to differentiated spermatogonia and that the expression persists in differentiated spermatogonia until the entry of meiotic cycle.

2.3.5 *STK31* is reactivated in multiple cancer and cell lines

Previous reports have demonstrated that *STK31* is reactivated in gastrointestinal and esophageal cancers through hypomethylation in promoter region of *STK31*²⁷. Here, the reactivation of *STK31* in cancer and cell lines originating from liver, ovary, nasopharynx and gastrointestinal tract was determined by RT-PCR. The results showed that *STK31* was reactivated in 7 out of 15 (46.7%) gastrointestinal cancer samples and 2 out of 4 (50%) ovarian cancer samples (Figure 2.8). In cell lines, 6 out of 7 (85.7%) nasopharyngeal cancer and 7 out of 10 (70%) liver cancer expressed *STK31* while no expression was detected in normal tissue cDNA (Figure 1.9). These results demonstrate that *STK31* is reactivated not only in gastrointestinal cancer, but in many different types of cancer as well.

To further characterize the expression of *STK31* in cancer, immunofluorescence study in Caco2 cells was carried out. The results showed that *STK31* was predominantly expressed in the cytoplasm (Figure 2.9). Observations from enlarged

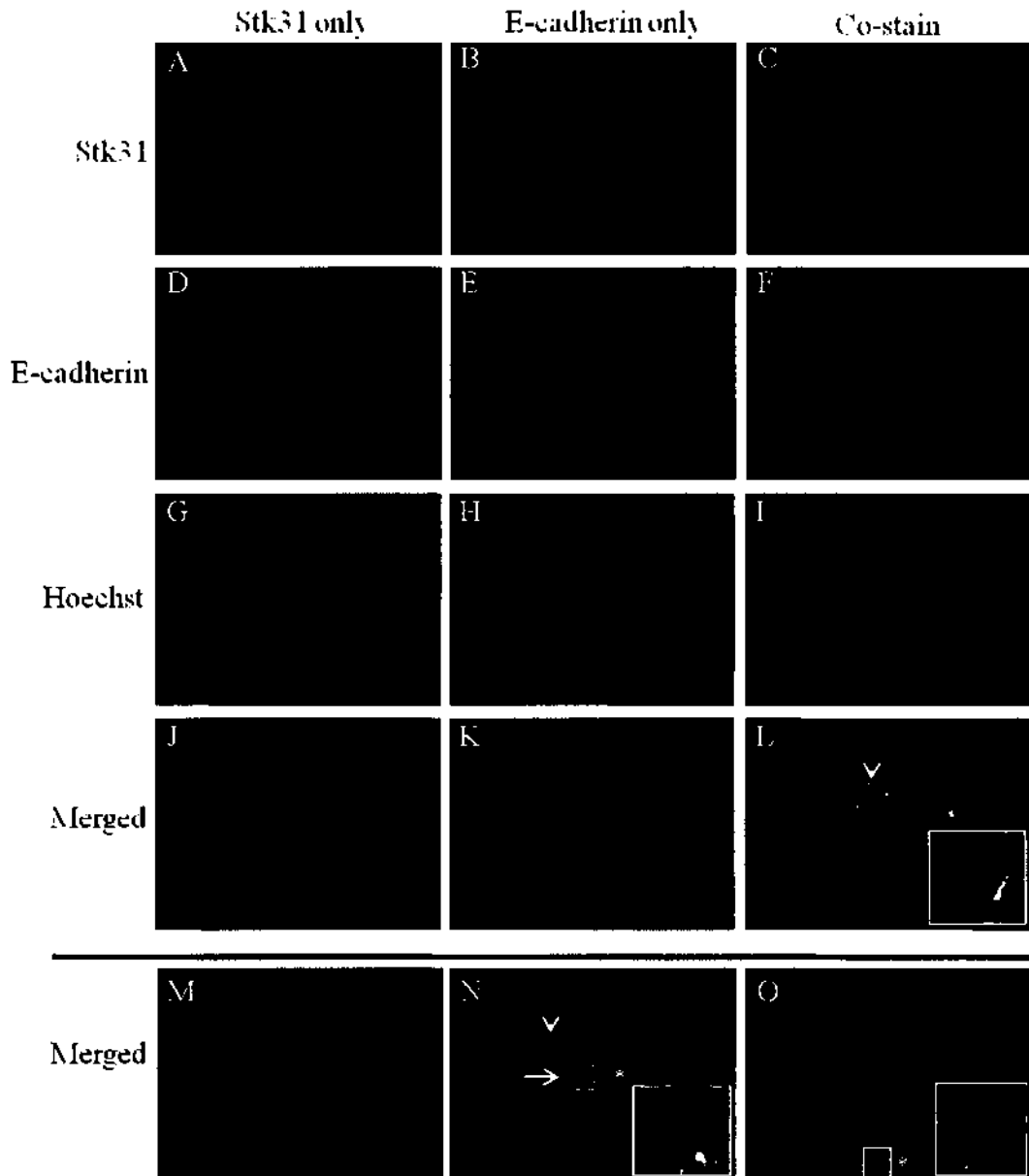


Figure 2.7| Co-immunofluorescence study of E-cadherin and *Stk31* in mouse testis. Adult mouse testis sections were stained with anti-STK31 antibody (A), anti-E cadherin antibody (E), both (C and F) or no antibody control (B and D). Nuclei were counterstained with Hoechst (G – I). Merged images for single antibody staining experiments are shown in J and K. Merged images for co-staining experiments are shown in L – O. Most spermatogonia were *E-cad*⁺/*Stk31*⁺ (Arrow head). A number of *E-cad*⁺/*Stk31*⁺ (Asterisk) and *E-cad*⁻/*Stk31*⁺ (Arrow) spermatogonia were also observed (inset). Magnification 400x (A – O).

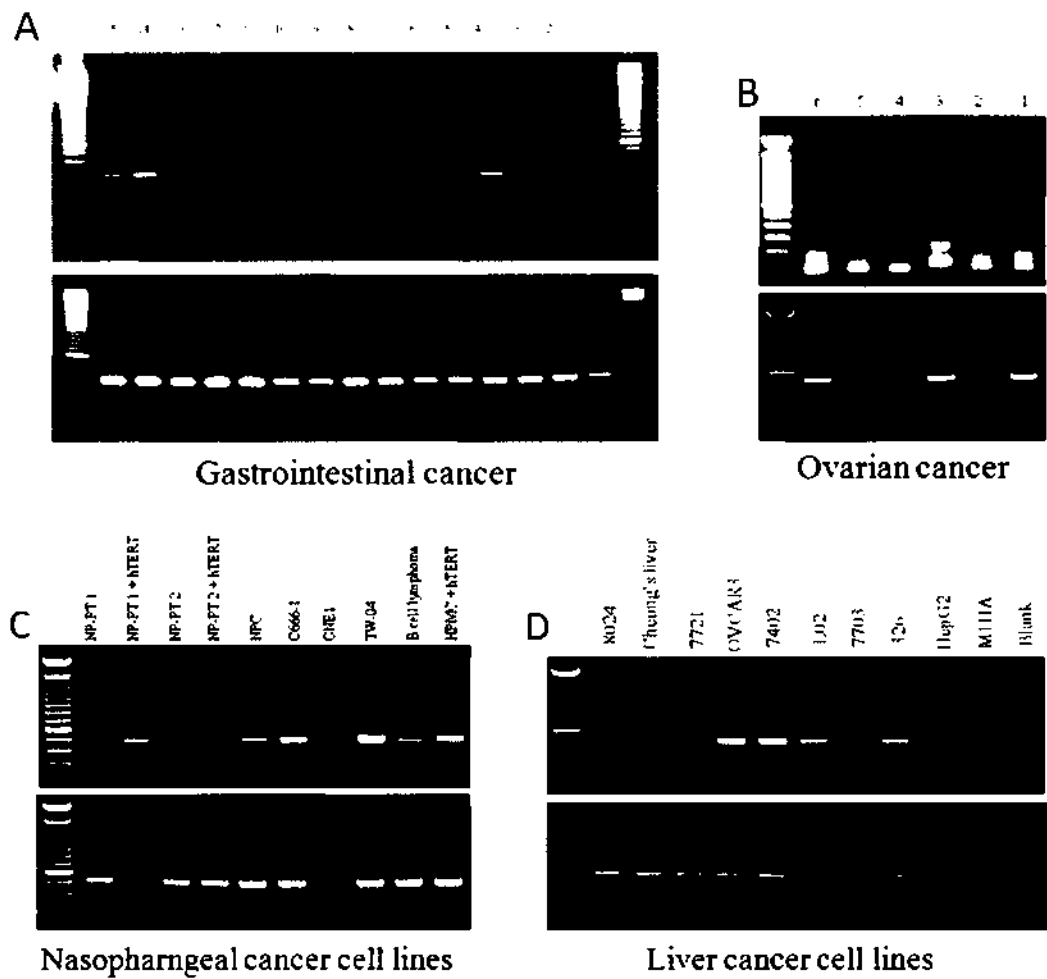


Figure 2.8| RT-PCR showing the reactivation of *STK31* in various cancer and cell lines. Expression of *STK31* (Top panel) was detected in patient samples of gastrointestinal cancer (A), and ovarian cancer (B), nasopharyngeal cancer cell lines (C) and liver cancer cell lines (D). GAPDH was used as internal control (Bottom panel).

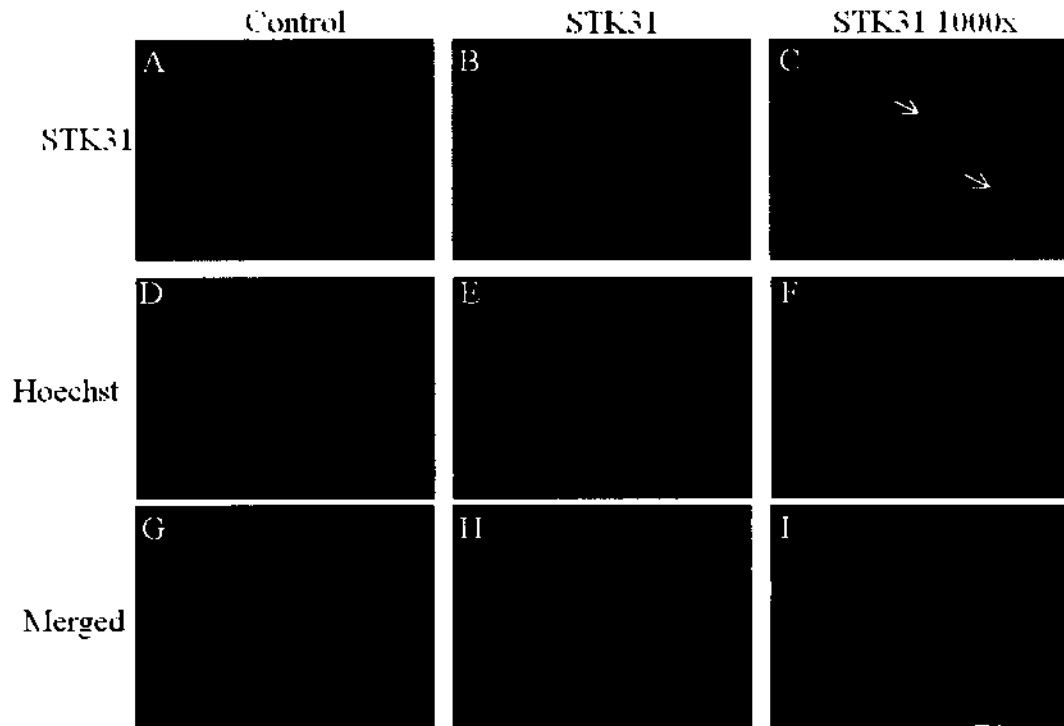


Figure 2.9| Immunofluorescence study of *STK31* in Caco2 cells. Human colon carcinoma cell line Caco2 were stained with anti-*STK31* antibody (B and C) or no antibody control (A). Nuclei were counterstained with Hoechst (D – F). Merged images are shown in bottom panel (G – I). Signals were detected in the cytoplasm and some granule-like signals were observed (Arrow). Magnification 400x (A, B, D, E, G, and H), 1000x (C, F, and I).

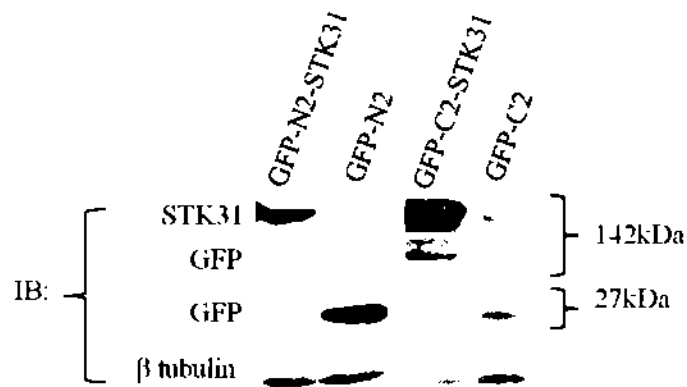


Figure 2.10| Western blot analysis of *STK31*-GFP fusion proteins. Whole cell lysates from HEK293 stable transfectants were probed with anti-*STK31* antibody (Top panel) and anti-GFP antibody (Two middle panels). β tubulin was used as loading control (Bottom panel). *STK31*-GFP fusion proteins in both terminuses (142kDa) were recognized by both *STK31* and GFP antibodies. GFP proteins (27kDa) were only detected in vector control lysate.

images showed that *STK31* formed granule-like structures. It is interesting to note that some cells showed stronger signal intensity, suggesting that the expression level of *STK31* is heterogenous even among the same cell lines.

2.3.6 *STK31* forms granular structures in HEK293 cells

To further characterize the cellular localization of *STK31* in live cells, GFPs were fused to either the N terminus or the C terminus of *STK31* and stably transfected to HEK293 cells. Expressions of both fusion constructs were determined by western blot analysis. It was estimated that STK31-GFP-N2 and STK31-GFP-C2 fusion proteins had a molecular weight of 142kDa; the expression of fusion proteins could be detected by anti-GFP and anti-*STK31* antibodies in fusion constructs transfected lysates, no fusion protein expression was detected in vector control lysates. GFP expression (27kDa) was detected in vector control transfected lysates but not fusion construct transfected lysates (Figure 2.10). These results indicated that the fusion proteins were stably expressed and there were no signs of proteolysis and cleavage of fusion proteins.

The cellular localizations of fusion proteins were then captured from live cells. Due to the lack of signaling peptides, GFP proteins expressed from the N2 and C2 vector were uniformly distributed in the cytoplasm (Figure 2.11). Both fusion proteins were also expressed in the cytoplasm; however, the localization was not uniform. The fusion protein aggregated to form a granular structure (Figure 2.11). This structure is similar to nuage in germ cell or stress granules in somatic cells, which are formed by tudor domain containing proteins³⁶⁻³⁹. Moreover, the tendency to form aggregates was different between the two fusion constructs. STK31-GFP-N2 fusion proteins (GFP located at C terminus) showed a higher tendency to aggregate instead of being uniformly distributed in the cytoplasm, however, STK31-GFP-C2

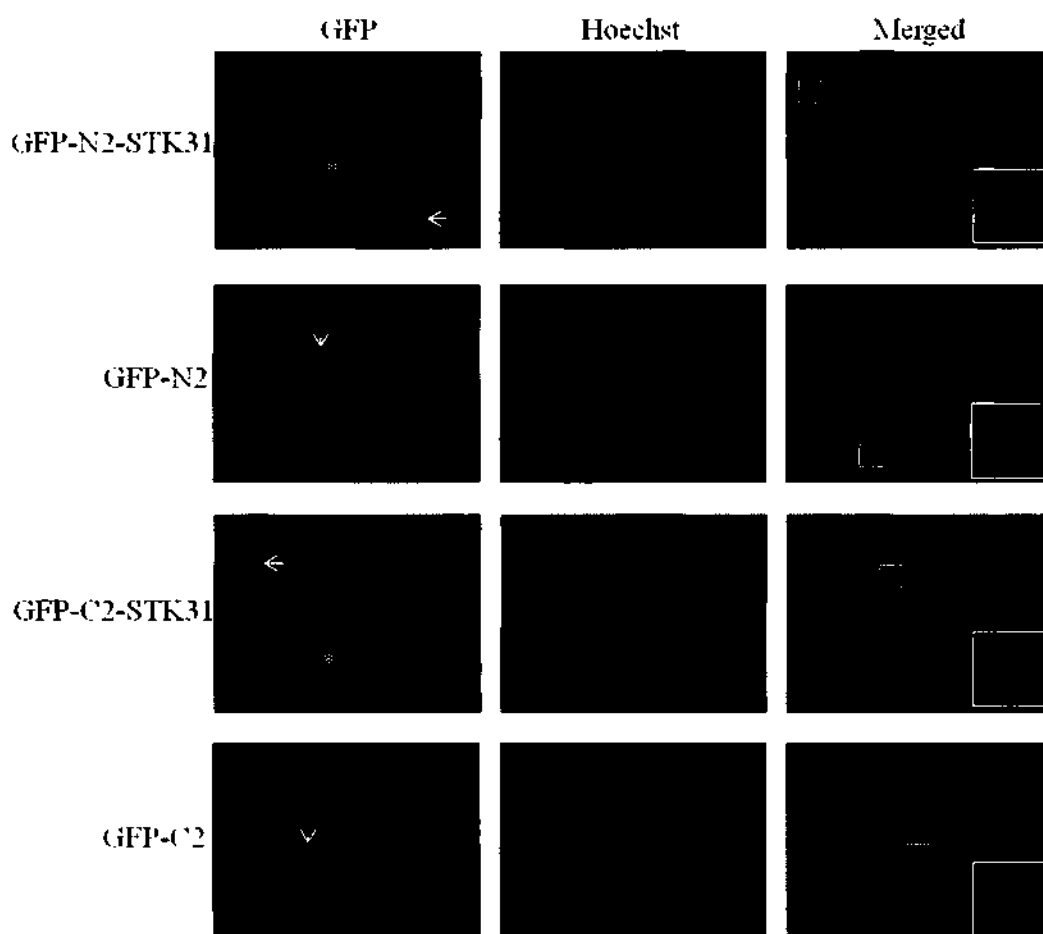


Figure 2.11| Live cell images of STK31-GFP fusion protein. Same numbers of HEK293 stable transfectants were seeded into 35 mm dish. GFP signals from STK31-GFP fusion proteins and GFP vector control were captured from live cells (Left panel). Nuclei were counterstained by Hoechst stain to visualize the total population of cells (Middle panel). Merged images are shown in right panel. GFP signals from N2 and C2 vector control are distributed uniformly in cytoplasm (Arrow head). Fusion proteins are located uniformly in the cytoplasm in some of the cells (Arrow), however, in another population of cells, the fusion proteins formed aggregated granules (Asterisk) instead of distributing uniformly. Magnification 100x.

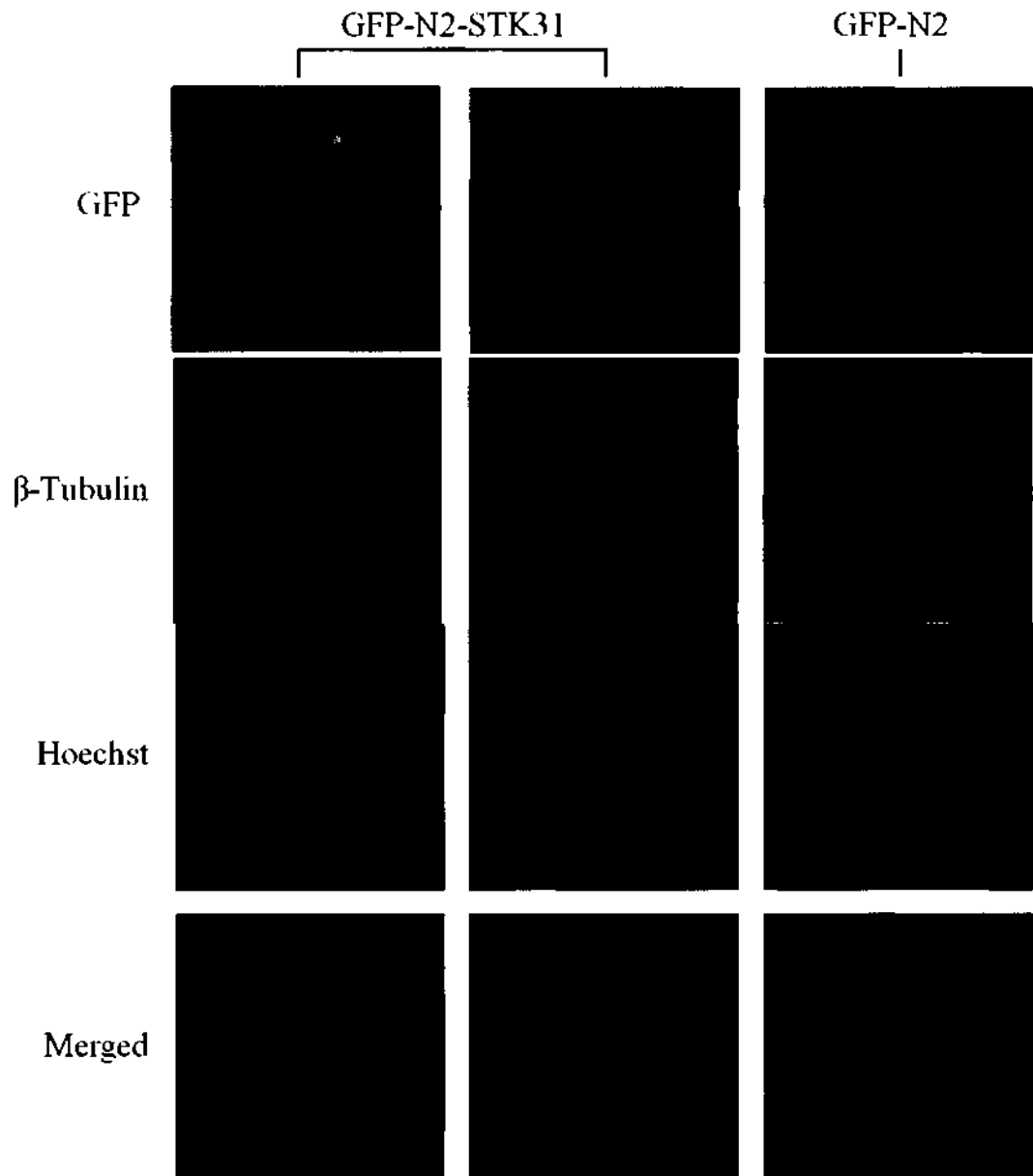


Figure 2.12| Immunofluorescence study of STK31-GFP fusion proteins during mitosis. HEK293 SPK-GFP-N2 stable transfectants were fixed on cover slips. GFP signals (Top panel) from fusion protein or vector control were captured directly. The mitotic spindle was stained with anti- β tubulin (2nd top panel). Condensed chromosomes were visualized by Hoechst stain (2nd bottom panel). Merged images are shown on the bottom panel. Two forms of distribution for fusion protein, uniform cytoplasmic distribution and aggregated granules were observed. The aggregated granules show asymmetric distribution while GFP alone show a uniform distribution during metaphase and anaphase. Magnification 1000x.

fusion protein (GFP located at N terminus) showed similar tendency to both types of localization (Figure 2.11). These data suggested that *STK31* is localized in the cytoplasm and aggregated into granular structures. Moreover, GFPs located at the N terminus may affect the granular structure formation.

2.3.7 Aggregated granules formed by *STK31* distributed asymmetrically during mitosis

Previous reports have demonstrated the presence of asymmetrically distributed proteins in male germline stem cell niche in *Drosophila*^{80,81,101,102}. Since *Stk31* is expressed in transition stage between undifferentiated and differentiated spermatogonia, therefore, it is possible that aggregated granules formed by *STK31* might also divide asymmetrically.

To study the cell division, *STK31*-GFP-N2 stable transfectants were used. The spindle fibers were stained with anti- β tubulin antibodies in order to determine the orientation of cytokinesis. The nuclei were stained with Hoechst in order to visualize the condensed chromosome. The results showed that a number of cells undergoing metaphase and anaphase expressed asymmetrical distribution of aggregated granules in the fusion protein group, as reflected by the unequal number of GFP signals observed from two poles (Figure 2.12). However, in the vector control group, the GFP signals were uniformly distributed during cell division (Figure 2.12). These results demonstrated that aggregated granules formed by *STK31* distribute asymmetrically during mitosis.

2.4 Discussion

2.4.1 Spermatogonia specific expression of *Stk31*

We reported a comprehensive study of expression profile and cellular

localization of *Stk31* during spermatogenesis. Previous studies have demonstrated that *Stk31* is expressed in all types of germ cells ranging from spermatogonia to spermatozoa using RT-PCR²⁵. Reports from another group have demonstrated that a Equine ortholog of *Stk31* is expressed in post-meiotic germ cells using immunostaining and western blot analysis¹⁰³. These results might be misleading due to the possible false positive results in PCR amplification and the discrepancy between the observed and expected molecular weight in the western blot analysis. In our previous studies, we have shown that *Stk31* RNA is first detected in primitive type A spermatogonia and restricted to spermatogonia but not differentiated germ cells. Here, we have further demonstrated that *Stk31* protein is only detected in mouse testis lysate but not in other organs, with an expected molecular weight of 113kDa. Immunofluorescent studies using the *STK31* specific antibody showed that *Stk31* is only expressed in spermatogonia, but not in more differentiated germ cells.

2.4.2 *Stk31* as markers for transitional state between undifferentiated and differentiated spermatogonia

Classification of mouse spermatogonia is a critical, yet challenging task due to the lack of stage specific markers. Researchers have attempted to characterize spermatogonia according to their microscopic morphologies⁶⁰, however, that would require complicated fixing procedures and experienced observational capacities. Therefore, cell surface markers are widely used for classification of spermatogonia. A number of spermatogonial stem cell markers have been identified due to their ability to enrich GSCs^{12,63}. Nonetheless, markers for differentiating spermatogonia are limited. c-kit is one of the differentiated spermatogonia marker identified due to its absence in GSCs^{104,105}. Here, we explored whether *Stk31* could be a potential marker for the spermatogonia that committed to differentiate. First of all, expression

of *Stk31* was not detected in spermatogonial stem cells that survived hyperthermia. Second, the expression of *Stk31* was observed in a number of undifferentiated spermatogonia as marked by the expression of E-cadherin, while another population of spermatogonia only expressed *Stk31* but not E-cadherin. This indicates that *Stk31* is expressed in the transition stage between undifferentiated and differentiated spermatogonia. Furthermore, expression of *Stk31* is upstream of c-kit since c-kit expression does not overlap with E-cadherin⁵⁹. Therefore, *Stk31* could be used as a marker for spermatogonia that are committed to differentiation.

2.4.3 Tudor domain and the intracellular localization of *STK31*

Recent reports have indicated that tudor domains are essential in the formation of nuage/germinal granules³⁶⁻³⁸ and stress granules³⁹. The formation of germinal granules requires tudor domain repeats while a single tudor domain is sufficient for the formation of stress granules. Here, we have demonstrated that *STK31*, which confers a tudor domain in the N-terminal, aggregate into granules in the cytoplasm. The aggregated granules were observed in both endogenous and GFP-tagged protein indicating that they were distinguishable from transfection-induced stress granules³⁹. However, its relationship with germinal granules and processing bodies, cytoplasmic structures closely related to stress granules¹⁰⁶, remains to be determined.

It is interesting to note that the location of GFP tag would affect the aggregate granules formation since more aggregated granules were observed in *STK31*-GFP-N2 fusion protein, where GFP was located in C-terminal. However, when GFP was tagged in the N-terminal, which was expected to be next to the Tudor domain, significant portions of fusion protein expression was observed throughout the cytoplasm. This could be explained by the fact that the bulky nature of the GFP protein affects the trafficking of *STK31* guided by the Tudor domain.

2.4.4 Asymmetric distribution of aggregated granules during mitosis

Nuage was observed in all stages of male germ cells with most prominent structures observed in post-meiotic germ cells^{36,107,108}. Polar granules, a form of nuage in oocytes and early embryos, was reported to partition asymmetrically and give rise to germ cell precursors¹⁰⁹. No reports so far have demonstrated that differentiation of male germ cells involve asymmetric segregation of nuage³⁶. We have demonstrated that *Stk31* expression in spermatogonia forms granular structure. Although whether these aggregated granules are indeed nuages remains to be determined, it is interesting to note that these aggregated granules may exhibit asymmetric distribution. In fact, we have demonstrated that aggregate granules formed by *STK31* distribute asymmetrically during mitosis of HEK293 cells. Traditional concepts on mitotic division state that daughter cells should inherit identical genetic materials. Mitosis in stem cells or cells with hierarchy, however, shows asymmetric segregation of protein determinants^{83,86,110}. In cell lines, there are only two reports on somatic cells mitotic asymmetry. The first study demonstrated the asymmetry in interphase but not anaphase⁹⁴, which indicated that daughter cells obtained identical maternal materials after cytokinesis. The second study demonstrated the asymmetry of aggresomes which were formed by diseased base misfolded proteins⁹⁵. Since there were no polyglutamine repeats, which formed the aggresome, in GFP-tagged STK31 protein, misfolding of the fusion protein was unlikely to happen. Hence, our results have demonstrated for the first time the somatic cell mitotic asymmetry during anaphase.

The mechanism of asymmetric division involves the interaction of determinants with the centrosome and mitotic spindle^{80,82,111}. We hypothesize that the asymmetry is set up by protein-protein interactions between the tudor domain and the

segregation machinery. This hypothesis is supported by the observed discrepancy between asymmetry in N2 and C2 fusion of *STK31*; asymmetry in C2 fusion was not observed. The mechanism of aggregate granule asymmetry remains to be elucidated.

2.4.5 Reactivation of *STK31* in multiple cancers

The reactivation of *STK31* by promoter hypomethylation was demonstrated in gastrointestinal cancer by RT-PCR and immunostaining ²⁷. In this chapter, expressions of full length *STK31* in various cancer and cell lines were further demonstrated by RT-PCR and western blot analysis. On top of gastrointestinal cancer, our results showed that more than 50% of cancer or cell lines in the liver, ovaries and nasopharynx show reactivation of *STK31*. Interestingly, previous report claimed that *STK31* expression was rarely observed in hepatocarcinoma cell line ²⁷, however, we have observed *STK31* expression in 7 out of 10 hepatocarcinoma cell line tested. These indicate that *STK31* is reactivated in multiple cancers and significantly increases the clinical applications of *STK31* as a candidate for diagnosis and therapy in multiple cancers.

2.4.6 Possible role of *STK31* in spermatogenesis and cancer

In short, we have demonstrated that *STK31* contains a highly conserved tudor domain. It is expressed in the cytoplasm with aggregated granules occasionally observed. It is reactivated in multiple cancers as a CT antigen and the mouse homolog is expressed in differentiating spermatogonia.

In mouse testis, nuage/germinal granules formed by tudor containing proteins have been demonstrated to take part in differentiation ^{36,37}. Together with our findings, we hypothesize that *Stk31* divides asymmetrically during mitotic division of spermatogonia and act as a cell fate determinant controlling daughter cells to

differentiation lineage.

Cancer occurrence has been speculated to be a stepwise process of gaining “stemness”, giving rise to cancer stem cells^{112,113}. On the other hand, asymmetric division was proposed to be a process of acquiring stem cell properties¹¹⁴⁻¹¹⁶. We hypothesize that *STK31* is reactivated during the process of acquiring stem cell properties and act as a regulator for “stemness” through asymmetric division of cancer stem cells.

2.5 Conclusion

In conclusion, we have found that *STK31* is reactivated in multiple cancers. *STK31* is localized in the cytoplasm, and forms aggregated granules that divide asymmetrically during mitosis. The localization of *STK31* might be guided by N-terminal Tudor domain. On the other hand, *Stk31* is expressed in the transition state between undifferentiated and differentiated spermatogonia and might be used as new marker for A_{pr} and/or A_{al} spermatogonia. Further studies are required for determining the functions of *STK31* in spermatogonia and cancer development.

Chapter 3

Functional studies of *Stk31* in mouse spermatogonia

3.1 Introduction

Spermatogenesis begins from male germline stem cells. Understanding the biology of this cell type facilitates the research on spermatogenesis.

3.1.1 Male germline stem cells (GSCs)

Male GSCs, also called spermatogonial stem cell (SSCs), are the stem cell population in the testis. The self-renewal and differentiation of GSCs are the foundation of spermatogenesis. The GSC is one of the most active stem cell systems in postnatal life giving rise to millions of spermatozoa daily and persist throughout the lifetime of a male. Although GSCs are physiologically important, the molecular identity of GSCs has not been characterized. One reason for this might be the rarity of GSCs; it is estimated that within 3000 – 5000 testicular cells, only one is a GSC (0.02% - 0.033%)^{117,118}. Until today, no unique marker was defined for GSCs and the most widely used strategy to identify GSCs was to use a combination of markers as described in earlier section (Section 2.1.3).

In mice, GSCs are formed from the transformation of gonocytes during 0 – 6 dpp¹¹⁹. The first appearance of GSCs was recorded in 3 – 4 dpp¹²⁰. In humans, the transformation process takes years. Studies on the transformation process indicated the presence of two subpopulations of gonocytes. The first subpopulation directly forms differentiated spermatogonia to support the first round of spermatogenesis while the second subpopulation forms the GSCs, which undergo self-renewal and differentiation to support subsequent rounds of spermatogenesis¹²¹.

3.1.2 Niche of male GSC

Niche refers to a specialized microenvironment, which supports the stem cell to maintain tissue homeostasis. Tissue homeostasis involves generation, maintenance and repair of the tissue through self-renewal and differentiation. The balance between self-renewal and differentiation is tightly regulated by both architectural support from cells and secretion of intrinsic and extrinsic factors within the niche ^{122,123}. The niche for male GSCs in mammals is poorly defined; however, the GSC system in *Drosophila* is well defined because of the simple anatomy and the availability of molecular markers in *Drosophila* ¹²⁴⁻¹²⁶.

In the *Drosophila* testis, GSCs are located in the apical tip, surrounded by clusters of somatic cells called hub cells ¹²⁷. Cell-cell interactions between GSC and hub cells are mediated by Adenomatous polyposis coli protein homologue (APC2), E-cadherin and Armadillo (Arm) ⁸¹. The division of GSCs is asymmetric, resulting in one GSC remaining in the niche and one committed progeny named gonialblast, which move away from the niche. Once away from the niche, gonialblasts are nursed by two somatic cyst cells (SCCs), which help sustain subsequent germ cell differentiation ¹²⁸. Gonialblasts then undergo transit amplifying divisions with incomplete cytokinesis to form 16-cell clusters of spermatogonia ¹²⁹.

Recent studies have suggested that the niche of GSCs in mouse testis is more complicated because of the involvement of Sertoli cells, Leydig cells, peritubular myoid cells and possibly other somatic cells ¹² (Figure 3.1). Among the various cell types, Sertoli cells are recognized as the major contributor to the GSC niche. This is supported by the fact that glial cell line-derived neurotrophic factor (GDNF) secreted by Sertoli cells is an essential factor for GSC self-renewal ¹³⁰⁻¹³³. Moreover, adhesion molecules β 1 integrin on both GSCs and Sertoli cells are required for the homing of GSCs to the basement membrane ^{134,135}. Furthermore, discovery of gonadotropin releasing hormone (GnRH) as a regulator of GSC biological activities also support

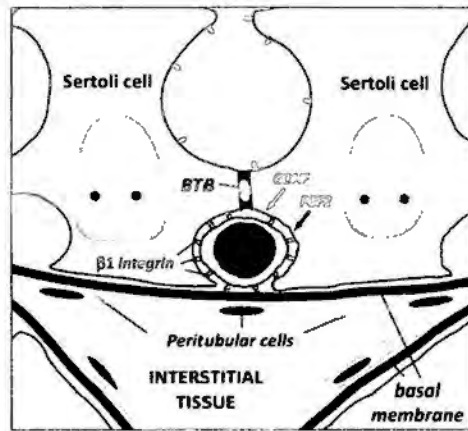


Figure 3.1| Niche of mouse male GSCs. Niche of mouse male GSCs involve Sertoli cells, Leydig cells, peritubular cells and possibly other somatic cells. GSCs are located on the basal membrane. Growth factors include GDNF and FGF2, which are essential for GSCs self-renewal, are secreted by Sertoli cells. Adhesion molecule $\beta 1$ integrin on both GSCs and Sertoli cells are required for the homing of GSCs to the basement membrane. Adapted from

134

the role of Sertoli cells in the GSC niche since the function of Sertoli cells is regulated by follicle stimulating hormone (FSH) and luteinizing hormone (LH), which are both regulated by GnRH¹³⁶. Leydig cells and myoid cells are also participators of the GSC niche. First, similar to Sertoli cells, Leydig cells are also regulated by FSH and LH. Second, undifferentiated spermatogonia showed biased localization to vascular network and accompanied Leydig cells and other interstitial cells *in vivo*¹³⁷. Moreover, colony-stimulating factor-1 (CSF-1), expressed by Leydig cells and select peritubular myoid cells, stimulate GSC self-renewal¹³⁸. These indicate the possible contribution of Leydig cells and myoid cells in the GSC niche.

3.1.3 Asymmetric division of GSCs

We have reviewed the concepts of asymmetric division in the previous chapter (Section 2.1.4). Here, we focus on asymmetric division in GSCs and review the mechanisms of asymmetric division.

In the *Drosophila* testis, GSCs normally undergo asymmetric division, which gives rise to one self-renewing progeny and one committed progeny¹²⁷. It is noteworthy that GSCs in *Drosophila* ovaries are able to undergo symmetric division to generate two self-renewing progeny that remains in the niche¹³⁹. In the mouse testis, GSCs were proposed to be able to undergo both symmetric and asymmetric divisions. In the symmetric division model, GSCs are able to give rise to either two self-renewing progeny or two progeny that commit to differentiate. In the asymmetric division model, GSCs give rise to one self-renewing progeny and one committed progeny which then further divide to form A_{pr} spermatogonia¹². Whether two models occur simultaneously is still a topic of debate. Moreover, whether A_{pr} spermatogonia originates from a second division of committed differentiating progeny or one of the A_{pr} progeny able to regenerate to GSCs is currently unknown.

Studies from neuroblasts and male GSCs in *Drosophila* have demonstrated that cell division asymmetry resulted from two general mechanisms: the asymmetric segregation of intrinsic cell fate determinants or asymmetric localization of daughter cells to specific microenvironments (niche) ¹¹¹. Both mechanisms require a polarized division that could be achieved by maintaining cell polarity or proper orientation of the mitotic spindle. Regulating spindle orientation could provide flexibility between symmetric and asymmetric division, however, this requires cautious control in order to prevent undesirable outcomes such as tumor growth ¹¹¹.

Male *Drosophila* GSCs sustain asymmetry through oriented division within a stem cell niche. Male GSCs orient to interact with hub cells through a specialized cortex region. These interactions are mediated by E-cadherin and Armadillo (*Arm*) and result in the correct orientation of Adenomatous Polyposis Coli homolog 1 (APC1), APC2 and centrosomin (*cnn*) ^{81,126}. This APC protein complex provides an anchor for astral microtubules and the result is one daughter cell that remains in contact with the hub cell in the niche while the other migrates away from the niche to differentiate.

Drosophila neuroblasts maintain asymmetry through asymmetric segregation of protein determinants. In contrast to male GSCs, the polarity of neuroblasts are set up through an evolutionally conserved mechanism involving the Par-3/6-aPKC polarity complex ^{81,82,111}. This complex is localized to the apical cortex, which is opposite to where the protein determinant is concentrated. During mitosis, aPKC phosphorylates the Lethal giant larvae (Lgl) protein. This protein has been found to bind with actin, myosin II, and proteins involved in exocytosis ^{140,141}. Due to the association with motor protein or trafficking molecules, Lgl has been speculated to regulate intracellular trafficking processes ¹⁴². Phosphorylation of Lgl by aPKC in the apical cortex is likely to inactivate Lgl and therefore protein determinants include Numb,

Pros and Brat concentrate on the basal side and ultimately segregate into daughter cells with the help of adaptor proteins Pons and Miranda^{80,143}. Besides, aPKC can phosphorylate the segregating determinant Numb directly¹⁴⁴. The phosphorylation releases Numb from the apical side suggesting the presence of an alternative Lgl independent segregating model.

In mouse GSCs, no evidence of asymmetric division had been found until a recent report demonstrating that UCH-L1 distributed asymmetrically in GSCs, which was associated with the basement membrane¹⁴⁵. This report did not provide direct evidence on the fate determining function of UCH-L1, although clues from transgenic mice showed that overexpression of UCH-L1 leads to the arrest of germ cells in a more differentiated pachytene stage¹⁴⁶. Moreover, the mechanisms for the asymmetric division in mouse GSCs have not been elucidated.

Previous studies in the mouse neural system suggest that mice and flies have similar asymmetric division mechanisms since target disruption of the key players like Lgl and Par-3 in mice and flies result in similar phenotypes^{147,148}. Alternatively, recent reports have demonstrated that the majority of neural progenitor divisions in mice do not occur along the apical-basal axis as it does in flies^{149,150}. Moreover, a recent report has demonstrated that the polarized distribution of protein determinant TRIM32 is independent of the polarity set up by Par-3/6-aPKC complex⁸³. These recent studies suggest that mice might have evolved an asymmetric division mechanism distinct from flies.

3.1.4 Self renewal of male GSCs

In the *Drosophila* testis, self-renewal of male GSCs is regulated by cell-cell interactions (Figure 3.2A) and networks of extrinsic and intrinsic factors^{12,125,127}. The GSCs attach to hub cells through various adhesion molecules that are



Figure 3.2| Regulations of GSCs self-renewal and differentiation in *Drosophila* and mouse testis. In *Drosophila* (A), asymmetric division of GSCs is determined by the cell-cell interaction with Hub cells (HC) through APC, E-cadherin and Arm. GSCs remaining in the niche would self-renew. The progeny that are committed to differentiate are called gonialblasts (GB) and leave the niche and are nursed by somatic cyst cells (SCC). In mice (B), self-renewal of GSCs is regulated by Sertoli cells through paracrine signaling. GDNF secreted from Sertoli cells bind to its receptor on GSCs and promotes self-renewal. Adapted from ¹²⁷.

indispensable in asymmetric division^{81,126}. Meanwhile, the interactions maintain the GSCs in close proximity with the niche and the short distances mediate signaling with extrinsic factors. Signaling cascades regulating male GSCs self-renewal include Janus Kinase-Signal Transduction and Activator of Transcription (JAK-STAT) and Bone Morphological Protein (BMP) and accomplish this through *Upd* and *gbb* from hub cells respectively^{124,151-154}. Other signaling pathways include *Piwi/Yb* and *zpg* mediated signaling^{155,156}.

Unlike *Drosophila*, knowledge of factors regulating GSC self-renewal in mammals is limited mainly due to the poorly defined niche and lack of model systems. However, with the recent breakthrough in establishing *in vitro* culture of GSCs and germ cell transplantation techniques, a number of intrinsic and extrinsic factors have been demonstrated to be involved in GSCs self-renewal (Figure 3.2B). GDNF and CSF-1 are the extrinsic factors provided by Sertoli cells and Leydig cells respectively. The addition of these factors in GSC cultures promote the expansion of GSCs^{130-133,138}. Subsequent studies on the underlying mechanisms of GDNF mediated self-renewal have demonstrated the involvement of Phosphoinositol 3 kinase/Akt (PI3K/Akt) and Src family kinase (SFK) intracellular signaling cascades and identified a number of intrinsic factors including *bcl6b*, *etv5*, and *lhx1*. These intrinsic factors are important for the maintenance of GSC self-renewal^{130,157,158}. Besides the PI3K/Akt and SFK pathways, BMP signaling has been demonstrated to take part in GSC self-renewal, although the mechanisms are still undefined^{159,160}. Other extrinsic factors include FGF and EGF, which are both secreted from Sertoli cells and shown to promote *in vitro* GSC expansion in a GDNF-dependent manner^{132,161-163}. However, the underlying mechanisms are yet to be determined. Targeted disruption experiments have identified *nanos2*, a TATA box binding protein associated factor 4b (*Taf4b*) and promyelocytic leukemia zinc finger protein (*Plzf*) as

intrinsic factors regulating GSC self-renewal since gene specific *null* mice showed significant germ cell loss or “Sertoli cell only” phenotype^{66,164-166}. Moreover, *in vitro* RNAi experiments have demonstrated the requirement of the transcription factor Oct3/4 in GSC self-renewal⁶⁸. However, how these intrinsic factors interact with GDNF mediated signaling cascade to regulated GSCs self-renewal remains to be determined.

3.1.5 Differentiation of GSC

Knowledge on GSC differentiation is limited when compared to self-renewal mechanisms because only fragments of evidence are available. In the *Drosophila* testis, differentiation of GSCs are also regulated by cell-cell interactions and intrinsic and extrinsic factors in the niche^{125,127}. *bam* is an intrinsic factor promoting differentiation of GSCs as indicated by the fact that overexpression of *bam* leads to GSC depletion^{151,167}. Therefore, *bam* should be repressed in self-renewing GSCs possibly through JAK-STAT and/or BMP pathways. On the other hand, gonialblast differentiation is regulated through communication between gonialblasts and SCCs. These communications are mediated by zpg mediated signaling^{168,169} and induction of EGFR signaling in SCCs by an unidentified signal/ligand from gonialblasts¹⁷⁰⁻¹⁷³. It is still unknown how the zpg signaling between gonialblasts and SCCs differ from that between GSCs and hub cells.

In the mouse testis, the regulation of GSC differentiation has been poorly studied. There are only a few known factors that promote GSC differentiation. Stem cell factor (SCF) produced by Sertoli cells is one of the most well known extrinsic factors to induce differentiation. Binding of SCF to c-kit, a tyrosine kinase receptor of SCF on germ cells, promotes differentiation while targeted disruption of the *Steel* locus (encodes SCF) or the *W* locus (encodes c-kit) results in the arrest of

spermatogonia differentiation^{75,174-176}. BMP4 and Activin A have also been demonstrated to induce the differentiation phenotypes of GSCs, and their actions are associated with induction of c-kit^{177,178}. Neurogenin 3 is a potential intrinsic factor proposed to take part in spermatogonial differentiation according to its molecular nature¹⁷⁹, however, experimental evidence supporting this hypothesis has not been published. At the moment, there is no report of an intrinsic factor that acts as a cell fate determinant in the differentiation of mouse GSCs.

3.1.6 Aim

Previous studies have demonstrated that *Stk31* is expressed in the transition stage between undifferentiated and differentiated spermatogonia. These same studies showed that *STK31* exhibits mitotic asymmetry in HEK293 cells (Chapter 2). Therefore, we hypothesize: 1. *Stk31* shows mitotic asymmetry in GSC division; and 2. *Stk31* is a cell fate determinant in GSCs.

The specific aims of this chapter are: first, to set up a *in vitro* GSCs model for the functional study of *Stk31*; second, to determine if *Stk31* asymmetry presence in GSCs; and third, to determine the function of *Stk31* in GSCs.

3.2 Materials and methods

3.2.1 Animals

C57/BL6 x DBA F1 (BDF1) hybrid mice and C57/BL6 mice were purchased from LASEC, CUHK. All procedures were approved by Animal Ethics Committee, CUHK (AEEC Number: 06/044/MIS).

3.2.2 Purification of GSCs

Ten BDF1 pups with age of 2 dpp were humanly terminated and their testes

were collected. The tunica albuginea was removed to release the seminiferous tubules. The seminiferous tubules were minced with scissors and testicular cells were released using a two-step enzymatic treatment^{177,180-183}. Minced tubules were placed in Solution I (1mg/ml Collagenase Type IV; 40µg/ml DNaseI, Sigma) for 10 minutes at 37°C. Tissues and cells were collected by centrifugation at 600 g for 7 minutes followed by incubation in Solution II (0.25% Trypsin, 1mM EDTA, Invitrogen; 40µg/ml DNaseI, Sigma) for 5 minutes at 37°C. The trypsin reaction was stopped by the addition of 10% FBS. Tissue debris was removed by filtering through a 60µm nylon mesh and testicular cells were collected by centrifugation at 600 g for 7 minutes.

3.2.3 Establishment of GSC cultures

Testicular cells were cultured in GSC medium [StemPro 34 SFM medium supplemented with StemPro supplement (Invitrogen); 25µg/ml insulin (Sigma); 100µg/ml iron-saturated transferrin (Sigma); 60mM putrescine (Sigma); 30nM sodium selenite (Sigma); 6mg/ml D-(1)-glucose (Sigma); 30µg/ml pyruvic acid (Sigma); 1µl/ml DL-lactic acid (Sigma); 5mg/ml bovine serum albumin (Sigma); 2mM L-glutamine (USB corp); 5×10⁻⁵M β-mercaptoethanol (Sigma); minimal essential medium (MEM) vitamin solution (Invitrogen); MEM nonessential amino acid solution (Invitrogen); 10⁻⁴M ascorbic acid (Sigma); 10µg/ml d-biotin (USB corp); 30ng/ml β-estradiol (Sigma); 60ng/ml progesterone (Sigma); 20ng/ml mouse epidermal growth factor (BD Bioscience); 10ng/ml human basic fibroblast growth factor (Sigma), 10³U/ml ESGRO (murine leukemia inhibitory factor; Chemicon), 10ng/ml recombinant rat glial cell line-derived neurotrophic factor (GDNF) (R&D Systems, Minneapolis, MN) and 1% fetal bovine serum (Gibco)] and maintained in 37°C in an atmosphere of 5% carbon dioxide in air. Germline stem cells were

obtained through differential plating and long term cultures were established according to established protocol¹⁶¹. $0.5 - 1 \times 10^5$ cells were seeded onto each well of a 0.2% gelatin coated 24 well plate. After 1 to 2 days *in vitro* (DIV), floating cells enriched in germ cells were transferred to another well after overnight attachment. After 3 DIV, floating cells were maintained in a 24 well plate for 12 days with the medium changed every 3 days. On the 15th DIV, GSC clumps were flushed off from attached cells through gentle pipetting and transferred to STO feeder layer (Section 3.2.4).

3.2.4 Long-term GSC cultures on STO feeder layer

STO cells were purchased from ATCC. STO culture were maintained in STO culture medium (DMEM, Gibco; 10% FBS, Gibco; 1% P/S, Gibco; 100 μ M β -mercaptoethanol, Sigma) and passaged as recommended.

For mitotic inactivation of STO cells, cultures at 90% confluence were treated with 10 μ g/ml mitomycin C (Sigma) for 3 hour at 37°C. Mitotic inactivated STO were washed with HBSS and either used immediately or frozen by addition of 10% DMSO for storage.

For preparation of the feeder layer, 5×10^5 of fresh or 1×10^6 of frozen mitomycin C treated STO cells were plated onto 0.1% gelatin coated 35 mm dish. The feeder layer was used 1 – 7 days after seeding.

On the 15th DIV, $1 - 2 \times 10^5$ GSCs were seeded onto the feeder layer with the medium changed every 2 – 3 days. The GSCs were passaged every 4 – 6 days. GSC clumps were flushed off by gentle pipetting, followed by centrifugation at 600 g for 7 minutes. GSC clumps were resuspended into a single cell suspension and seeded onto the feeder layer at a 1:2 to 1:3 ratio.

3.2.5 Serum free and feeder free culture

For serum free culture, all procedures were the same as indicated (Section 3.2.4) except that 1% FBS in GSCs medium was replaced by B-27 supplement (Gibco, Invitrogen).

For feeder free culture, all procedures were the same as indicated (Section 3.2.4) except that GSCs were seeded onto 20 μ g/ml laminin (BD Bioscience) coated 35 mm dish.

3.2.6 Time Lapse Imaging of GSCs culture

GSCs were cultured onto MatTek glass bottom culture dish (MatTek) under feeder layer culture condition. Images were taken every 20 minutes for 60 hours by Time Lapse Imaging System (CarlZwiss) 3 days after seeding.

3.2.7 Collection of GSCs for molecular analysis

GSCs were collected for molecular analysis as described^{58,184}. GSCs were flushed off from feeder layer by gentle pipetting and pelleted by centrifugation at 600 g for 7 minutes. This protocol yields GSCs with purity over 95% and minimizes the background signal from feeder layer.

3.2.8 RT-PCR

RNA from GSCs were extracted using TRIzol reagent (Invitrogen). The RNA was dissolved in DEPC-treated ddH₂O. RNA concentrations were measured by Nanovue Spectrophotometer (GE Healthcare).

For reverse transcription, 2.5 μ g RNA were mixed with 0.5 μ g/ μ l Oligo dT primer (Invitrogen) followed by incubation at 70°C for 10 minutes. Oligo dT was annealed to RNA by incubating on ice for 2 minutes. RT mix (1X PCR buffer; 2mM

MgCl₂; 8mM DTT; 0.25mM dNTP) was then added to the reaction followed by incubation at 42°C for 5 minutes. 200U MMLV-RT (Invitrogen) was then added and the RT reactions were completed by incubating at 42°C for 50 minutes followed by 70°C for 15 minutes. RNA in cDNA mixture were degraded by addition of 1U of RNase H (Invitrogen) and incubated at 37°C for 20 minutes.

Primer pairs used in this study were Stk31, SSEA-1, EpCAM, β 1-integrin, E-cadherin, Cd9, Oct3/4, c-kit, Ccna1, Hlf3, and Gapdh (Appendix). 1 μ l of cDNA were used for RT-PCR as indicated (Section 2.2.3).

3.2.9 Recipient mice

According to histocompatibility^{185,186}, C57/BL6 or BDF1 mice were used as recipient mice. To deplete endogenous germ cells, 40mg/kg busulfan (Sigma) was injected into mice at 4 weeks of age through intra-peritoneal injection. Mice were kept for 6 – 8 weeks before transplantation.

3.2.10 Germ cell transplantation

Germ cells transplantation was carried out as described^{183,187,188}. To prepare GSC suspension for transplantation, GSCs were flushed off from feeder layer followed by three times wash in HBSS. GSCs were resuspended in injection solution (0.04% Trypan blue, Sigma; 100 μ g/ml DNase I; in HBSS, Gibco) with concentration of 10⁷ cells/ml.

Recipient mice were anesthetized with a Ketamine/Xylazine mix. Incision was made at the mid-line of the lower abdomen. The testes were pulled out and placed on sterilized paper. The cells suspensions were loaded into micropipettes and injected into the seminiferous tubule through efferent duct injection. Sham transplantation were made by injecting the injection solution. Any leaked cells were washed away

with physiological saline and the wound was sealed with sutures. The mice were allowed to recover and comfortably housed for 2 months to allow regeneration of spermatogenesis. 3µg/kg Temgesic were given via intra-subcutaneous injection when needed after surgery. Recipient mice were allowed to mate with female mice and their testes were collected after these mating experiments. The numbers of pups was counted per recipient.

3.2.11 Retinoic acid treatment of GSCs

GSCs were treated 5 days after passaged. 1µM Retinoic acid (Sigma) were added to the culture medium and cultured for 3 days. GSCs were collected for RT-PCR studies as indicated. For immunofluorescence study, 3 days after RA treatment, cultures were fixed for immunofluorescence study.

3.2.12 Immunofluorescent studies

GSCs were fixed by 4% PFA, permeabilized and blocked in 5% normal goat serum (Invitrogen) in 1X PBST for 30 minutes at room temperature. The sections were then probed with 1:100 Mouse Anti-STK31 MaxPab (Abnova) at 4°C overnight. Non-specific binding of primary antibodies were washed off with 1X PBST and the sections were probed with Alexa®488 Anti-mouse high cross absorbed Ab (Molecular Probe) for 1 hour at room temperature. The sections were then washed with 1x PBST and the nuclei were counterstained with 100ng/ml Hoechst 33342 (Invitrogen) for 5 minutes at room temperature. The slides were mounted by Anti Fade Gold mounting media (Invitrogen) and images were taken with a Nikon ECLIPSE 80i imaging system (Nikon) and analyzed via SPOT Advanced software (SPOT Diagnostic Inc.). Daughter GSCs from a single mitotic division were characterized by the presence of an intercytoplasmic bridge ¹⁴⁵.

3.2.13 Cloning of *Stk31*

The mouse homolog *Stk31* was cloned from mouse adult testis cDNA. Primer pairs *Stk31* FL was used in this experiment. The full-length coding region of *Stk31* was amplified by *FideliTaq* polymerase (USB corp) as indicated (Appendix). PCR products were purified with *illustra*TM *GFX*TM PCR DNA and Gel Band Purification Kit (GE Healthcare) and cloned into pQCXIH retroviral vector (Clontech) using *NotI* and *BamHI* restriction sites. Plasmid DNA was prepared using Mini Plus or Midi Plus Plasmid DNA Extraction Kit (Viogene).

3.2.14 Retrovirus production

Retroviral system was used in *Stk31* overexpression studies. Retrovirus was produced using BD Retro-XTM Universal Expression System (Clontech). GP2-293 packaging cells were maintained in DMEM (Gibco) supplemented with 10% FBS (Gibco), 1% P/S (Gibco), 4mM L-glutamine (USB corp) and 1mM Sodium Pyruvate (Sigma). To produce the retrovirus, 3×10^6 GP2-293 cells were transfected using 5 μ g of overexpression vector, 5 μ g of pAmpho and 20 μ l of Lipofectamine 2000 reagent (Invitrogen) in a 60 mm culture dish. To increase viral titre, packaging cells were seeded onto the culture dish with the DNA:liposome complex pre-loaded in medium. 24 hours post-transfection, the medium was changed to full medium supplemented with MEM nonessential amino acid solution (Invitrogen). Viral supernatant was collected 72 hour post-transfection.

Cell debris in both the retroviral supernatant was removed by filtering through MILLEX-HV[®] PVDF 0.45 μ m filter unit (Millipore). Viral titres were determined by transducing NIH3T3 cells.

3.2.15 Transduction

GSCs were cultured for 3 days after passage for transduction. 1ml viral supernatants (10^4 TU/ml, ~0.1 MOI) were pre-incubated with 6 μ g/ml polybrene (Sigma) for 5 minutes followed by adding to GSCs culture containing 1ml GSCs medium. 20 hours post-transduction, viral containing medium was changed to GSCs medium.

3.2.16 Selection of transduced GSCs

Hygromycin resistant feeder layers were prepared by retroviral transduction of the pQCXIH vector (Clontech) into STO cells.

To obtain stable transduced GSCs, transduced GSCs were passaged onto antibiotics resistant feeder layer 3 days after transduction. 3 days after passage, GSCs were selected with 40-200 μ g/ml Hygromycin (Invitrogen). 4-5 days after selection, resistant GSCs were passaged to new feeder layer with addition of normal GSCs to maintain cell confluence¹⁸⁹. Selection cycles were repeated until resistant GSCs colonies acquired sufficient cell confluence for maintaining the proliferation status.

3.3 Results

3.3.1 Establishment of GSCs culture on STO feeder cells

To study the functions of *Stk31* in spermatogonia, an *in vitro* culture of GSC were established. This experiment was based on previous established GSC cultures¹⁶¹ and maintained on STO feeder layers. Germ cells were first extracted from neonatal BDF1 mice through double enzymatic treatments^{177,180-183} and germ cells were enriched by differential plating. During the differential plating periods, somatic cells were attached to gelatin-coated plate while germ cells, which were distinguished by their large size, remained floating. After three rounds of negative

selection, the majority of somatic cells were removed and the floating population was enriched in germ cells. These steps resulted in a favorable somatic cell: germ cell ratio, which is critical for the initiation of GSC cultures. The germ cells and the small amount of somatic cells were seeded onto a 24 well plate in the presence of GDNF, FGF, EGF and LIF, which have been shown to be required or enhanced GSCs maintenance and self-renewal^{132,161,177,180,182,190-192}. After 3 – 15 DIV, somatic cells began to attach, proliferate and spread on the well. GSCs attached to the somatic cell layer, proliferated and formed cell clumps. These clumps were recovered from the attached cells and seeded onto STO feeder layers for further culturing.

To characterize the GSC cultures on STO feeder cells, the growing properties of the culture were compared with previous studies¹⁶¹. During the first 1 – 2 days on fresh STO feeder, GSCs attached to the feeder layer as a single cell (Figure 3.3A). On day 3, GSCs began to proliferate and form small clumps (Figure 3.3B). On day 4 – 5, GSCs formed large clumps of cells (Figure 3.3C and D), which is a characteristic of self-renewing divisions of GSC^{132,161,181}. Chains of proliferating cells, resembling the *A_{al}* spermatogonia *in vivo*, were observed (Figure 3.3E). However, unlike the previous studies, the clusters of cells had distinct borders instead of unclear borders^{132,161,181}.

Furthermore, GSCs attached preferentially to laminin¹⁶² and self-renew on laminin-coated plates in feeder free conditions¹⁶². In order to determine whether GSCs on STO feeder maintain this property, GSCs were seeded onto laminin-coated plates after passage. GSCs on STO feeder attached to laminin one day after seeding exhibits a flattened round morphology (Figure 3.4). Consistent with previous report¹⁶², the attached cells proliferated during days 2 – 5 and upon reaching confluency, the morphology of the cells switched from being flattened and round to being fibroblast-like (Figure 3.4).



Figure 3.3| Culturing properties of GSCs on STO feeder layer. GSCs morphologies were captured 1 – 2 days (A), 3 days (B), and 4 – 5 days (C – E) after seeding onto fresh STO feeder layer. Individual cells were observed on day 1 – 2. Small clusters of cells were observed on day 3. Large clumps of proliferating GSCs were observed on day 4 – 5. GSCs in clumps with distinct borders (Arrow) and chains of proliferating GSCs were observed (Arrow head). Magnification 100x.

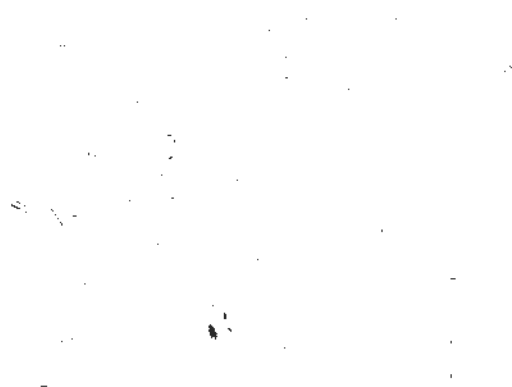


Figure 3.4| Culturing properties of GSCs on laminin. GSCs morphologies were captured 1 day (Left) or 5 days (Right) after seeding onto laminin-coated plate. Individual GSCs attached on to laminin with a flattened round morphology (Arrow) (Inset). GSCs proliferated on laminin and upon reaching confluence, fibroblast-like morphology were observed (Arrow head) (Inset). Magnification 100x.

Besides laminin binding activity, GSCs have been shown to be able to be cultured on MEFs in serum-free condition¹⁶². To study whether this property could be applied in GSCs on STO feeder, serum in the GSC culture medium was replaced by B-27 nutrient supplement. On the first day of serum replacement, the STO feeder layer rounded up and detached from culture plate, which were the signs of apoptosis (Figure 3.5). This indicated that GSCs are not suitable for culturing on STO feeder layers under serum-free conditions. However, it is interesting to note that large cell clumps with unclear borders were found 5 days after serum replacement (Figure 3.5). This morphology is similar to GSCs under anchorage independent culturing conditions¹⁹³.

3.3.2 Molecular characterization of GSCs culture

On top of cell morphology and culturing properties, the identities of GSCs on STO feeder layers were further characterized by studying the expression of molecular markers. Markers for the testis (Histone 1t)^{194,195}, primordial germ cells (SSEA-1)^{196,197}, spermatogonial stem cells (β 1-integrin and Oct3/4)^{61,68,198}, spermatogonia (CD9, EpCAM and E-cadherin)^{62,63,199}, differentiated spermatogonia (c-kit)¹⁰⁵, and primary spermatocytes (Ccna1)²⁰⁰ were used in this experiment. GSCs from initial cultures (7 DIV) and prolonged cultures (100 DIV) were compared to a commercially available mouse spermatogonia cell line GCI-spg. STO feeder was used as a control to eliminate possible contamination of feeder in GSC cultures.

Both initial and prolonged GSC cultures expressed a testis specific histone isoform, Histone1t. No expression was detected in STO feeder control confirming their testicular origin. Similar to previous reports^{68,161,162}, both initial and prolonged cultures maintained the expression of spermatogonial stem cell markers, β 1-integrin and Oct3/4. They also expressed undifferentiated spermatogonia markers, CD9 and

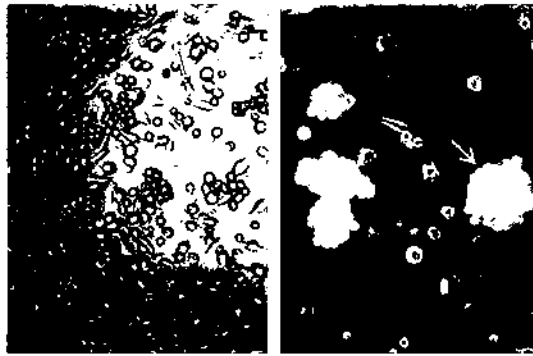


Figure 3.5| Culturing properties of GSCs on STO feeder under serum-free condition. GSC morphologies were captured 1 day (Left) or 5 days (Right) after serum replacement. STO feeder layer detached from culture plate 1 day after serum replacement. Large clumps with unclear borders similar to anchorage independent growth were observed (Arrow) 5 days after serum replacement. Magnification 100x.

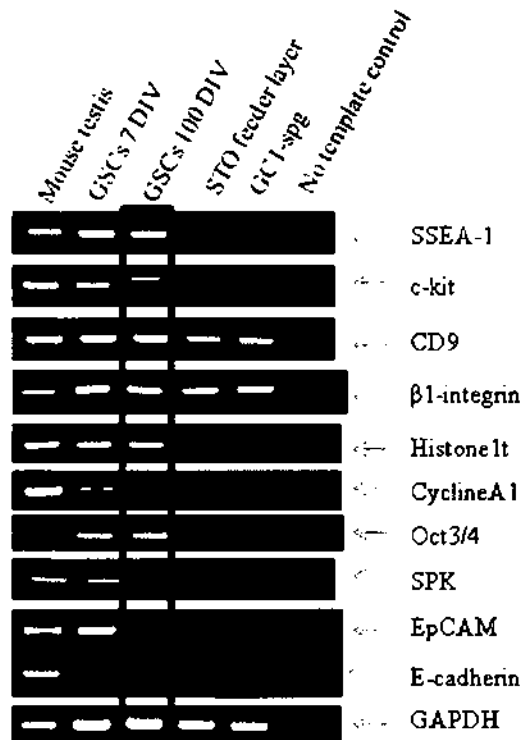


Figure 3.6| Expressions of stage specific germ cell markers in GSCs cultured on STO feeder layer. Expressions of testis specific marker (Histone 1t), markers for primordial germ cells (SSEA-1), spermatogonial stem cells (β 1-integrin and Oct3/4), spermatogonia (CD9, EpCAM and E-cadherin), differentiated spermatogonia (c-kit), and primary spermatocytes were determined (Upper panels). GAPDH was used as internal control (Bottom panel). Expression in prolonged culture (Red rectangle) were compared with initial cultures and the GC1-spg cell line. STO feeder was used to eliminate possible contamination in GSCs. Mouse testis cDNA were used as positive control.

E-cadherin (Figure 3.6). The expression of more differentiated stage markers, c-kit and *Ccn1* were detected in the initial culture. However, after prolonged culture, the expression of these markers was lost, indicating that only undifferentiated stem cells are able to self-renew under this culture condition. In contrast to GSCs on MEF feeder, which are negative in SSEA-1 and positive in EpCAM expression^{161,162}, GSCs on STO feeder were positive for SSEA-1 expression. EpCAM expression significantly decreased after prolonged culture (Figure 3.6). This suggested that GSCs on STO feeder might maintain more primitive properties. In our previous studies, it was demonstrated that *Stk31* is expressed in the transition state from undifferentiated to differentiated spermatogonia (Section 2.3.4). Interestingly, the present study showed that *Stk31* was expressed in initial cultures, but not prolonged cultures.

3.3.3 GSC cultures maintain spermatogonial stem cell activity

Spermatogonial stem cell activity, the most critical property of GSCs, is characterized by the ability to repopulate the seminiferous tubules and regenerate spermatogenesis¹⁸⁷. The only known method to test this is by germ cell transplantation. In order to determine whether our GSC cultures maintained this property, the GSCs were transplanted to histocompatible, germ cell depleted recipient mice. After two months of regeneration, the fertilities of recipient mice was determined by mating and their testes morphologies was recorded. Upon GSC transplantation, the recipient mice testes recovered to a size similar to normal adult testes, however, testes from sham-transplantation groups were significantly smaller due to the depletion of germ cells (Figure 3.7). Furthermore, GSC transplanted mice regained fertility as shown by the ability to impregnate female mice. No pups were found on sham-transplanted group (Table 3.1).

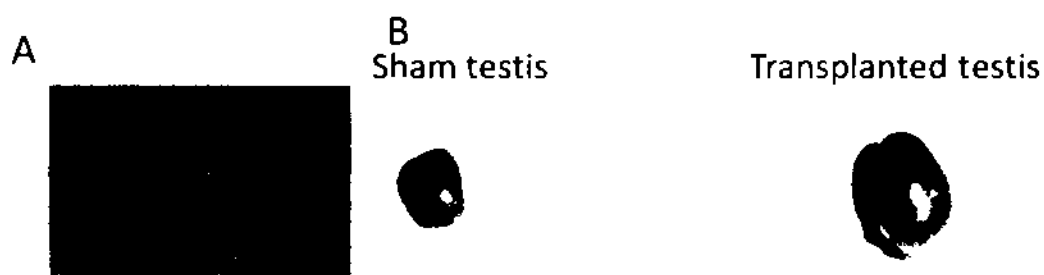


Figure 3.7| Morphology of testis after germ cell transplantation. GSCs were transplanted into recipient mice testes through efferent duct injection (A, Adapted from ¹⁸³). After regeneration, testes from GSC transplanted (Right) and sham transplanted (Left) mice were excised and imaged (B). The testes that received GSCs showed regeneration of spermatogenesis as reflected by testis size.

Treatment	No. of replicates	No. of pregnant female	No. of pups laid	% of male	% of female	Days for pups after transplantation
GSCs transplanted	2	4	20	55	45	~ 3 months
Sham	2	0	0	N/A	N/A	N/A

Table 3.1| Regeneration of spermatogenesis and restoring fertility of recipient mice after germ cell transplantation. Recipient mice received GSCs transplantation or sham transplantation were mated with female mice. Numbers of pups lay by female mice were counted. Upon transplantation, recipient mice restored fertility while sham transplanted mice remained sterile.

These results indicate that our GSCs maintain similar culturing properties, germ cell marker expressions, and more importantly, spermatogonial stem cell activity. Therefore, these GSCs were suitable for subsequent analysis.

3.3.4 Retinoic acid induce differentiation in GSCs

Since the GSCs were maintained in undifferentiated states and did not express *Stk31*, it was necessary to induce differentiation in order to study the transition state between undifferentiated to differentiated spermatogonia. Retinoic acid, which has been demonstrated to induce differentiation in various stem cell systems²⁰¹⁻²⁰⁴, has also been found to be able to induce differentiation in GSCs⁶⁸. It was therefore used to induce the differentiation of GSCs, and subsequently the transition state of GSCs.

The GSCs started to differentiate three days after the induction via retinoic acid. This differentiation was characterized by changes in two culturing properties: clump dissociation and detachment from feeder layers. While the earlier section and previous studies demonstrated that self-renewal division occurs preferably in clumps of GSCs (Section 3.3.1), the current study showed that after RA induction, the clumps began to dissociate, forming small clusters of not more than 15 cells. GSCs in vehicle control groups remained in normal mounds (Figure 3.8). Furthermore, it has been suggested that differentiating GSCs would detach from feeder layers after induction by retinoic acid^{58,181}. In this study, during the collection of GSCs, RA-induced GSCs readily detached from feeder layer in response to light vibration. The vehicle treated group, however, required repeated pipetting in order to flush the GSCs off the feeder layer. These results suggested that RA is able to induce differentiation in GSCs culture on STO feeder layers.

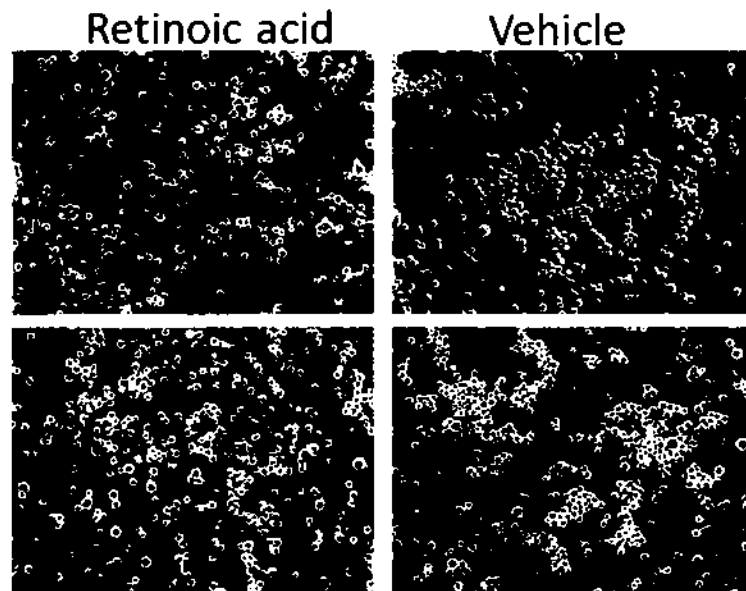


Figure 3.8| Induction of GSCs differentiation by retinoic acid. GSCs on STO feeder layer were treated with $1\mu\text{M}$ retinoic acid (Left panel). 4 days after treatment, cell morphologies were recorded. Absolute ethanol was used as vehicle control (Right panel). GSCs clumps were dissociated into small clusters of cells (<15 cells/cluster) (Arrow) after RA treatment. Sizes of clumps remain unchanged in the vehicle control group. Magnification 100x.

3.3.5 Induction of *Stk31* expression upon RA-induced differentiation

It has been demonstrated that Oct3/4, which is required for spermatogonial stem cell self-renewal, is down-regulated during RA induced differentiation⁶⁸. In this experiment, RNA was extracted from GSCs 3 days after RA induction. Expression of these germ cell markers were analyzed by RT-PCR. Consistent with the previous studies⁶⁸, Oct3/4 was down-regulated after induction by RA in this study. Despite the weak expression of EpCAM, its expression was still down-regulated in concomitant with Oct3/4. The expressions of SSEA-1, β 1-integrin and CD9 were not affected by RA induction. Strikingly, the expression of *Stk31* was induced upon RA induction (Figure 3.9).

In order to study whether the induced *Stk31* expression would be translated into protein, an immunofluorescence study was carried out. In this experiment, GSCs cells 3 days after RA induction or vehicle treatment were fixed and stained with anti-STK31 antibody. Consistent with the RT-PCR results, protein of *Stk31* was detected in the RA treated group, but not the vehicle control group (Figure 3.10). Interestingly, the induction of *Stk31* expression was heterogeneous. Strong expression of *Stk31* was detected from individual cells dissociated from clumps. Weak expression of *Stk31* was detected from cells that remained in small clusters (Figure 3.10). In contrast to the RA-treated group, GSCs in the vehicle group remained in clumps of more than 15 cells, and were negative in *Stk31* staining.

These results indicate that self-renewal of GSCs decreases upon differentiation as reflected by decrease in Oct3/4 expression. Meanwhile, the expression of *Stk31* is induced. These data further support our hypothesis that *Stk31* is expressed in the transition state between undifferentiated and differentiated spermatogonia.

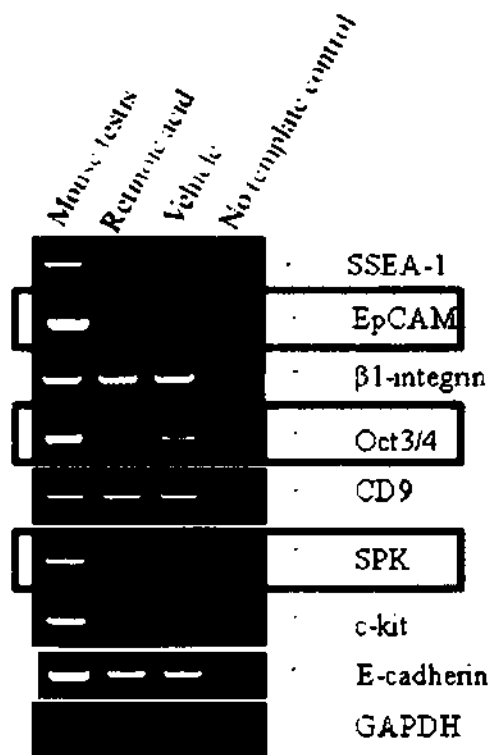


Figure 3.9| Expressions of stage specific germ cell markers in GSCs after RA induced differentiation. Expressions of markers for primordial germ cells (SSEA-1), spermatogonial stem cells (β 1-integrin and Oct3/4), spermatogonia (CD9, EpCAM and E-cadherin), and differentiated spermatogonia (c-kit) were determined (Upper panels). GAPDH was used as internal control (Bottom panel). Differential expressed genes, Oct3/4, EpCAM and *Stk31*, were marked (Red rectangle). Oct3/4 and EpCAM were down-regulated while expression of *Stk31* was induced upon differentiation.

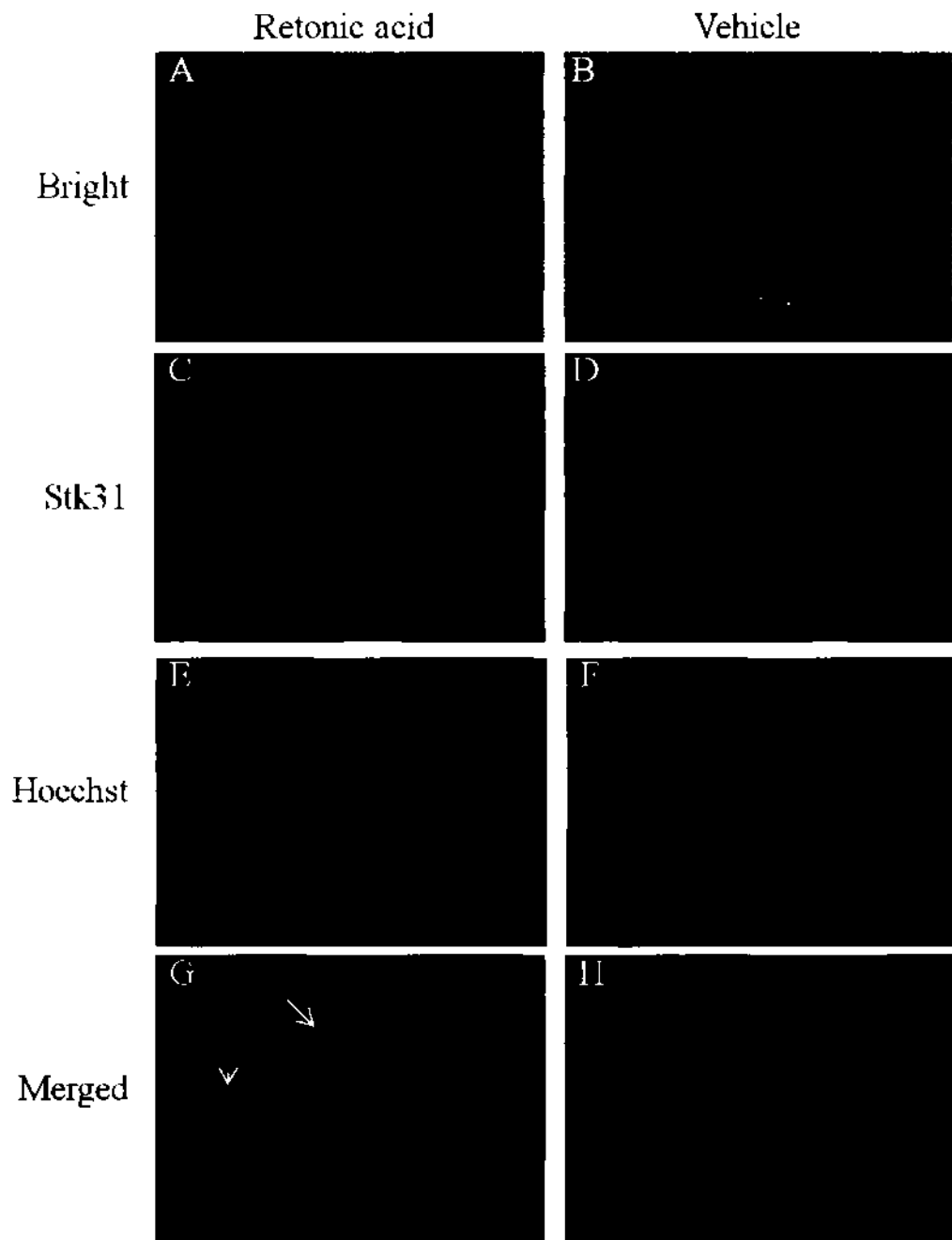


Figure 3.10| Immunofluorescence study of *Stk31* in differentiating GSCs. GSCs on STO feeder layer were treated with 1 μ M retinoic acid (A, C, E and G) or vehicle control (B, D, F and H). 4 days after treatment, cells were fixed and stained with anti-STK31 antibody (C and D). Nuclei were counterstained with Hoechst (E and F). Bright fields are shown on the top panels; merged images are shown on the bottom panels. Heterogeneous *Stk31* expression was induced upon differentiation. Strong expressions were detected in dissociated cells (Arrow) while weak expressions were detected in small clusters (Arrow head). Magnification 200x.

3.3.6 Asymmetrical distribution of induced *Stk31* protein during GSCs mitotic division

Studies in *Drosophila* have shown that GSCs in males divide asymmetrically during differentiation. The asymmetry was proposed to be determined by cell-cell interaction, cell-ECM interaction, localization of extrinsic and intrinsic factors^{81,101,137,205,206}. From our previous results, *Stk31* was found to be expressed in the transition state during GSC differentiation. Moreover, the induction of *Stk31* was heterogeneous. This suggested that *Stk31* might be the intrinsic factor that acts as a cell fate determinant in mouse GSC system. To study this, immunofluorescent studies were used to study the expression of *Stk31* from daughter cells of a single mitotic division of GSCs. These two daughter cells were characterized by the presence of an intercellular cytoplasmic bridge¹⁴⁵.

Immunofluorescent studies showed that *Stk31* localized asymmetrically within daughter cells derived from individual cells dissociated from clumps (Figure 3.11). More importantly, asymmetrical distributions were found in cells with two nuclei, which mimics the stage before division/cytokinesis (Figure 3.11), indicating that the asymmetry was set up before division instead of being induced after division. Uniform cytoplasmic distribution and aggregated granules expression patterns, as suggested by GFP fusion protein, were also found in GSCs exhibiting asymmetrical division (Figure 3.11).

3.3.7 *Stk31* induce differentiation phenotype in GSCs

As a intrinsic factor which is divided asymmetrically during GSCs division, it would affect the cell fate of the daughter cells through altering the self-renewal or differentiation^{83,207,208}. To study the consequence of asymmetric distribution of *Stk31*, whether or not it acts as a cell-fate determinant, we overexpressed *Stk31* in GSCs

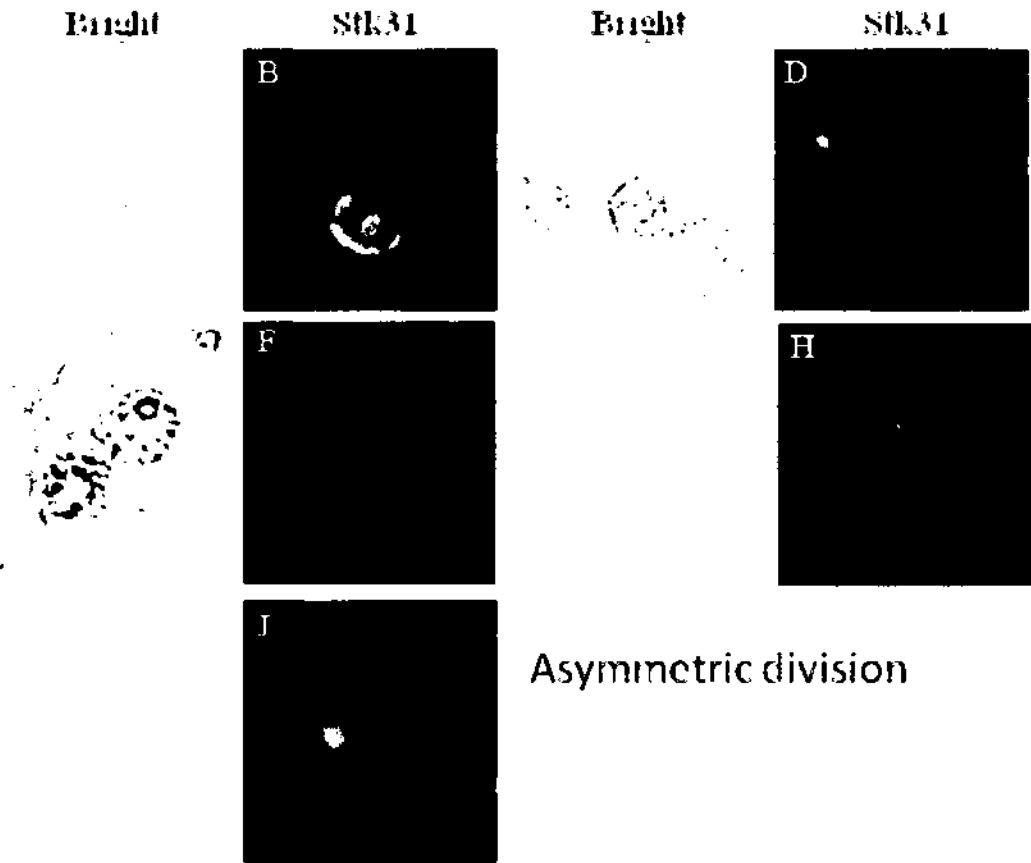


Figure 3.11| Asymmetry of *Stk31* in GSCs division. After RA treatment, GSCs were fixed and stained with anti-STK31 antibody. Nuclei were stained by Hoechst. Merged images were showed on the right panel. Bright field were showed on the left panel. Daughter cells from single parental cells were characterized by intra-cytoplasmic bridge. *Stk31* distributed asymmetrically in two daughter cells after division (A – J). Uniform cytoplasmic distribution (C and D) and aggregated granules (G and H) were observed in the asymmetric division. The asymmetry was set up before division/cytokinesis (I and J). Magnification 400x.

using retroviral transduction. The results showed that retrovirus was able to overexpress *Stk31* in GC1-spg and STO cells (Figure 3.12A). The expression of *Stk31* in GSCs was not checked since transduced cells were used for subsequent selection. Nonetheless, the success of transduction was monitored by the expression of GFP.

Before transduction, GSCs grew in mounds (Figure 3.12B). After transduction, *Stk31*-overexpressed groups showed a significant decrease in the number of mounds as compared to the vector control group (Figure 3.12B). This indicated that *Stk31* overexpression was able to initiate a differentiated phenotype in GSCs.

3.4 Discussion

3.4.1 GSCs on STO layers enhance the flexibility of genetic manipulation

We have demonstrated that by using established serum-containing culture condition¹⁶¹, GSCs are able to self-renew and expand on STO feeder layers. Early reports have demonstrated the feasibility of GSC cultivation in the presence of STO feeder layer²⁰⁹. Although proliferation was noted during cultivations, the number of GSCs could only be maintained for 4 months without expansion. After the discovery of GDNF, the key regulator for expansion of undifferentiated spermatogonia^{64,210}, long term GSC cultures have been established¹⁶¹. Subsequent experiments on genetic manipulation of GSC culture have been successfully conducted^{189,211,212}. These systems utilize MEFs instead of STO as the feeder layer, possibly due to the better maintenance of mES cells on this feeder layer²¹³. Soon after the establishment of the long term culture method, another group has reported an improved culture condition using serum-free conditions with specialized supplements where STO was used as feeder layer^{58,132,192}. Yet, no genetic manipulation using this culture condition has been reported. Although MEFs confer more reproducible

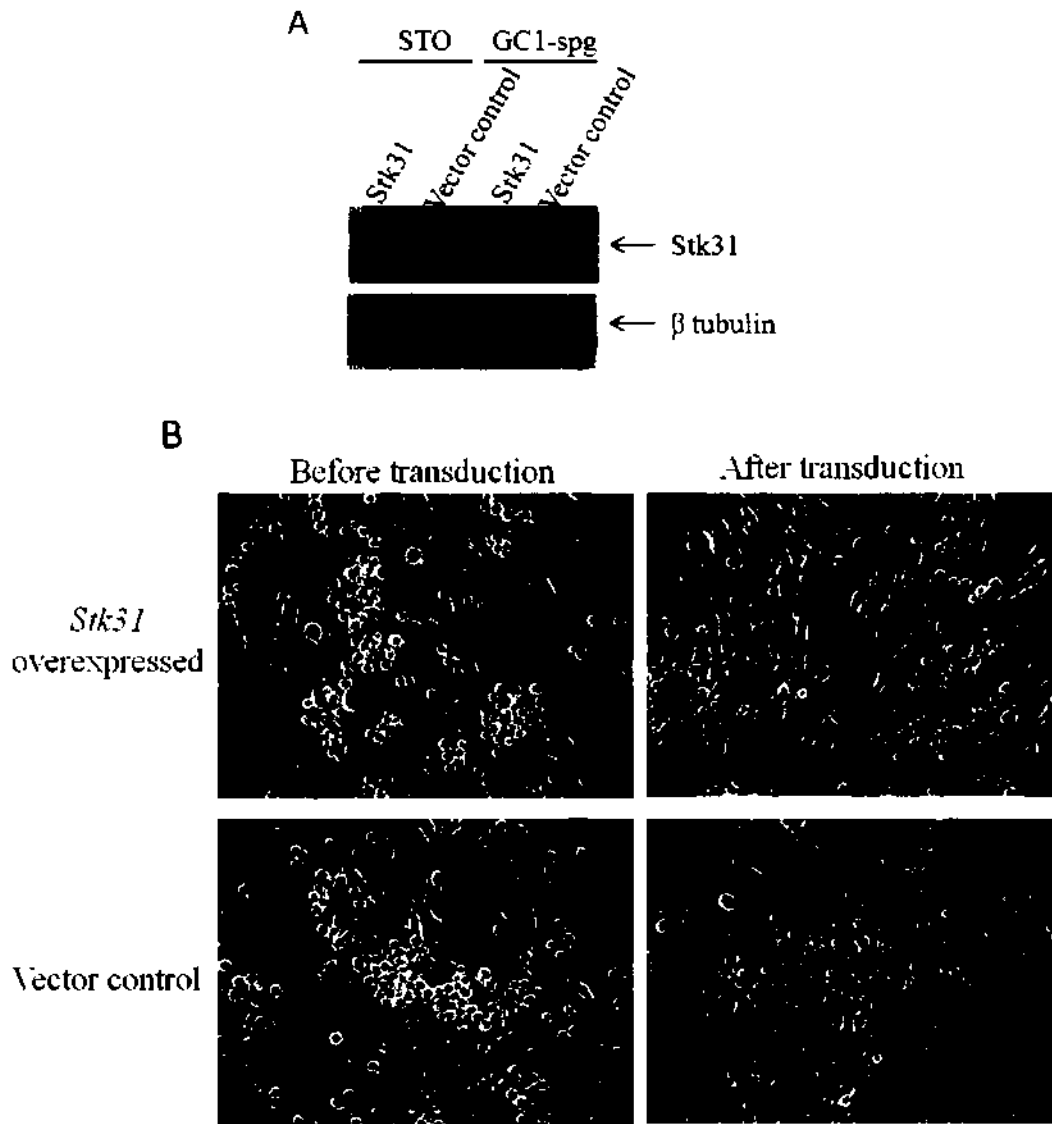


Figure 3.12| Induction of differentiation phenotypes by *Stk31*. GSCs were transduced with retrovirus carrying *Stk31* overexpression vector. Overexpressions of *Stk31* by retrovirus were confirmed by western blot in GC1-spg and STO cells (A). Cell lysates of transduced cells were probed with anti-STK31 antibody (A – top panel) and β tubulin was used as loading control (A – bottom panel). Morphologies of GSCs were recorded before and after transduction (B). *Stk31* overexpression initiates clump dissociation after transduction (B – top panel). Mounds of GSCs were still observed in vector control group after transduction (B – bottom panel).

characteristics than STO, the flexibility of genetic selection, which usually involves various antibiotic selections, is limited due to the lack of resistant MEFs. Due to the immortalized nature of STO, introduction of antibiotic resistances are more feasible and therefore greatly enhances their flexibility for genetic manipulation.

3.4.2 Cultures on STO layers shows primitive GSCs signatures

GSCs on STO layers share various similarities regarding morphological characteristics and molecular signatures with GSCs on MEFs. These included the chains and clump formations; expression of GSC markers such as CD9 and β 1-integrin; and laminin binding and anchorage independent growth properties^{161,162,193}. The discrepancies lie on the cell border morphology and expression of primordial germ cell marker SSEA-1. GSCs grown on STO exhibit flattened clumps with distinct borders. On the other hand, GSCs on MEFs exhibit clumps with unclear borders. This morphology is more comparable with early reports on maintaining GSCs on STO for 4 months²⁰⁹. However, in our system, GSCs were able to expand and passage for more than 3 months.

SSEA-1 is expressed in ES/EG cells, which are only available during embryonic period. FACs analysis showed that GSCs on MEFs did not express SSEA-1¹⁶¹. In our system, GSCs were obtained from postnatal mice and therefore should be negative for SSEA-1. However, the cells in our experiment expressed SSEA-1. This indicated that either the cultured cells were ES/EG cells or that they retained some properties of their lineage progenitors. It is unlikely that the cultured cells were ES/EG cells because the cultured cells were morphologically distinguishable from ES/EG cells. Moreover, transplantation of ES/EG cells into seminiferous tubules results in tumor formation and causes the death of recipient¹⁸⁸. However, transplantation of our culture cells into seminiferous tubules did not result in tumor

formation and death. Instead, spermatogenesis was regenerated and fertility was restored. Therefore, we speculate that GSCs on STO retain some properties of their progenitors. Further study on the expression of the SSEA-1 protein is necessary for clarification of this interesting phenomenon.

3.4.3 Induction of *Stk31* during GSCs differentiation

Since the cells in GSCs culture were heterogenous, it was postulated that only a portion of cells display Oct3/4 expression are the spermatogonial stem cell ⁶⁸. However, it is reasonable to consider that these cells as undifferentiated spermatogonia due to: first, the presence of undifferentiated markers; second, the absence of differentiated markers; and third, the chain morphologies resembling A_{pr} and A_{al} spermatogonia. Retinoic acid is able to induce differentiation in GSC cultures as indicated by changes in growing properties and marker expression. This differentiation should start from undifferentiated to differentiated spermatogonia. Consistent with our hypothesis, *Stk31* expression was induced after differentiation; meanwhile, expression of Oct3/4 was down-regulated, further supporting that *Stk31* is a differentiating spermatogonia (A_{pr} to A_1) marker. A_s spermatogonia is thought to be the spermatogonial stem cell. Oct3/4 is among one of the proteins expressed in this subset of cell type ^{133,214-217}. It would be interesting to examine if there are co-relations between the expression of *Stk31* and Oct3/4, as this would provide a hint on the hierarchy of spermatogonia. Positive co-relations might indicate that spermatogonial stem cell presents in A_{al} population. Positive co-relations might also indicate that A_s spermatogonia may differentiate into A_1 spermatogonia directly.

On top of Oct3/4, c-kit was reported to be induced during RA induced differentiation ⁶⁸. However, in our system, after 3 days of treatment, c-kit expression was not detected. This may due to the fact that our GSCs have a more primitive

phenotype. Also, this indicates that induction of *Stk31* may be upstream of c-kit. Longer periods of induction may be necessary in order to determine the co-relations between *Stk31* and c-kit.

3.4.4 Mechanisms for *Stk31* asymmetry in GSCs

Asymmetric segregation of protein determinants have been reported in various mammalian stem cells system such as neural progenitors cells⁸³, hematopoietic stem cells and progenitors cells⁸⁴ and muscle satellite cell⁸⁵. Asymmetric division has also been demonstrated in cell systems with hierarchies such as T cells⁸⁶. The spermatogonial stem cell system differs from these systems in that mitotic division in spermatogonial stem cells undergo incomplete cytokinesis^{55,57,218}. The intercellular cytoplasmic bridge resulting from incomplete cytokinesis allows for the exchange of materials between daughter cells. Therefore, asymmetric segregation should require unique machinery for maintaining this asymmetry. Our results showed that the asymmetry of *Stk31* was set up before cytokinesis occurs. Interestingly, a gradient distribution of *Stk31* was observed. This indicated that such machinery would have been set up before cytokinesis and is able to set up a protein gradient. Previous reports on *Drosophila* suggested that asymmetry in GSC systems was determined by the niche through protein-protein interactions with the cortex region of GSCs^{81,126}. A recent report on mitotic asymmetry in mouse GSC systems also suggested the involvement of the basement membrane¹⁴⁵. The niche of mouse GSCs is likely to consist of Sertoli cells which are epithelial cells. However, *in vitro* cultures of GSCs were maintained on a fibroblast feeder. Due to the differences in surface protein architectures of the two cell types, this culture condition was not suitable for mimicking the niche. This also suggested that *Stk31* asymmetry was unlikely to be set up by protein-protein interaction between GSCs and the niche. Further studies are

needed to elucidate the molecular mechanism underlying *Stk31* asymmetry, which might be independent of Par-3/6-aPKC polarity complex as in the case of TRIM32.

3.4.5 *Stk31* is a cell fate determinant in GSCs

Cell fate determinants are discerned by their asymmetric distribution in stem cell division and the ability to regulate the cell fate after division. In mouse GSCs, cell fate determinants have not yet been identified. In our experiments, we have demonstrated the asymmetry of *Stk31* and more importantly, when overexpressed, *Stk31* is able to initiate the differentiated phenotype of GSCs. These results indicated that *Stk31* is a cell fate determinant in mouse GSCs. This is the first evidenced cell fate determinant in mouse GSCs.

What is the underlying mechanism for the cell fate specifications by *Stk31*? C-kit is a potential candidate since the expression of c-kit was down-regulated by *Plzf*, which is responsible for GSC self-renewal ²¹⁷. Interestingly, c-kit might be a downstream target of *Stk31* as suggested by the delayed induction of c-kit after retinoic acid treatment. BMP-SMAD signaling cascade would be another target due to their conserved role in GSC differentiation in *Drosophila* and mice, which were also associated with c-kit expression ^{177,178}. Indeed c-kit and SMAD1 were down-regulated in *STK31* knocked-down Caco2 cells in a dose-dependent manner (Chapter 4). Besides receptor signaling pathways, the cell cycle regulator cyclin D2, which has been demonstrated to take part in GSCs self-renewal induced by Ras ²¹⁹, was up-regulated in *STK31* knocked-down Caco2 cells (Chapter 4). This suggested that *Stk31* might also regulate GSC self-renewal through cell cycle regulation.

Taken together, we hypothesize that upon stimulation from extrinsic factors, expression of the cell fate determinant *Stk31* is induced. *Stk31* may be distributed asymmetrically in GSC division through unique asymmetry machinery. The

accumulation of *Stk31* in committed progeny will trigger the BMP-SMAD pathways, which would result in the induction of c-kit expression and subsequent differentiation processes. On the other hand, the accumulation of *Stk31* would suppress cyclin D2 expression and prevent GSC self-renewal. These pathways together with the niche regulate the homeostasis of male mouse GSCs.

3.5 Conclusion

In conclusion, we have demonstrated that GSCs can be cultured on STO feeder without the loss of GSC properties. Expression of *Stk31* was induced in RA-induced differentiation. *Stk31* is distributed asymmetrically during GSC division and overexpression of *Stk31* in GSCs induces the differentiation phenotype. We propose the involvement of BMP-SMAD cascade and c-kit in the cell fate specification by *Stk31*. Further studies are required to elucidate the molecular mechanisms underlying the *Stk31* asymmetry and the requirement of *Stk31* in spermatogenesis *in vivo*.

Chapter 4

Functional studies of *STK31* in human colon cancer

4.1 Introduction

Cancer is one of the most common lethal diseases. Research has been focused in the origin of cancer. Recently, the emerging concept of the “cancer stem cell” has facilitated the understanding of tumor origin and progression.

4.1.1 Cancer stem cells

One common characteristic of all cancers or tumors is the variability in diverse properties among the cancer cells within a tumor. These properties include the expression of surface antigens, cell morphology (differentiation stages), proliferation properties, metastatic capacity, tumorigenicity and therapeutic resistance^{220,221}. These variables in tumors are referred to as tumor heterogeneity²²². Currently, there are two models accounting for tumor heterogeneity: the “cancer stem cell” model and the “clonal evolution” model^{6,223} (Figure 4.1). The clonal evolution model states that cancer cells acquire genetic alterations over time. Combinations of these changes provide growing advantages to cells that undergo natural selection. Therefore, during tumor initiation and progression, a cell that received mutations would have more progeny that might in turn acquire additional genetic alterations. Meanwhile, another cell would acquire other advantageous mutations. The result of this is a mixture of tumor cells that have acquired different mutations or characteristics, in a single tumor. Furthermore, all cancer cells can potentially become invasive, tumorigenic and resistant to therapeutic strategies²²³⁻²²⁶. In the cancer stem cell model, only a particular subset of cells within the tumor contains stem cell properties. These stem cell properties determine the invasiveness, therapeutic resistancy and tumorigenicity of the tumor. This particular subset of cells is called “Cancer stem cells (CSCs)”. In

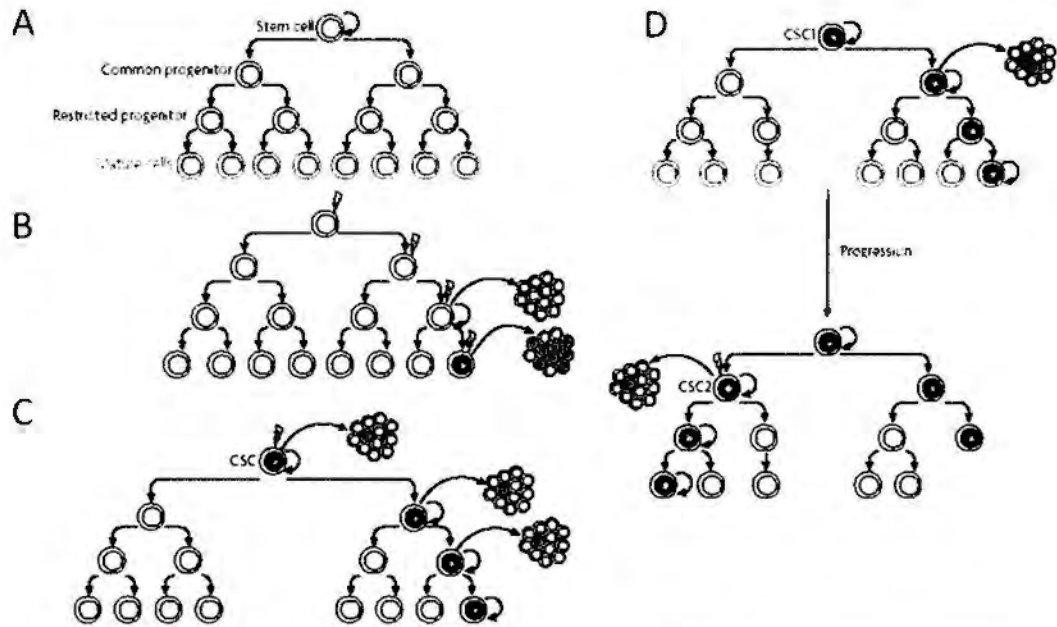


Figure 4.1| “Cancer stem cell” and “Clonal evolution” model for cancer heterogeneity. Under normal conditions, stem cells undergo differentiation and form a cell hierarchy (A). In the “Clonal evolution” model (B), all cells may acquire genetic alteration and have similar tumorigenic potential. In the “Cancer stem cell” model (C), only the “cell-of-origin” acquires CSC properties. Tumor heterogeneity arises from the differentiation of CSCs. The two models are not mutually exclusive. CSC1 have been demonstrated to undergo clonal evolution, acquiring additional alteration such as metastatic potential to become CSC2 (D). Adapted from ⁶.

the cancer stem cell model, tumor heterogeneity is explained by the hierarchical alignment of cells according to their self-renewal and differentiation status²²⁷⁻²³⁰. These two models share the common concept that cancer cells express stem cell properties, although these properties may not be completely acquired in the clonal evolution model. The major difference between the two models is the explanation for tumor heterogeneity. Whereas acquisitions of selective advantageous genetic events are used in the clonal evolution model, stem cell hierarchy is used in the cancer stem cell model. Despite the difference, the two models are not mutually exclusive since CSCs have been demonstrated to undergo clonal evolution²³¹. A common misunderstood concept in the cancer stem cell model is that cancer stem cells must originate from normal stem cells. Emerging evidence suggests that CSCs do not necessarily originate from normal stem cells²³², instead, they can also originate from committed progenitors or differentiated progenies. Therefore, a recent discussion published in *Cell Stem Cell* revised the term cancer stem cell to refer to the cancer cells that fulfill the classic stem cell criteria²³³.

CSCs can be identified by the formation of tumors after serial transplantation into immuno-compromised or immuno-deficient mice. The existence of CSCs was first evidenced in acute myeloid leukemia. Since then, CSCs have been identified from tumors originating from the brain, breast, lung, liver, colon and pancreas²³⁴⁻²⁴⁴. The frequency of CSCs in different populations varies from 0.03%²⁴⁵ to nearly 100%²⁴⁶. The high occurrence of tumorigenic cells can be explained through the clonal evolution model because the majority of cells can acquire tumorigenic properties in this model. Some investigators hypothesize that the low occurrence of tumorigenic cells found in some tumors is due to non-optimal microenvironments for particular tumor types after transplantation⁷. In the identification of CSCs, cell surface markers were used to isolate subsets of cells that were rich with CSCs. These

subsets of cells were not purely CSCs since there was no unique marker for CSCs available at the moment. The cell surface markers used include CD133, CD44, CD24, CD90 and EpCAM²³⁴⁻²⁴⁴ (Table 4.1). Among these markers, CD133 and CD44 could enrich CSCs across various tissue origins while the others show certain degrees of tissue specificity.

In the war against cancer, delayed diagnosis, resistance to chemotherapy or targeted therapy and cancer relapse often result in poor clinical outcomes. The central question in these cases is: are we targeting the right cells (Figure 4.2)? The discovery of CSCs could explain the limitation of current diagnostic method, therapeutic resistance and recurrence. Furthermore, it sheds light on the solutions for these problems and opens up new possibilities for cancer therapy. Currently, most of the tumor markers, such as prostate-specific antigen (PSA) in prostate cancer, are found on differentiated cell types⁵. These types of cells are formed from cancer stem cells during the late stages of carcinogenesis. Therefore, these markers might not reflect earlier steps of carcinogenesis. In these cases, elucidation of gene signatures associated with cancer stem cells would greatly improve the prognosis. Indeed, “stem cell gene” signatures have been recently reported in 10 different types of malignancies^{247,248}. Current chemotherapy agents often target the active proliferation properties of cancer cells. These agents include cell cycle inhibitors and DNA damaging agents which induce apoptosis in actively proliferating cancer cells. However, there is evidence that suggests certain types of cancer stem cells are quiescent and remain dormant in G₀ phase^{249,250}, and are therefore resistant to cell cycle dependent apoptosis. Besides, stem cells often have enhanced DNA repair and anti-apoptotic ability^{251,252}, and hence, CSCs might also be resistant to DNA damaging agents. The anti-apoptotic activities also account for their resistance to cytotoxic chemotherapy agents⁵. Together, these therapeutic strategies would kill

Tumour type	CSC marker	Tumour cells expressing CSC marker, %	Minimal number of cells expressing CSC markers for tumour formation	Injected in Matrigel	Transplantation site	Strain
Breast	CD44 ⁺ /CD24 ^{low}	11-15	200	+	Mammary fat pad	NOD-SCID
Breast	CD44 ⁺ /CD24	ND	2×10^4	-	Mammary fat pad	NOD-SCID
Breast	ALDH1 ⁺	9-10	500	++	Mammary fat pad	NOD-SCID
Brain	CD133 ⁺ /CD133 ⁺ /CD133 ⁺ (VIB)	17-20 0-23	10 ⁵ 100	-	Brain Cerebrum	129/SVJ 129/SVJ
Brain	CD133 ⁺	2-3	500	-	Brain	nu/nu
Colon	CD133 ⁺	0.8-25	200	+	Kidney capsule	NOD-SCID
Colon	CD133 ⁺	0.7-6	3×10^4	-	Subcutaneous	SCID
Colon	EpCAM ⁺ /CD44 ⁺	0.03-38	200	+	Subcutaneous	NOD-SCID
Head and neck	CD44 ⁺	0.1-42	5×10^4	+	Subcutaneous	Rag2 ^{fl} /DKO, NOD-SCID
Pancreas	CD44 ⁺ /CD24 ^{low} /ESA ⁺	0.2-0.8	100	+	Pancreas	NOD-SCID
Pancreas	CD133 ⁺	1-3	500	-	Pancreas	NMRI-nu/nu
Lung	CD133 ⁺	0.32-22	10 ⁵	-	Subcutaneous	SCID
Liver	CD90 ⁺	0.03-6	5×10^4	-	Liver	SCID/Beige
Melanoma	ABCBS ⁺	1.6-20	10 ⁶	-	Subcutaneous	NOD-SCID
Mesenchymal	Side population (Hoechst dye)	0.07-10	100	-	Subcutaneous	NOD-SCID

Table 4.1| CSC markers used in various cancer. Various surface markers have been used to isolate or enrich cancer stem cells. Among these, CD133 and CD44 are the two most commonly used markers. Adapted from ⁶.

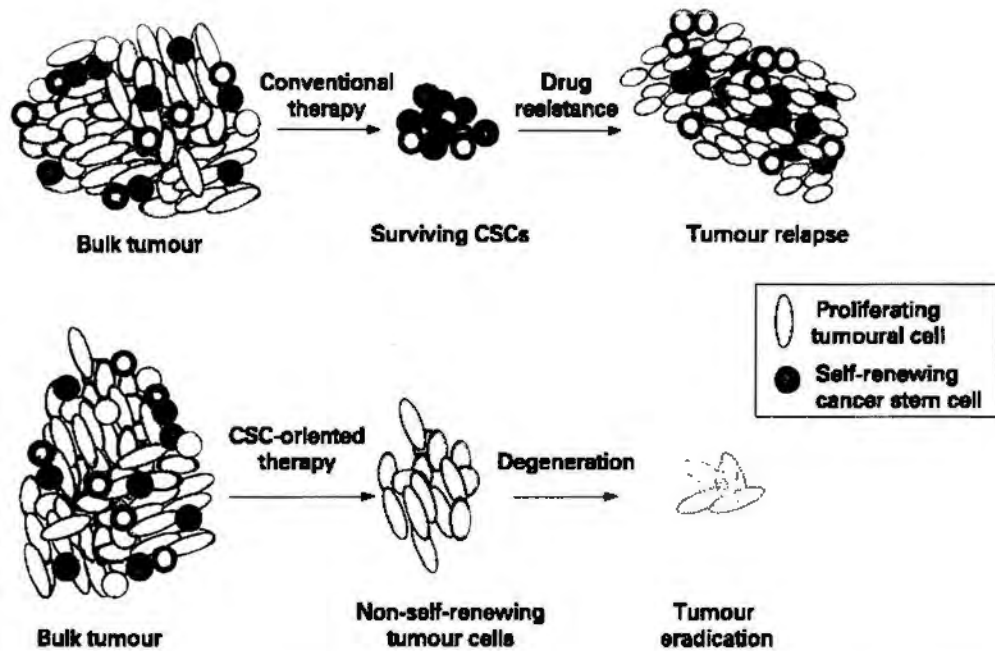


Figure 4.2| Comparison between conventional cancer therapy and CSC targeted therapy. Conventional cancer therapy targets tumor cells at low hierarchy. The survived CSCs regenerate and cause tumor relapse. In CSC targeted therapy, termination of CSCs would leave behind a non-self-renewing tumor population that is not tumorigenic, hence, cancer could be cured. Adapted from ²⁵³.

flimsy differentiated progeny from CSCs but not the CSCs themselves. This would lead to the degeneration of tumors and transient clinical improvements, however, survived CSCs would lead to the relapse of the tumor. In these cases, selectively targeting CSCs but not normal stem cells would be a more efficient method to treat cancer. Emerging therapeutic strategies include: 1. antibody based therapy which target CSCs specific surface antigen for targeted therapy; 2. inhibition of stem cell signaling such as Notch and Hedgehog cascades; and 3. differentiation therapy which attenuate tumor forming ability of CSCs through enforced differentiation^{5,6,223}.

4.1.2 Properties of cancer stem cells

Since cancer stem cells are defined as cancer cells that fulfill the classic stem cell criteria²³³, CSCs share various properties with normal tissue stem cells. These properties include the ability to self-renew, the ability to differentiate, the ability to migrate and metastasize. On top of these properties, CSCs also have the ability to form tumors i.e. tumorigenicity^{5,233}. Self-renewal in CSCs and normal stem cells represent their ability to proliferate and divide into daughter cells which sustain stem cell identity. Differentiation in CSCs and normal stem cells represent the ability to form multi-lineage cells found in the tissues. A classical example is the hematopoietic stem cell system in which the stem cell is able to differentiate into leukocytes, erythrocytes and thrombocytes²⁵⁴. Homeostasis of self-renewal and differentiation in normal stem cells is achieved by asymmetric division (Section 2.1.4). It is still unknown whether CSCs adhere to this homeostasis. Interestingly, asymmetric division has been postulated as a path for CSCs formation^{81,115,227}. Migration properties confer to normal stem cells the ability to migrate to regions that require cell generation or replacement such as wounds. Migration and metastasis of CSCs allows the tumor to invade the adjacent region within the primary site or

voyage through the circulating system and/or lymphatic system to the secondary site⁵ where they show the fourth property, the ability to initiate the formation of new tumors.

At the moment, research on CSCs mainly focuses on subsets of cells which express CSCs markers in primary tumors. However, the availability of these primary CSCs are limited due to the limited number of clinical samples and low occurrence frequency of CSCs in certain tumor types. Recently, argument that cancer cell lines could be used as alternative models of cancer stems cells has arisen^{255,256}. During the establishment of cancer cell lines, primary tumors were dissociated and tumor cells were plated on culture dishes. After at least 30 passages, only small subsets of cells within the primary tumor showed immortality. These cells were established into cell lines while others cells were not able to go through crisis. The molecular profiles of these cell lines were remarkably different from *in vivo* tumors probably due to the low occurrence frequency of CSCs in *in vivo* tumors. However, these cell lines do show similar CSC phenotypes such as indefinite growth through self-renewal (immortality), the ability to differentiate and tumor formation²⁵⁵. In support of this argument, CSC-like cells have been identified in various cancer lines originating from mammary, breast, liver and nasopharyngeal cancers²⁵⁷⁻²⁶⁰.

4.1.3 Signaling involved in cancer stem cell

As discussed earlier, initiation of tumor formation by CSCs involve self-renewal and differentiation. Similarly, these two processes are also important in normal stem cell functions. Therefore, it is reasonable to speculate that CSCs and normal stem cell systems share some molecular mechanisms underlying self-renewal and differentiation. The proposed signaling pathways regulating self-renewal and differentiation in CSCs include Sonic Hedgehog (Shh), Wnt/ β catenin, Notch and

Bmi-1 cascade. Besides, regulators for cellular responses to DNA damage such as PTEN and INK4A and regulators for genomic integrity such as telomerase have also been proposed as alternative mechanisms^{6,261,262}. These pathways have been proved to be involved in regulating the self-renewal and differentiation of normal stem cells. In addition, key players in these pathways have been found to be mutated or mis-regulated in various cancers. Their roles have been implicated in tumor growth, migration, metastasis and maintenance *in vivo*²⁶³⁻²⁶⁵. However, the precise pathways activated in CSCs remains to be determined^{6,262}.

Regarding the signaling pathways in CSCs, several key concepts have emerged recently¹¹³. First, since the function of CSCs involve the homeostasis of self-renewal and differentiation, it is important to consider the coordination and crosstalk between different pathways, for example promoting self-renewal versus inhibiting differentiation and *vice versa*. Second, signaling pathways involved in the molecular control of CSCs are not simply switched on or off. Instead, they are fine-tuned with thresholds to achieve a desired set point¹¹³. An excellent example in normal stem cell counterparts is the morphogen gradient, which is set up during development. Third, pathways involved in regulation of CSCs by the stem cell niche should be considered. As discussed earlier, the niche determines the fate of stem cells (Section 3.1.2). There is increasing evidence suggesting the existence of CSC niches which might regulate the formation, maintenance and metastasis of CSCs²⁶⁶. Therefore, it is important to consider regulations from the niche as well when elucidating the signaling pathways involved in CSCs.

4.1.4 Colon cancer stem cell

Colon cancer is one of the most common cancers in developed countries²⁶⁷. Although the tumorigenesis initiates locally, tumor cells often migrate to secondary

sites such as the liver causing death^{268,269}. CSCs have been identified in colon cancer simultaneously by two independent research groups using CD133 as CSCs surface markers^{238,239}. Later reports demonstrated that CD133⁺ was not restricted to stem cells and both CD133⁺ and CD133⁻ population are able to initiate tumor formation²⁷⁰. So subsequent studies on colon CSCs used CD44, which is functionally important for colon CSCs²⁷¹, in combination with CD133 or other markers such as CD24, EpCAM and Lgr5 for enrichment of colon CSCs^{240,272-274}.

Although the origin of tumors in many tissues is still a topic of debate, the “cell-of-origin” in intestinal cancer has been proposed to localize in the stem cell population of colonic crypt²⁷⁵. Supporting evidence for this proposal is that colonic tumors take years to develop while the turnover of colonocytes usually cycle within days. Therefore, stem cell populations may have a higher chance to accumulate mutations and initiate tumor²⁷³. Moreover, expression of CD133 is observed in normal crypt stem cells. The increment in number of CD133⁺ cells in colon cancer sample further indicates their colonic crypt stem cells origin²⁵³. Furthermore, the crypt stem cells has been beautifully demonstrated as the “cell-of-origin” in intestinal cancer using transgenic mice model where mouse homolog of adenomatous polyposis coli (*Apc*) was conditionally knocked out in crypt stem cells²⁷⁶. Together with the existence of CSCs in colon cancer, it is reasonable to hypothesize that colon CSCs originate from colonic crypt stem cells. However, arguments have been raised claiming that committed precursor cells could also be the “cell-of-origin”²⁷⁵. Further experiments are required in order to clarify these hypotheses.

As discussed earlier, CSCs and their normal stem cell counterparts might share similar signaling pathways. Therefore, reviewing the signaling pathways involved in normal crypt stem cells may provide clues to signaling in CSCs. In the human intestine, epithelial renewal is supported by crypt stem cells. These stem cells divide

asymmetrically in order to maintain homeostasis²⁷⁷. Upon asymmetric division, the daughter cells commit to two lineages, the absorptive and the secretory lineage (Figure 4.3). Progeny in the absorptive lineage will ultimately form enterocytes while progeny in the secretory lineage will form three different cell types: enteroendocrine cells, goblet cells and Paneth cells. Wnt signaling promotes the proliferation/self-renewal of stem cells and/or transit amplifying cells. The proliferative effects of Wnt signaling have been linked to cell cycle regulator c-Myc²⁷⁸, cyclin D1^{279,280} and possibly D2^{277,281}. Wnt signaling may also promote differentiation; however, supporting experimental data has not been published²⁷⁷. Alternatively, the differentiation of crypt stem cells and/or transit amplifying cells might be regulated by Wnt counteracting pathways, TGF- β and BMPs cascades. TGF- β shows a strong cytostatic response in intestinal culture *in vitro*²⁸² while BMP inhibits intestinal stem cells renewal *in vivo*²⁸³. These suggested that the counteracting role of TGF- β and BMP against Wnt cascade. Since BMP also belongs to the TGF- β superfamily, they share the intracellular messenger SMADs proteins. There are three subclasses of SMADs protein: Receptor-regulated SMADs (SMAD1, 2, 3, 5, and 8), common SMAD (SMAD4) and inhibitory SMAD (SMAD 6 and 7). Upon stimulation, receptor-regulated SMADs are phosphorylated and associate with common SMAD. The complex then translocates into the nucleus where it regulates transcription²⁸². Other signaling such as Notch and Hedgehog pathways are not reviewed here. However, these pathways also take part in the regulation of normal crypt stem cells.

Although the above signaling pathways have been demonstrated in the regulation of normal crypt stem cells system, their roles in colon cancer stem cells remain to be elucidated.

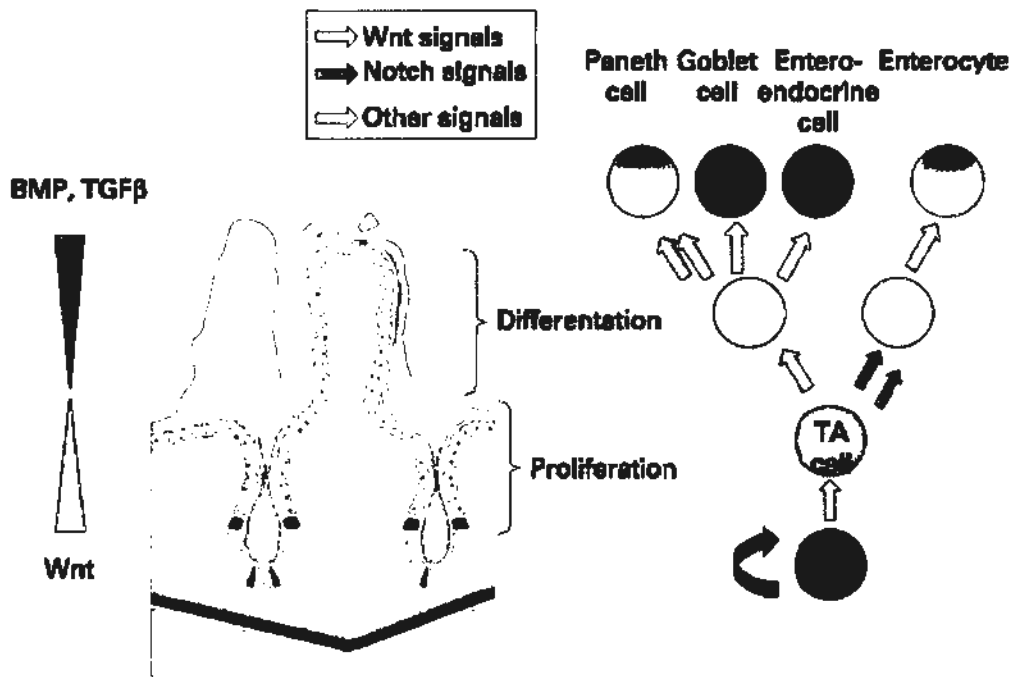


Figure 4.3| Cell hierarchy in colon stem cells. Asymmetric division of stem cells drive the differentiation process. Progeny differentiate into the secretory and the adsorptive lineages. Progeny in adsorptive lineage will form the enterocyte while progeny in the secretory lineage will form enteroendocrine cell, goblet cells and Paneth cells. Wnt signaling promotes the proliferation/self-renewal of stem cells whereas the TGFβ superfamily signaling promotes the differentiation. Adapted from ²⁵³.

4.1.5 Aim

Previous studies have demonstrated that *Stk31* is a cell fate determinant in GSCs (Chapter 3). *STK31* is reactivated in multiple cancers and the expression in Caco2 exhibits heterogeneity (Chapter 2). Therefore, we hypothesize that *STK31* regulates the cell fate in CSCs through regulating the self-renewal and differentiation. The homeostasis between these cell fates determines the “stemness” of CSCs. The specific aims of this chapter were: first, to determine the function of *STK31* in colon cancer; and second, to determine the underlying mechanisms of *STK31* functions in cancer cells.

4.2 Materials and methods

4.2.1 miR RNAi against *STK31*

microRNA mimics against human homologs of *STK31* were designed by RNAi designer online (Invitrogen). Pairs of designed oligos (Appendix) were annealed and cloned into pcDNATM6.2-GW/EmGFP-miR vector (Invitrogen). Two to three separate designs were used to target *STK31*, design against LacZ were used as control. Plasmids DNA were prepared using Mini Plus or Midi Plus Plasmid DNA Extraction Kit (Viogene). Sequence of miR RNAi designs were proof read by DNA sequencing (Tech Dragon HK Ltd).

The efficiency of miR RNAi knock down were determined by co-transfecting *STK31* expression vectors and *STK31* miR RNAi vectors into HEK293 cells followed by western blot analysis.

4.2.2 Cell culture and transfection

Caco2 cells and HEK293 cells were maintained as described (Section 2.2.8).

HEK293 cells were transfected with 2.5 ug DNA and 6ul Lipofectamine 2000

reagent (Invitrogen). For overexpression experiments, 2.5µg overexpression vector were used. For knock down experiments, a mixture of 1.5µg overexpression vector and 1.5µg miR RNAi vector were used. In order to obtain maximum transfection efficiency, 8×10^5 HEK293 cells were seed onto 35 mm culture dish with DNA:liposome complex pre-loaded in medium. For overexpression and knock down experiments, cells were collected 48 hours post-transfection for western blot analysis.

Caco2 cells were transfected using 2µg vector and 4µl Lipofectamine 2000 reagent (Invitrogen). In order to obtain maximum transfection efficiency, 5×10^5 Caco2 cells were seed onto 35 mm culture dish with DNA:liposome complex pre-loaded in medium. Stable transfectant were selected with 8µg/ml Blasticidin and maintained in 5µg/ml Blasticidin containing medium.

4.2.3 Western blot

Western blot for HEK293 cells and Caco2 stable transfectant were performed as described in section 2.2.4.

4.2.4 Contact inhibition assay

Stable transfectant were seeded onto 6 well plate at three confluences, 1×10^5 cells/well; 3×10^5 cells; and 6×10^5 cells/well. 48 hours after seeding, cells morphology at sub-confluence, confluence and post-confluence were recorded by inverted microscope (Nikon).

For flow cytometry analysis, cells at different confluence were collected by trypsin followed by three times wash in 1x PBS. Cells were fixed in chilled 70% ethanol for 30 minutes at 4°C. DNA ploidy were stained with Propidium Iodide solution (20ug/ml Propidium Iodide; and 10ug/ml RNase A)(Sigma) at 37°C for 30

mins followed by analysis in CALIBUR flow cytometer (Beckman Dickson). Cell cycle and apoptosis profiles were analyzed by FCS express software (De Novo Software).

4.2.5 Proliferation assay

Cell proliferations were determined by direct cell counting and Cell Titre96[®] AQueous Cell Proliferation assay kit (Promega).

For cell counting experiment, stable transfectant were seeded onto 24 well plate 1 day before counting at a density of 5×10^4 cells/well. Single cell suspensions were obtained by trypsin treatment and cell viability were determined by Trypan blue stain (Sigma). Viable cells were counted from day 1 to day 7.

For MTS proliferation assay, stable transfectant were seeded onto 96 well plate 1 day before experiment at a density of 5×10^3 cell/well. On each time point, 20 μ l MTS reagent were added to each well containing 100 μ l medium followed by incubation at 37°C for 2 hours. Cell proliferations were reflected by optical density of MTS reagent at 490nm. Data were recorded from day 1 to day 7.

4.2.6 Migration assay

Stable transfectant were seeded onto 6 well plates at a density of 3×10^5 cells/well. V-shape plastic rods were placed in each well to make a “cell-free channel”. 72 hours after seeding, the plastic rods were removed followed by two times wash in DMEM free medium. Cells were incubated in DMEM free medium and migrations to “cell-free channel” were recorded by Time Lapse Imaging System (CarlZwiss) at 6 hour interval for 96 hours. Cell migrations were determined by measuring distances between parallel lines from initial sites to migrated sites.

4.2.7 Attachment assay

96 well plate were pre-coated with 20ug/ml laminin (BD Bioscience), 0.1% gelatin (Sigma), 10ug/ml fibronectin (Biosource); 25ug/ml poly-L-lysine (Sigma); and matrigel (1:8; BD Falcon) at 4°C overnight. 5×10^4 cells/well were seed and allowed to attach for 1 hr or 2 hr. Unattached cells were washed off with 100µl DMEM free medium. Numbers of attached cells were determined by Cell Titre96® AQueous Cell Proliferation assay kit (Promega) as described in section 4.2.4.

4.2.8 Enterocytic differentiation assay

Stable transfectant were seeded onto 24 well plates at a density of 6×10^4 cells/well. After confluences were reached, medium was changed to DMEM free medium. Medium was changed twice a week and cell morphology was recorded 5 – 14 days post-confluence. Dome and cyst structure, which were morphological features of enterocytic differentiation, were observed and captured under inverted microscope.

4.2.9 Colony formation assay

Base agar (0.5% Agar; DMEM supplemented with 10% FBS and 1% P/S) were prepared by mixing pre-warmed (40°C) DMEM medium with 1% agar at 1:1 (v/v) ratio. 1.5 ml base agar was solidified per 35 mm dish. Top agar (0.35% Agar; DMEM supplemented with 10% FBS and 1% P/S) were prepared by mixing pre-warmed (40°C) DMEM medium with 0.7% agar at 1:1 (v/v) ratio.

Stable transfectants were mixed with top agar before seeding at a density of 3.3×10^3 cell/ml. 1.5 ml cell-containing top agar was solidified and covered with DMEM medium. Medium was changed twice every week. Colonies were visualized and counted two to three weeks after seeding by staining with 0.005% crystal violet

(Sigma) solution for 1 hour.

4.2.10 Human whole genome microarray

RNA from stable transfectant was extracted using TRIzol reagent (Invitrogen). RNA was dissolved in DNase/RNase free ddH₂O. RNA concentrations were measured by Nanovue Spectrophotometer (GE Healthcare).

RNA was labelled and hybridized onto Agilent Whole Genome Oligo Microarray 44K (G4112F, Two colored with dye swapped, Agilent Technologies)(Core Facilities, Li Ka Shing Institute of Health Sciences, The Chinese University of Hong Kong). Data were analyzed by GeneSpring GX10 software (Agilent Technologies).

4.2.11 Real-time PCR

Reverse transcription were performed as described in section 3.2.8 except that 5µg RNA was used. Primers were designed by qPrimerDepot²⁸⁴. Primers used in this study were KIT, SMAD1Realtime PCR were amplified using Power SYBR[®] Green PCR Master Mix (Appendix) and analyzed by 7500 software v2.0.1 using comparative $\Delta\Delta\text{Ct}$ method (Applied Biosystems).

4.2.12 Tumorigenicity assay

Nude and NOD/SCID mice were purchased from LASEC, CUHK. Stable transfectant were collected by trypsin treatment followed by three times wash in 1X PBS. Cells were resuspended in DMEM free medium to a density of 1×10^7 for nude mice injection and 5×10^7 cells/ml for SCID mice injection. 1×10^6 cells or 5×10^6 cells were injected subcutaneously into nude and SCID mice respectively. Mice were housed for 12 – 16 weeks for nude mice experiment and 8 – 10 weeks for SCID mice

experiment. Solid tumor formation was recorded. All procedures were approved by Animal Ethics Committee, CUHK (AEEC Number: 06/049/MIS).

4.2.13 Statistical analysis

Statistical analyses were performed by Prizm 3.0 software. Results were presented by mean \pm S.E.M.. Groups of data were compared by student *t*-test or One-way ANOVA analysis. *p* value <0.05 was considered statistically significant.

4.3 Results

4.3.1 Generation of *STK31* stable knock-down Caco2 cells

Functional genomic studies rely on gain-of-function and loss-of-function models. To prepare for the functional studies of *STK31*, overexpression and RNAi clones for *STK31* were made.

For the human homolog, a vector of *STK31* ORF under the control of CMV promoter was purchased (Genecopoeia) and transfected to HEK293 cells. Whole cell lysates were then used for western blot analysis. The result showed that *STK31* protein with a molecular weight of 115kDa was detected in *STK31* transfected lysate but not in vector control lysate (Figure 4.4). This indicated that the *STK31* clone could be overexpressed in HEK293 cells. Next, the miR RNAi was designed and cloned to be expressed with GFP, in a co-cistronic manner, under the control of CMV promoter. The RNAi vectors were then co-transfected with overexpression vector and the lysates were again used for western blot analysis. The result showed that all three RNAi designs could knock down *STK31* overexpression with different efficiency when compared with LacZ RNAi control (Figure 4.4). Design 2 and 453 were the most effective designs and were used for the generation of *STK31* stable knock down cell lines.

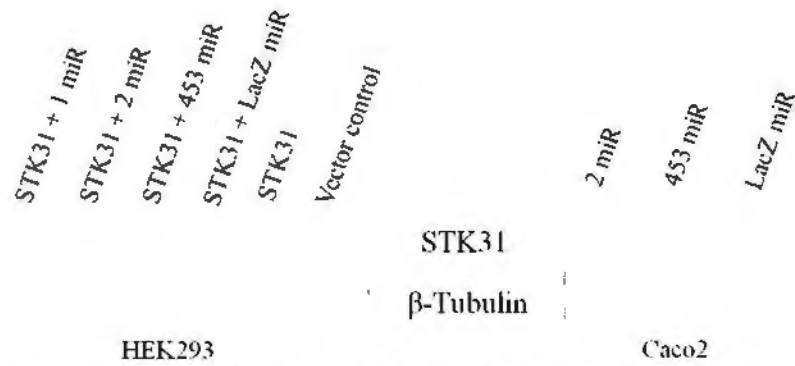


Figure 4.4| Overexpression and knock down of *STK31* in HEK293 cells and Caco2 cells. Overexpression and knock down of *STK31* in HEK293 cells and knock down of endogenous expression of *STK31* in Caco2 cells were analyzed by western blot analysis. Whole cell lysate were probed with anti-*STK31* antibody (Top panel). β tubulin was used as loading control (Bottom panel). Both miR RNAi design 2 and 453 efficiently knock down overexpressed and endogenous *STK31* when compared to LacZ control.

To study the function of *STK31* in cancer, a colorectal adenocarcinoma cell line Caco2 was used for the following reasons. First, *Stk31* is expressed in the transition state between undifferentiated to differentiating spermatogonia in mouse testis (Section 2), therefore it is possible that it may take part in cancer stem cells functions. CD133 and CD44, both of which are well-characterized colon cancer stem cells markers, are expressed in Caco2 cells^{272,285}; Second, *STK31* has been reported to be reactivated in gastrointestinal cancer²⁷; and lastly, Caco2 was shown to have strong *STK31* expression (Section 2.3.5).

Caco2 cells were transfected with effective RNAi against *STK31* and stable transfectant were selected with antibiotics. The knock down efficiencies were confirmed by western blot and the result showed that design 2 (designated Caco2^{miR 2}) could effectively knock down the endogenous expression while design 453 (designated Caco2^{miR 453}) could completely abolish the endogenous expression when compared to LacZ RNAi control (designated Caco2^{LacZ}) (Figure 4.4). After the establishment of stable knock-down cell line, various properties of CSCs including self-renewal or proliferation, migration, differentiation and tumorigenicity were studied.

4.3.2 Knock-down of *STK31* decreases cell proliferation in confluent culture

Since *STK31* was shown to be reactivated in cancers, it might take part in oncogenic activities such as enhancing cell proliferations of cancer or self-renewal of cancer stem cells. In these experiments, proliferations of stable knock-down cell lines were studied by cell counting and MTS assay. Same numbers of stable transfectants were seeded into 24 well plates or 96 well plates respectively. Cell proliferations were recorded from day 1 to day 7 after seeding.

In cell counting experiment, during the sub-confluent period (day 1 – 3), no

significant difference was observed among the three lines. Upon reaching confluence (day 4), growth of Caco2^{miR 453} began to decrease. Significant decrease was observed in Caco2^{miR 453} ($p < 0.05$) from the first day of post-confluent culture (day 5) and the rate of proliferation in Caco2^{miR 453} further decreased on day 6 ($p < 0.001$) and 7 ($p < 0.01$) when compared to Caco2^{LacZ} control. On the other hand, significant decrease on proliferation of Caco2^{miR 2} line was found only on day 6 and 7 ($p < 0.05$) when compared to Caco2^{LacZ} control (Figure 4.5A).

In MTS assay, consistent with the cell counting results, no significant difference was observed among the three lines on day 1 – 4 after seeding. Starting from day 5, Caco2^{miR 2} and Caco2^{miR 453} showed significant decrease in rate of proliferation ($p < 0.001$ and $p < 0.01$ respectively). The decrease persisted in Caco2^{miR 453} on day 6 ($p < 0.001$) and Caco2^{miR 2} on day 6 and 7 ($p < 0.001$ and $p < 0.01$ respectively) (Figure 4.5B).

From the results, we found that knock-down of *STK31* in Caco2 cells results in decrease in proliferation rate and that the decrease was only observed after the cultures reached confluence, no significant differences were observed in sub-confluent cultures. More importantly, as reflected by the cell counting experiments, the decreases in proliferation were dependent on the *STK31* expression level.

4.3.3 Knock-down of *STK31* reactivates contact inhibition

The cell cycle of normal cells, upon reaching confluence, is arrested. This phenomenon is described as contact inhibition^{286,287}. Loss of contact inhibition is a hallmark property obtained by transformed cells during transformation^{288,289}. The contact inhibition of Caco2, a transformed cell line, was lost and grew into multiple layers after reaching confluence²⁹⁰. To study if the decreases in proliferation in

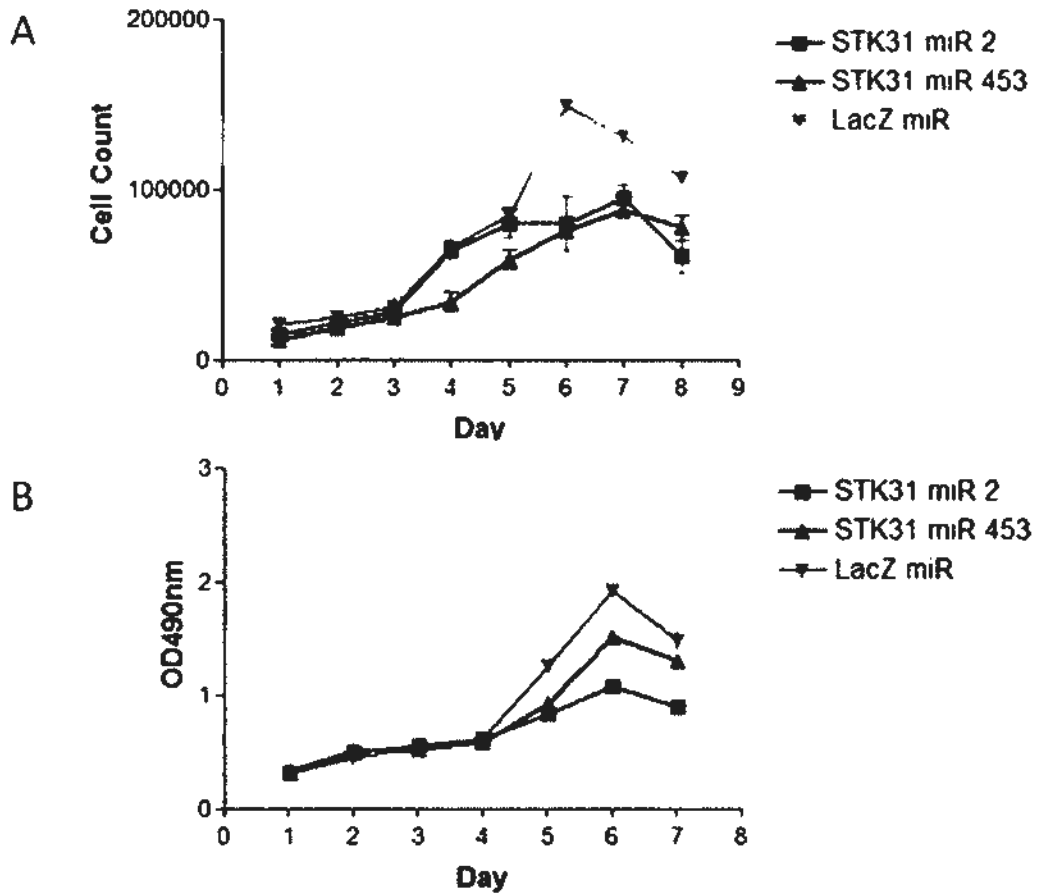


Figure 4.5| Proliferation studies of *STK31* knock down Caco2 cells. Proliferation of *STK31* knock-down Caco2 cells were studied by cell counting (A) and MTS assay (B). No significant differences were obtained in sub-confluent culture (day 1 – 4). After reaching confluence, *STK31* knock-down Caco2 cells showed decrease in proliferation compared to LacZ control. (Data were presented by mean \pm S.E.M.; Significance were calculated by t-test * $p < 0.05$; ** $p < 0.01$; *** $p < 0.001$)

STK31 knock-down cells were due to the reactivation of contact inhibition, cell morphologies were recorded in cultures of different confluences. In this experiment, same number of Caco2 stable transfectant were seeded into 6 well plate and cell morphology were recorded at different confluences.

The results showed that Caco2 cells exhibited normal epithelial morphology, no significant difference in growing properties were found among three lines in sub-confluent condition (Figure 4.6). However, after reaching confluence, the growth of Caco2^{miR 453} arrested as indicated by the 2D monolayer of cells. In contrast, Caco2^{LacZ} continued to grow, forming multiple layers of cells. The growth of Caco2^{miR 2} lied between the Caco2^{miR 453} and Caco2^{LacZ}, which also showed multiple layers formation but significantly less than Caco2^{LacZ} group (Figure 4.6). It was interesting to note that cells that grew into multiple layers were significantly smaller than cells that grew in monolayer (Figure 4.6). These data demonstrated that knock-down of *STK31* results in reactivation of contact inhibition and the degrees of reactivations were dependent on the expression level of *STK31*. Therefore, *STK31* would be responsible for inactivating the contact inhibition in Caco2 cells.

4.3.4 Knock-down of *STK31* causes G1/S arrest upon confluence

Decrease in proliferation could be resulted from cell cycle arrest²⁹¹. On the other hand, contact inhibition could also cause cell cycle arrest at G1/S phase²⁹². To further elucidate the results from proliferation and contact inhibition studies, the cell cycle profiles of *STK31* knock-down cells were analyzed by flow cytometry. In this experiment, cells were seeded at three densities and collected at sub-confluent, confluent and post-confluent. DNA ploidy were stained by propidium iodide and analyzed by flow cytometer.

The results showed that as the Caco2^{LacZ} cells started to grow from

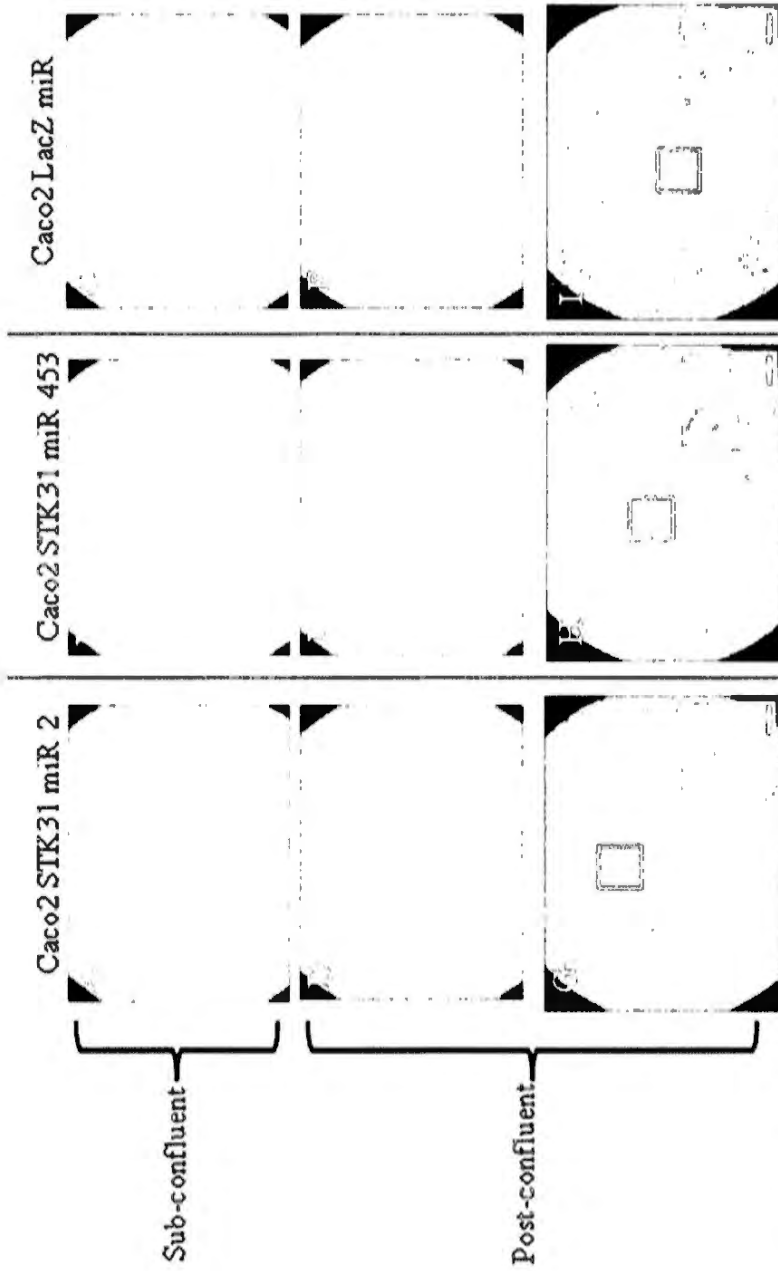


Figure 4.6] Morphologies of *STK31* knock down cells under different confluence. Morphologies of *Caco2*^{miR 2} (Left panel), *Caco2*^{miR 453} (Middle panel) and *Caco2*^{LacZ} (Right panel) cells were recorded at sub-confluence (A – C) and post-confluence (D – I). No observable differences were found among three groups at sub-confluence. In post-confluence stage, *Caco2*^{LacZ} grew into multiple layers while *Caco2*^{miR 453} remained in a monolayer due to reactivation of contact inhibition. Significant decrease in the multiple layers of cells was observed in *Caco2*^{miR 2}. *Caco2*^{LacZ} cells were significantly smaller in multi-layered cells (G – I) (Inset). Magnification 100x (A – F), 200x (G – I).

sub-confluent to confluent stage, the percentage of cells at G1 phase increased from 38% to 48%. In post-confluent environment, the G1 population further increased from 48% to 54% (Figure 4.7). These results were consistent with previous report that contact inhibition would cause cell cycle arrest of Caco2 cells in G1 phase²⁹². The cell cycle profile in sub-confluent Caco2^{miR 453} and Caco2^{miR 2} were similar to Caco2^{LacZ} control (Figure 4.7). However, upon reaching confluence, the population of Caco2^{miR 453} cells shifted from S phase to G1 phase where G1 population of cells increased from 39% to 54% while S population decreased from 27% to 16%. The G1 population was significantly higher while the S phase population was significantly lower than that in Caco2^{LacZ} control (48% G1 population; 23% S population) ($p < 0.01$ and $p < 0.001$ respectively). The cell cycle profile did not show significant difference in Caco2^{miR 2} group in confluent situation (Figure 4.7). In post-confluent situations, Caco2^{miR 453} showed significant G1 arrest (64% G1 population) when compared to Caco2^{LacZ} control (54% G1 population) ($p < 0.001$). Meanwhile, the population of S phase and G2/M phase significantly decreased ($p < 0.01$ and $p < 0.05$ respectively). On the other hand, Caco2^{miR 2} also had the trend to increase in G1 population while S phase population was also significantly decreased ($p < 0.05$) (Figure 4.7). These results demonstrated that knock-down of *STK31* would cause G1 arrest in post-confluent condition.

Together, these observations indicate that *STK31* promote proliferation of Caco2 cells after confluent through inactivating/by passing the contact inhibition resulting in G1 cell cycle arrest.

4.3.5 Knock-down of *STK31* enhances binding to ECM

The second property of cancer stem cells is the ability to migrate from one site to the other. This process involves several steps including detachment from ECM,

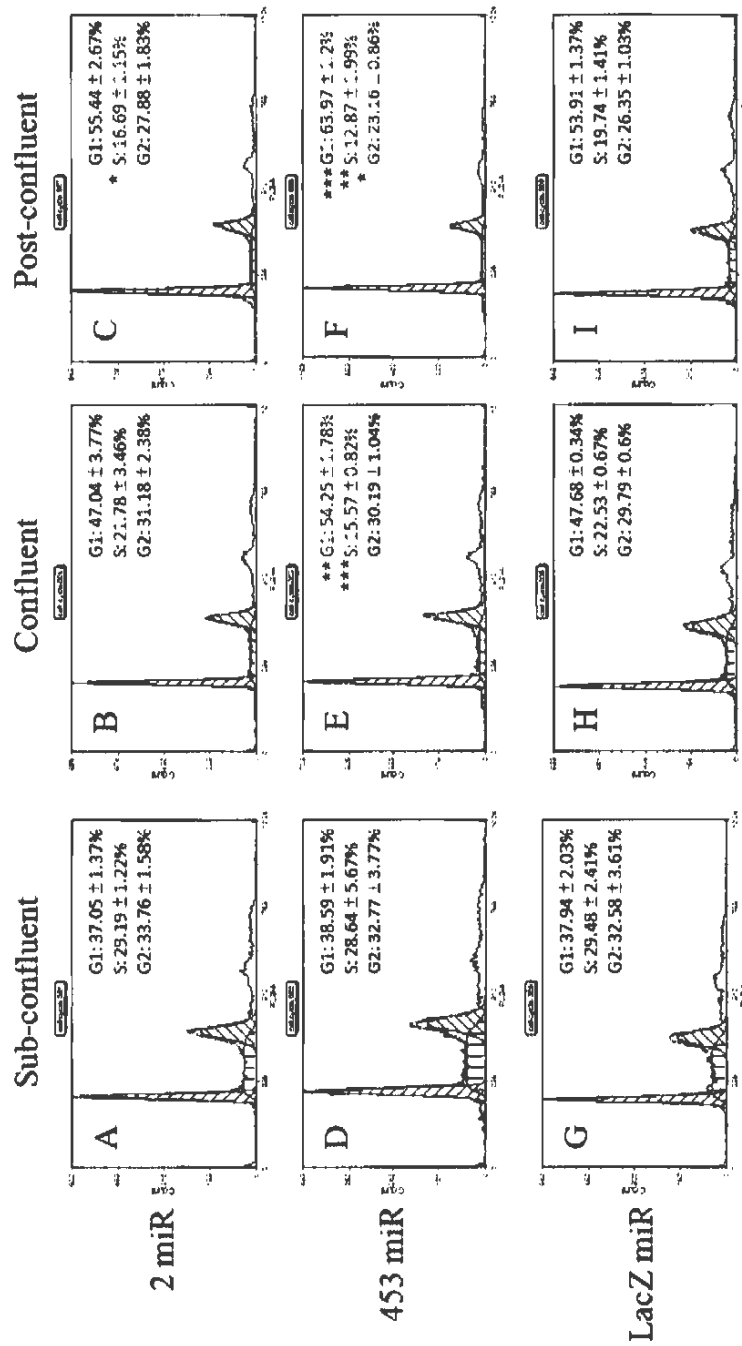


Figure 4.7] Cell cycle profile of *STK31* knock-down cells under different confluences. Cells were seeded in three different confluences 2 days before FACs analysis. DNA ploidys were stained with PI. DNA profiles were shown in Figure A – I. No significant differences were observed in sub-confluence condition (Left panel, A, D, and G). Upon reaching confluence, the proportion of G1 population increased in all groups (Middle panel, B, E, and H). However, the degree of increase was significantly higher in the *Caco2*^{miR453} group. In post-confluent conditions, the proportion of G1 arrested cells was significantly higher in *Caco2*^{miR453} than *Caco2*^{LacZ} (Right panel, C, F, and I). (Data were presented by mean ± S.D.; Significance were calculated by t-test * $p < 0.05$; ** $p < 0.01$; *** $p < 0.001$)

entry of circulating system, invasion into secondary site and attachment to microenvironment of new site^{293,294}. In the following experiments, the effects of *STK31* knock-down on binding affinities to ECM were studied by attachment assay. In these experiments, 96 well plates were coated with purified ECM matrigel or component of the ECM including laminin, gelatin or fibronectin. Poly-L-lysine was used as positive control. Cells were allowed to attach for 1–2 hrs and the number of attached cells were measured by MTS assay.

The results showed that *Caco2*^{miR 453} and *Caco2*^{miR 2} had significantly higher binding affinities to matrigel than *Caco2*^{LacZ} control ($p < 0.001$). Furthermore, *Caco2*^{miR 453} had significantly higher binding affinities to laminin ($p < 0.001$), gelatin ($p < 0.001$) and fibronectin ($p < 0.05$) which were components of the ECM (Figure 4.8). It was interesting to note that *Caco2*^{miR 2} and *Caco2*^{miR 453} had higher binding affinities to poly-L-lysine ($p < 0.05$) when compared to *Caco2*^{LacZ} control. These results indicate that knock-down of *STK31* results in stronger binding to ECM and hence less tendency to migrate.

4.3.6 Knock-down of *STK31* decreases cell migration

To study whether enhanced ECM binding affinities resulted in decreased migration ability, cell migration assays were carried out. Same numbers of cells were seeded onto 6 well plates with the introduction of “cell-free channel”, upon reaching confluence, cell migration in the “cell-free channel” were recorded by calculating the migrated distances.

The results showed that *Caco2*^{miR 453} had a significantly lower cell migration when compared to *Caco2*^{LacZ} control (Figure 4.9) and that the cell migration decreased from 4.74 μ m to 3.07 μ m ($p < 0.01$). The migration of *Caco2*^{miR 2} also decreased from 4.74 μ m to 4.63 μ m.

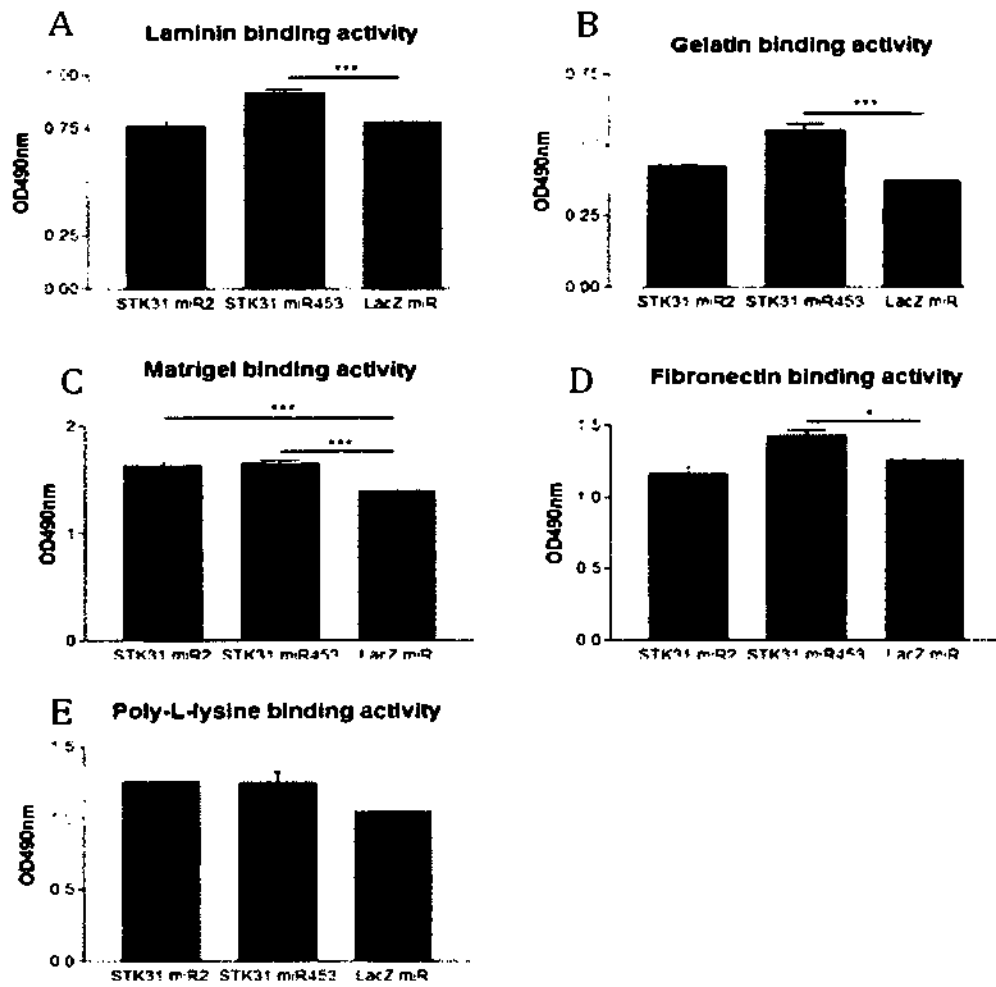


Figure 4.8| Attachment assay of *STK31* knock-down cells. Same numbers of cells were allowed to attach to various ECM components. Numbers of attached cells were determined by MTS assay. Binding affinities to various ECM components were shown in Figure A – D. Poly-L-lysine was used as positive control (E). Binding affinities to Matrigel were significantly higher in *STK31* knock-down cells (C). *Caco2^{miR 453}* attached more readily to laminin (A), gelatin (B) and fibronectin (D) when compared to *Caco2^{LacZ}* control. (Data were presented by mean \pm S.E.M.; Significance were calculated by One way ANOVA:Turkey test * $p < 0.05$; *** $p < 0.001$)

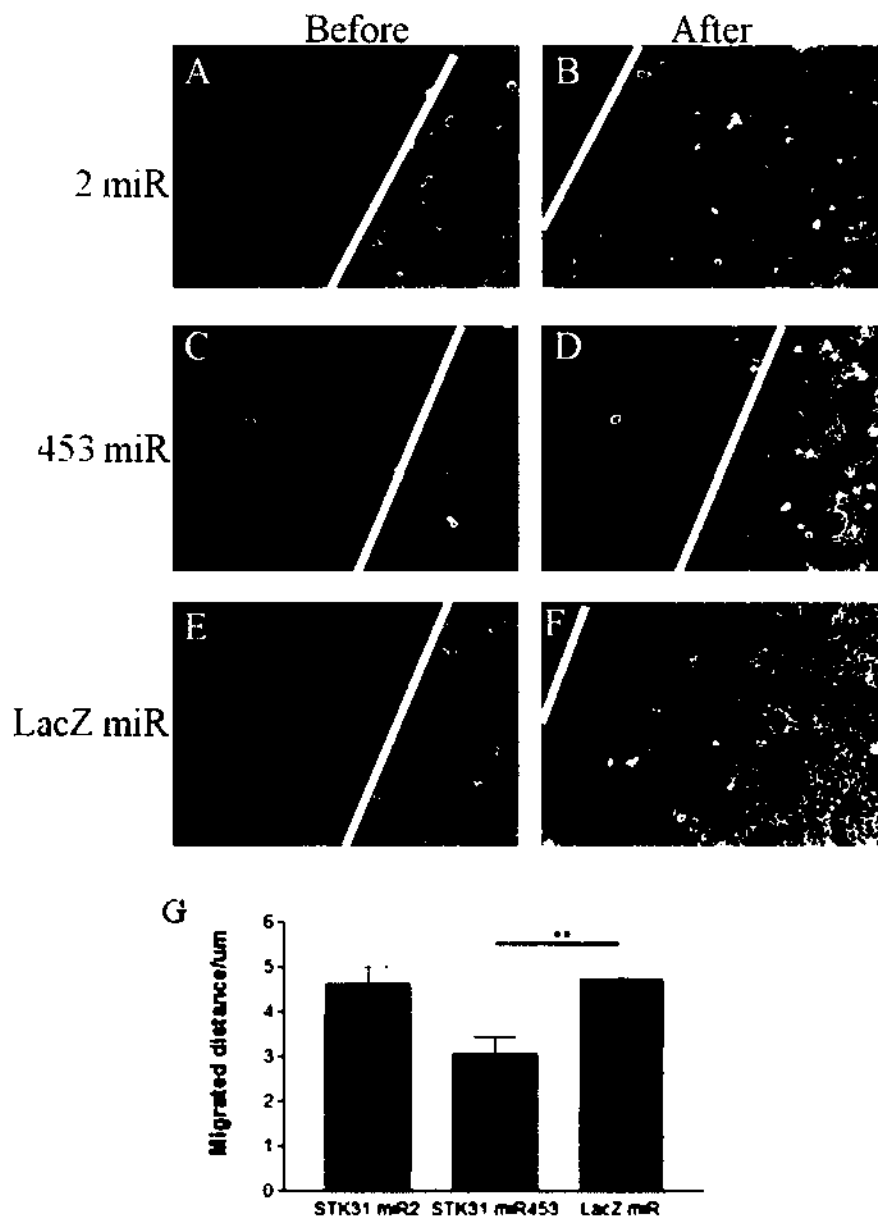


Figure 4.9| Migration assay of *STK31* knock-down cells. Cell free channels were made by placing a V-shape glass rod into culture well. Cells were seeded in confluent density.. Migration was recorded by Time Lapse Imaging and migrated distances were measured. Photomicrography of the front line of cells before and after assay were shown in figure A – F. Knock down of *STK31* results in a decrease in the migration rate of Caco2 cells (A – F). The migration rate was significantly lowered in Caco2^{miR 453} cells compared to Caco2^{LacZ} control ($p < 0.05$) (G). Magnification 100x (A – F) (Data were presented by mean \pm S.E.M.; Significance was calculated by One way ANOVA: Turkey test ** $p < 0.01$)

Taken together, the results confirmed that *STK31* promotes migration of Caco2 cells probably through decreasing the binding affinities to ECM as shown above.

4.3.7 Knock-down of *STK31* induces enterocytic differentiation

The third property of cancer stem cells is the ability to differentiate into different lineages of cells in that organ^{5,112}. Colon cancer stem cells from patients were found to be able to differentiate into two possible lineage-restricted cell types, enterocytes and goblet cells after *in vitro* expansion^{274,295}. Caco2 cells express colon cancer stem cells markers CD133 and CD44^{272,285}. Moreover they were shown to undergo enterocytic differentiation *in vitro*²⁹⁶, therefore, they are a good model to study the effect of *STK31* knock-down in enterocytic differentiation. It had been reported that Caco2 cells are able to differentiate under serum²⁹² or serum-free²⁹⁷ conditions where insulin:transferring:selenium are supplemented in serum free condition. In this experiment, both serum and serum-free (without supplement conditions) were used. Same numbers of stable transfectants were seeded into 24 well plates at confluent density. After attached, the medium was changed to serum-free medium for serum-free condition. Cells were cultured for 14 days. The medium was changed twice a week and images were captured at indicated time points.

5 days after incubation, the degrees of differentiation were limited. After 14 days in culture, Caco2^{LacZ} undergo enterocytic differentiation under serum containing condition as remarked by the formations of cyst and dome structure. The differentiation was serum-dependent as few cells were differentiated under serum-free conditions probably due to the absence of ITS supplement. Strikingly, under both conditions, Caco2^{miR 453} and Caco2^{miR 2} significantly enhanced the differentiation as reflected by the number and size of cysts and dome (Figure 4.10).

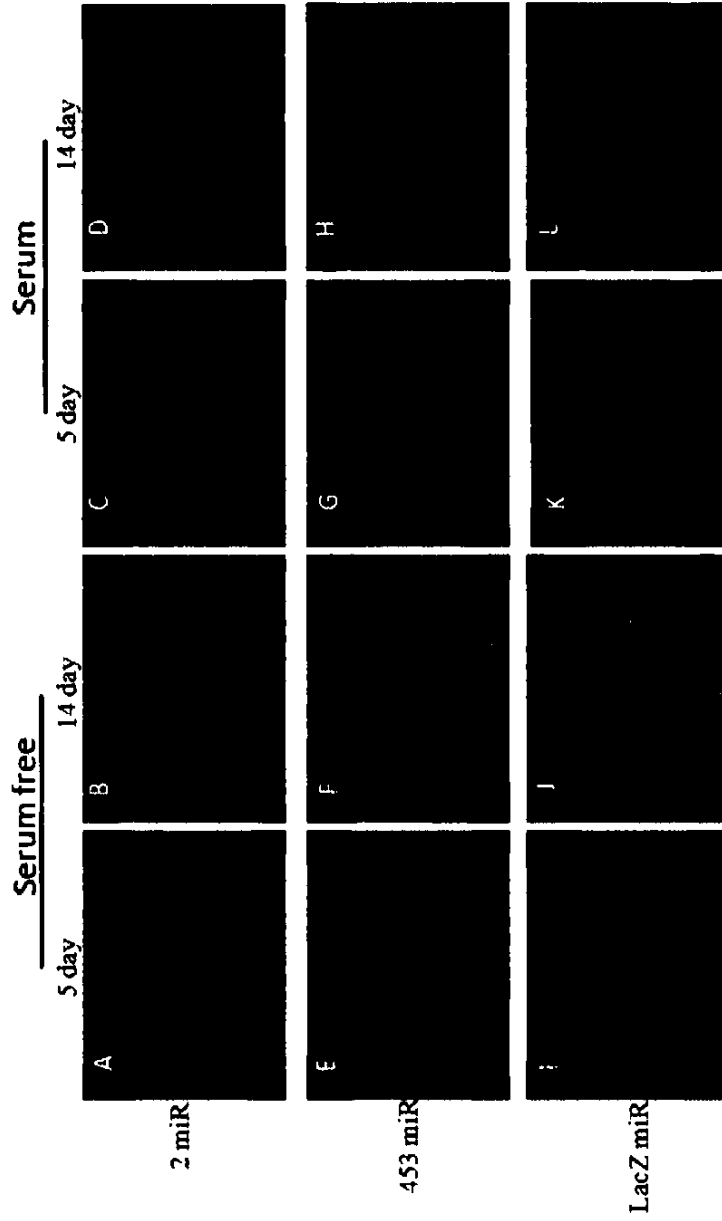


Figure 4.10| Enterocytic differentiation of *STK31* knock down cells. Cells were grown to confluence and allowed to undergo spontaneous enterocytic differentiation under serum (C, D, G, H, K and L) or serum-free conditions (A, B, E, F, I, and J). Images were taken at indicated time points. Differentiation was identified by the presence of cysts (Red arrow) and domes (Dashed red circle). Under traditional serum containing differentiation model, knock down of *STK31* resulted in enhanced differentiation at day 14 compared to LacZ control (D, H, and L). Under serum-free condition, where enterocytic differentiated in LacZ control was minimized due to the lack of ITS supplement, knock down of *STK31* resulted in induction/enhancement of enterocytic differentiation (B, F, and J).

These indicated that knock down of *STK31* resulted in enhancement of spontaneous enterocytic differentiation under serum-containing condition. On the other hand, knock-down of *STK31* might decrease the self-renewal as remarked by differentiation potential under serum-free condition.

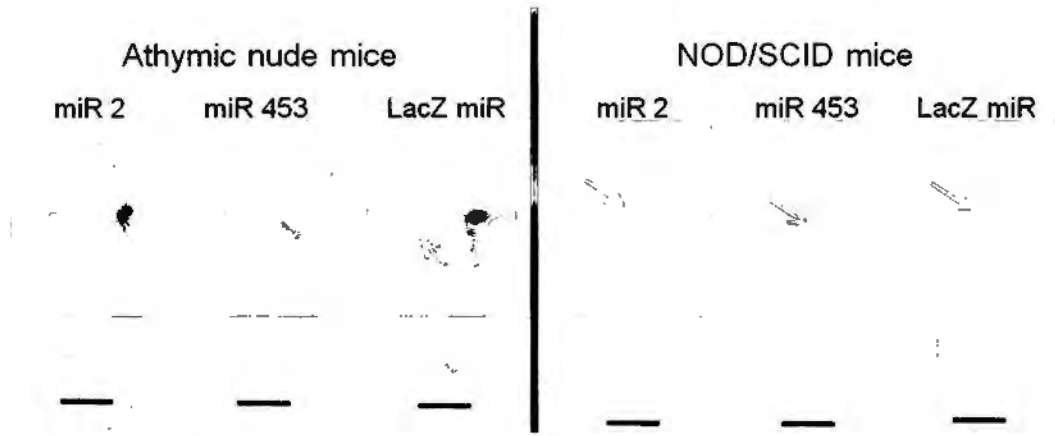
Taken together, the results suggest that *STK31* might promote the maintenance of un-differentiated state. It might also take part in the de-differentiation process for acquisition of “stemness” in Caco2 cells.

4.3.8 Knock-down of *STK31* decreases tumorigenicity *in vitro* and *in vivo*

Despite the fact that tumorigenicity of cancer stem cells in different mouse models is controversial^{246,298}, it is widely accepted that tumorigenicity was the hallmark of cancer stem cells¹¹². Since *STK31* is able to alter three cancer stem cell properties, it might be possible that *STK31* also takes part in controlling the tumorigenicity of Caco2 cells. In the hierarchy of cancer cells, only cancer stem cells are able to form new tumor. The ability to form tumors could be reflected by the ability to grow in anchorage-independent conditions²⁹⁹. Therefore, in this section, the effects of *STK31* knock-down in anchorage-independent grow was determined by colony formation assays. In this experiment, stable transfectant were seeded into agar gel, which mimiced the anchorage-independent condition. Then, the numbers of colonies formed were counted.

The results showed that knock-down of *STK31* significantly inhibit the colonies formation of Caco2 cells (Figure 4.11). Moreover, the inhibitions were dependent on the expression level of *STK31*, since the number of colonies in Caco2^{miR 453} was less than that in Caco2^{miR 2}. These results suggest that *STK31* promote anchorage-independent growth of Caco2 cells.

To address whether inhibition of anchorage-independent growth in *STK31*



Athymic nude mice

Group	No. of mice formed solid tumor	Occurrence rate	Average weight of tumor (mg)
Caco2 miR 2	10 / 15	66.66%	48.3
Caco2 miR 453	9 / 15	60%	127.1
Caco2 LacZ miR	9 / 12	75%	55.3
Sham	0 / 5	0%	N/A

NOD/SCID mice

Group	No. of mice formed solid tumor	Occurrence rate	Average weight of tumor (mg)
Caco2 miR 2	1 / 5	20%	40
Caco2 LacZ miR	3 / 4	75%	59.5
Sham	0 / 1	0%	N/A

Figure 4.12| Tumorigenicity of *STK31* knock-down cells *in vivo*. Cells were intrasubcutaneously injected into nude or NOD/SCID mice. The numbers of solid tumor formed were counted. Knock down of *STK31* decreased the tumorigenicity of Caco2 cells as reflected by the percentage of mice that formed solid tumor.

knock-down cells would result in reduced tumor formation *in vivo*, stable transfectant were injected into *nude* and NOD/SCID mice intra-subcutaneously. The results showed that knock-down of *STK31* decreased the tumorigenicity *in vivo* as reflected by the decrease in number of mice that formed tumor (Figure 4.12).

4.3.9 Signaling pathways involved in CSCs properties alteration in *STK31* knock-down cells

Together, we have showed that *STK31* plays a role in regulating the four “stemness” properties in cancer stem cells. So the next question is how *STK31* regulate the “stemness”? What are the underlying mechanisms? To address these questions, the transcriptomes of Caco2^{miR 453} were compared with Caco2^{LacZ} by whole genome microarray analysis. In this experiment, two experimental groups were compared by two-color microarray duplicated with dye swap labeling. Differentially expressed transcripts with $p < 0.08$ and fold change > 2 were reported.

The results showed that 96 genes were differentially expressed in *STK31* knock-down cells. Among the 96 genes, 28 genes were up-regulated while 68 genes were down-regulated (Table 4.2). Common pathways among these 96 genes were not reported indicating the possible involvement of novel signaling pathways. To confirm the microarray results, primers for ten genes, of particular interest due to their co-relations with cancers, were designed from database for realtime PCR studies.

The real-time PCR results showed that KIT, ARL11, PTPN13, HDGFRP3 and SMAD1 were significantly down-regulated in *STK31* knock down cells, meanwhile, the down-regulations were depended on the remaining level of endogenous *STK31* (Figure 4.13). On the other hand, LUM and FGF12 were significantly down-regulated only in Caco2^{miR 453} cells where endogenous *STK31* level was

GeneSymbol	Accession number	Regulation	Fold	Description
ICAI	NM_004968	down	3.4146283	Homo sapiens islet cell autoantigen 1
KIT	NM_000222	down	7.151116	Homo sapiens v-kit Hardy-Zuckerman 4 feline sarcoma viral oncogene homolog (KIT)
ZNF383	NM_152604	up	2.5891101	Homo sapiens zinc finger protein 383 (ZNF383)
ICAI	NM_004968	down	3.33008	Homo sapiens islet cell autoantigen 1 (ICAI)
SNCA	NM_007308	up	8.976191	Homo sapiens synuclein, alpha (non A4 component of amyloid precursor) (SNCA)
GPR81	ENST00000356987	down	7.85881	Probable G-protein coupled receptor 81 (G-protein coupled receptor 104)
COL9A3	NM_001853	down	2.6798186	Homo sapiens collagen, type IX, alpha 3 (COL9A3)
ARL11	NM_138450	down	21.697128	Homo sapiens ADP-ribosylation factor-like 11 (ARL11)
A_24_P802562	A_24_P802562	up	3.640206	
SMAD1	NM_005900	down	183.8287	Homo sapiens SMAD family member 1 (SMAD1)
KIAA0774	NM_001033602	up	9.298044	Homo sapiens KIAA0774 (KIAA0774)
THC2651751	THC2651751	down	2.2437162	
TMEM16B	NM_020373	down	7.471941	Homo sapiens transmembrane protein 16B (TMEM16B)
MEX3A	AK125482	down	2.2988076	Homo sapiens cDNA FLJ34393 fs, clone OCEBF3009279
ARHGAP22	NM_021236	up	2.9474616	Homo sapiens Rho GTPase activating protein 22 (ARHGAP22)
SNCAIP	NM_005460	down	15.861969	Homo sapiens synuclein, alpha interacting protein (synphilin) (SNCAIP)
PTHR2	NM_005048	down	5.920434	Homo sapiens parathyroid hormone receptor 2 (PTH2)
TRERF1	ENST00000372922	down	8.426428	Transcriptional-regulating factor 1 (Transcriptional-regulating protein 132)
ASNS	NM_001673	up	2.7862954	Homo sapiens asparagine synthetase (ASNS)
BC069781	BC069781	down	19.874887	Homo sapiens cDNA clone IMAGE:762583
TRAM1L1	NM_152402	down	5.8407736	Homo sapiens translocation associated membrane protein 1-like 1 (TRAM1L1)
GBPI	NM_002053	down	4.0890856	Homo sapiens guanylate binding protein 1, interferon-inducible, 67kDa (GBPI)
IL12RB2	NM_001559	down	3.2558742	Homo sapiens interleukin 12 receptor, beta 2 (IL12RB2)
UNC13C	NM_001080534	down	10.522095	Homo sapiens unc-13 homolog C (C. elegans) (UNC13C)
KIAA1212	NM_018084	down	2.9093002	Homo sapiens KIAA1212 (KIAA1212)
CACNG6	NM_145814	down	2.0964401	Homo sapiens calcium channel, voltage-dependent, gamma subunit 6 (CACNG6)
AKR1D1	NM_005989	down	3.3498344	Homo sapiens aldo-keto reductase family 1, member D1 (AKR1D1)
ENST00000390625	ENST00000390625	down	8.666279	Immunoglobulin heavy chain V gene segment

Table 4.2| Differential expressed genes in STK37 knock-down cells. Genes are presented by symbols and descriptions. Genes that were up-regulated are highlighted by Red while down-regulated genes are highlighted by Green. Differences between groups are presented by fold-change. Differentially expressed transcripts with $p < 0.08$ and fold change > 2 are reported.

GeneSymbol	Accession number	Regulation	Fold	Description
ZNF585A	NM_152655	up	4.9115605	Homo sapiens zinc finger protein 585A (ZNF585A)
LOC130940	NM_138803	up	2.1387844	Homo sapiens hypothetical protein BC015395 (LOC130940)
KLHL29	ENST00000288548	down	12.984759	Kelch-like protein 29 (Kelch repeat and BTB domain-containing protein 9)
TNS4	NM_032865	down	3.884351	Homo sapiens tensin 4 (TNS4)
RGS22	NM_015668	up	6.347687	Homo sapiens regulator of G-protein signalling 22 (RGS22)
NAP1L2	NM_021963	down	27.1446	Homo sapiens nucleosome assembly protein 1-like 2 (NAP1L2)
NRG1	NM_013961	down	7.9805786	Homo sapiens neuregulin 1 (NRG1)
HPR	NM_020995	down	3.0184093	Homo sapiens heparin-binding epidermal growth factor-like protein (HPR)
CDH11	NM_001797	down	56.160797	Homo sapiens cadherin 11, type 2, OB-cadherin (osteoblast) (CDH11)
FLJ35024	AF424541	up	7.190414	Homo sapiens unknown mRNA
ZDHHC11	NM_024786	up	4.929765	Homo sapiens zinc finger, DHHC-type containing 11 (ZDHHC11)
ENST00000358356	ENST00000358356	down	3.4419708	Runt-related transcription factor 1 (CBF-alpha 2)
LOC388630	XM_371250	down	2.1555758	PREDICTED: Homo sapiens similar to CDS35.5 (LOC388630)
CPA2	NM_001869	down	11.078192	Homo sapiens carboxypeptidase A2 (pancreatic) (CPA2)
C10orf8	NM_001010924	down	2.8706174	Homo sapiens chromosome 10 open reading frame 38 (C10orf8)
AR	NM_000044	down	19.963991	Homo sapiens androgen receptor (AR)
THC2692669	THC2692669	down	3.090093	ALU1_HUMAN (P99188) Alu subfamily J sequence contamination warning entry
FLJ25801	NM_173553	down	2.9704669	Homo sapiens hypothetical protein FLJ25801 (FLJ25801)
CRYGC	NM_020989	down	2.098044	Homo sapiens crystallin, gamma C (CRYGC)
CX165016	CX165016	up	10.864277	HIESC2_23_G02.g1_A035 NIH_MGC_258
ART4	NM_021071	down	3.6033022	Homo sapiens ADP-ribosyltransferase 4 (Dombrock blood group) (ART4)
LYPD6	NM_194317	down	5.1668916	Homo sapiens LY6PLAUR domain containing 6 (LYPD6)
AKI23649	AKI23649	down	2.2850277	Homo sapiens cDNA FLJ41655 fs
TNNT1	BC107798	up	4.2640505	Homo sapiens troponin T type 1 (skeletal, slow)
LOC641518	BC020624	down	8.874491	Homo sapiens hypothetical protein LOC641518
FAM59A	NM_022751	down	5.0541063	Homo sapiens family with sequence similarity 59, member A (FAM59A)
ODAM	NM_017855	down	6.744882	Homo sapiens odontogenic, ameloblast associated (ODAM)
HDCFRP3	NM_016073	down	26.74375	Homo sapiens hepatoma-derived growth factor, related protein 3 (HDCFRP3)

GeneSymbol	Accession number	Regulation	Field	Description
AADAC	NM_001086	down	5.591344	Homo sapiens acylacarnitide deacylase (esterase) (AADAC)
ALB	NM_000477	up	3.797428	Homo sapiens albumin (ALB)
MID2	NM_012216	down	2.0684547	Homo sapiens midline 2 (MID2)
DCP1B	NM_152640	down	3.7756503	Homo sapiens DCP1 deapping enzyme homolog B (S. cerevisiae) (DCP1B)
DDIT4	NM_019058	up	2.554159	Homo sapiens DNA-damage-inducible transcript 4 (DDIT4)
GJA1	NM_000165	down	17.796864	Homo sapiens gap junction protein, alpha 1, 43kDa (GJA1)
AKL30118	AKL30118	down	2.7743442	Homo sapiens cDNA FLJ26608 fs
AMT	NM_000481	up	5.431919	Homo sapiens aminomethyltransferase (AMT)
ROBO3	NM_022370	up	9.494382	Homo sapiens roundabout, aron, guidance receptor, homolog 3 (Drosophila) (ROBO3)
A_32_P158376	A_32_P158376	up	3.1824343	
PDLIM3	NM_014476	down	3.0463061	Homo sapiens PDZ and LIM domain 3 (PDLIM3)
FABP5	NM_001444	up	4.188141	Homo sapiens fatty acid binding protein 5 (prolactin-associated) (FABP5)
C20orf133	NM_080676	down	2.1129348	Homo sapiens chromosome 20 open reading frame 133 (C20orf133)
PTPN13	NM_080685	down	48.20727	Homo sapiens protein tyrosine phosphatase, non-receptor type 13 (PTPN13)
FGF12	NM_004113	down	22.807621	Homo sapiens fibroblast growth factor 12 (FGF12)
GOLGA2L1	NM_017600	down	4.2053185	Homo sapiens golgi autoantigen, golgin subfamily a, 2-like 1 (GOLGA2L1)
PLOD2	NM_182943	down	10.724174	Homo sapiens procollagen-lysine, 2-oxoglutarate 5-dioxygenase 2 (PLOD2)
FMOD	NM_002023	down	4.4760766	Homo sapiens fibronectin (FMOD)
KIAA0672	NM_014859	up	2.4549687	Homo sapiens KIAA0672 gene product (KIAA0672)
AK05438	AK05438	down	16.544527	Homo sapiens cDNA FLJ30876 fs
ZNF93	AK096342	up	7.0374765	Homo sapiens cDNA FLJ39023 fs
SCIN	NM_033128	down	7.0213957	Homo sapiens scindelin (SCIN)
KIAA1324L	NM_152748	down	159.09808	Homo sapiens KIAA1324-like (KIAA1324L)
TMEM27	NM_020665	down	3.1779554	Homo sapiens transmembrane protein 27 (TMEM27)
C5orf30	NM_033211	down	3.5162504	Homo sapiens chromosome 5 open reading frame 30 (C5orf30)
HYLS1	NM_145014	down	46.971718	Homo sapiens hydroleibhaus syndrome 1 (HYLS1)
CTSS	NM_004079	down	8.874509	Homo sapiens cathepsin S (CTSS)
CCND2	NM_001759	up	3.1284049	Homo sapiens cyclin D2 (CCND2)

GeneSymbol	Accession number	Regulation	Fold	Description
LUM	NM_002345	down	68.77325	Homo sapiens lumina (LUM)
SFRP3	NM_005416	up	9.475463	Homo sapiens small fibroin-rich protein 3 (SFRP3)
CST6	NM_001323	up	3.1878228	Homo sapiens cystein EAM (CST6), mRNA [NM_001323]
CA8	NM_004056	down	7.105368	Homo sapiens carbonic anhydrase VIII (CA8)
GAD1	NM_000817	down	7.0805674	Homo sapiens glutamate decarboxylase 1 (brain, 67kDa) (GAD1)
CLIC5	NM_016929	up	2.8027687	Homo sapiens chloride intracellular channel 5 (CLIC5)
Cl6orf74	BC009078	up	2.2154946	Homo sapiens chromosome 16 open reading frame 74, mRNA
ZNF93	AK096342	up	9.571887	Homo sapiens cDNA FLJ39023 fs
ALPK1	NM_025144	down	2.2798724	Homo sapiens alpha-kinase 1 (ALPK1)
LYZ	NM_000239	down	2.2735894	Homo sapiens lysozyme (renal amyloidosis) (LYZ)
ILIRAP	NM_002182	down	5.5767126	Homo sapiens interleukin 1 receptor accessory protein (ILIRAP)
AK094342	AK094342	up	2.099423	Homo sapiens cDNA FLJ37023 fs

Differential expression of various genes in *STK31* knocked down Caco2 cells

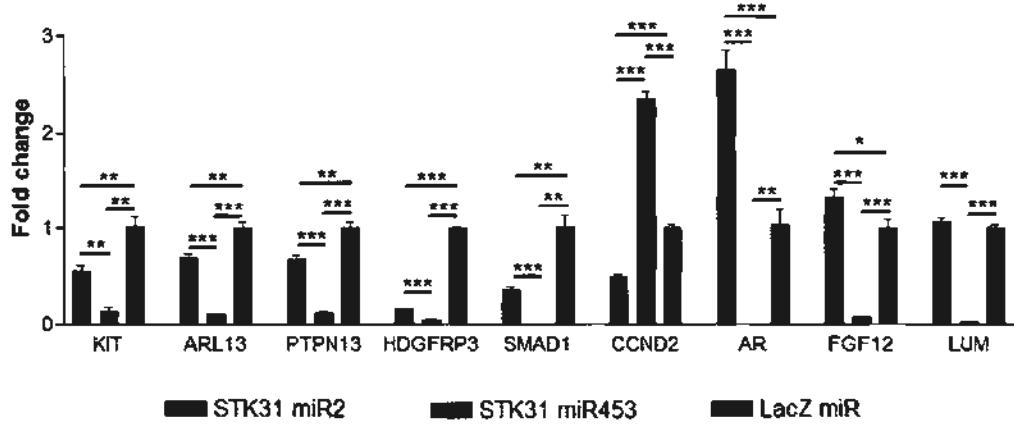


Figure 4.13| Real-time PCR for selected differentially expressed genes in *STK31* knock-down cells. Gene expressions were compared by comparative $\Delta\Delta Ct$ method and data were presented by fold change. KIT, ARL11, PTPN13, HDGFRP3 and SMAD1 were regulated in a *STK31* expression dependent manner. Down-regulation of FGF12 and LUM were only observed in Caco2^{miR453} only. CCND2 and AR showed an antagonistic expression among two *STK31* knock-down cells and the antagonistic expressions were significantly differed from LacZ control. (Data were presented by mean \pm S.E.M.; Significance were calculated by unpaired test * $p < 0.05$; ** $p < 0.01$; *** $p < 0.001$)

completely abolished. No significant differences were found between Caco2^{miR 2} and Caco2^{LacZ} control (Figure 4.13) suggesting that trace amount of *STK31* was sufficient to drive the expression of these two genes. Interestingly, *CCND2* and *AR* showed an antagonistic expression profiles in the two *STK31* knock-down cells. *CCND2* was up-regulated in Caco2^{miR 453} but down-regulated in Caco2^{miR 2} cells. *AR* was down-regulated in Caco2^{miR 453} but up-regulated in Caco2^{miR 2} cells (Figure 4.13). These results suggested that the expression threshold of *STK31* was crucial in those signaling cascades.

Together, we have identified differentially expressed genes in *STK31* knock-down cells that might take part in controlling the “stemness” properties in Caco2 cells.

4.4 Discussion

4.4.1 Regulators of “stemness” in colon cancer stem cell

Since the discovery of cancer stem cells, research has focused on the identification of CSCs in various tissues using different cell surface markers. Colon CSCs have been identified using mainly CD133 and CD44 as markers ^{238-240,272-274}. Although CD44 has been shown to be functionally important to colon CSCs ²⁷¹, genes involved in “stemness” have not been identified. Here, we reported a novel gene *STK31* as a potential regulator of “stemness” in colon CSCs. Expression of *STK31* in colon carcinoma cell line Caco2 was crucial for loss of contact inhibition, cell migration, maintaining differentiation potential and tumor formation. These are the hallmark properties of CSCs. Interestingly, low levels of *STK31* expression are sufficient for cell migration whereas contact inhibition, differentiation and tumor formation are regulated in a *STK31* level dependent manner. These modes of regulation perfectly match with emerging concepts that molecular control of CSCs

involve fine-tuned with thresholds to achieve a desired set point ¹¹³.

When using cell line models to study CSCs, the most debatable property is the self-renewal. Self-renewal describes the division that results in daughter cells that maintain the differentiating potential. Since differentiations are not well characterized in cell line, one can argue that proliferation in cell line does not equal to CSCs self-renewal. However, proliferation of Caco2 could be defined as self-renewal since daughter cells maintains the differentiation potential after division. The differentiation potential of Caco2 would be lost after confluence and in the presence of serum which were known to induce differentiation. Hence, the proliferation after confluence in a serum free condition could reflect the self-renewal properties of Caco2 cells. Our results demonstrated that knock down of *STK31* results in post-confluence cell cycle arrest and induces differentiation in serum free condition. These clearly indicated that *STK31* regulates the self-renewal of Caco2 cells. Together with its role in migration, differentiation and tumorigenicity, *STK31* is the first protein reported to regulate the “stemness” properties of CSCs.

4.4.2 Signaling pathways regulating “stemness”

Signaling pathways involved in CSCs have not been elucidated. The emerging concept is that coordination and cross talk between pathways are crucial ¹¹³. Our microarray profiling results indicated that there was no outstanding pathway underlying the “stemness” properties regulated by *STK31*. Instead, expressions of players from various pathways in cancer cells were altered. Among these, CCND2 (Cyclin D2), KIT and SMAD1 were well studied to take part in cell cycle regulation, differentiation, cell survival, tumor growth and invasion ³⁰⁰⁻³¹⁰.

Cyclin D2 belongs to the cyclin D family. Its association with Cdk4 was required for cell cycle progression through G1 phase ³¹¹. Interestingly, its role in cell

cycle progression is cell type specific. There are reports suggesting that expression of cyclin D2 was responsible for G1 arrest^{312,313}. Besides, cell cycle independent expressions of cyclin D2 have been proposed to take part in differentiation of macrophages³¹⁴. Interestingly, expression of cyclin D2 was down-regulated during differentiation in human colon cell line³¹⁵. From our results, cyclin D2 expression was up-regulated in Caco2^{miR 453} which endogenous *STK31* expression completely abolished. This would cause G1 arrest in confluent and post-confluent culture. Moreover, this would assist the differentiation process.

KIT is a tyrosine receptor kinase. Binding with its ligand, stem cell factor (SCF), would trigger signaling cascade that has been demonstrated to promote cell migration in human umbilical vein endothelial cells³¹⁶. It also enhances proliferation and invasion in prostate³⁰⁰ and colon cancer through PI3K/Akt pathway³⁰². Moreover, SCF/KIT signaling has been demonstrated to inhibit erythroid differentiation through modulating the G1-cyclin dependent kinase complex activity³⁰⁴. From our results, knock down of *STK31* resulted in down-regulation of KIT in a *STK31* expression level dependent manner. This in turn would cause the decrease in proliferation in confluent and post-confluent culture. On the other hand, this would also cause the decrease in cell migration. Regarding the differentiation, down-regulation of KIT decreased the SCF/KIT signaling. This might associate with up-regulation of cyclin D2 which enhances the differentiation in Caco2^{miR 453} cells. In Caco2^{miR 2} cells, cyclin D2 was down-regulated. In this case, the crosstalk between SCF/KIT and cell cycle regulator might be absent. The increase in differentiation in Caco2^{miR 2} cells might have resulted from KIT alone or association with other pathways.

SMAD1 belongs to the receptor-regulated SMAD family. It transduces signaling from BMP receptor in response to BMP sub-family ligands BMP2, 4, and 7. Besides, recent reports have suggested that TGF β also transduces signals through

phosphorylation³⁰⁶ and alteration in expression of SMAD1³¹⁷. SMAD1 dependent signaling have been implicated in anchorage independent growth³⁰⁶ and tumorigenicity³⁰⁷. It is also responsible for induction of pancreatic cancer cell invasiveness partially through increasing MMP2 activity³⁰⁹. From our results, knock down of *STK31* resulted in down-regulation of SMAD1 in a *STK31* expression level dependent manner. This would suppress the anchorage independent growth *in vitro* and the tumor forming ability *in vivo*.

Although cyclin D2, KIT and SMAD1 could explained the observed phenotype in *STK31* knock down Caco2 cells, other differential expressed genes in the microarray would also contribute to the “stemness” properties. Moreover, the crosstalk between these pathways remains to be clarified.

4.4.3 Acquisition of “stemness”

Reactivation of *STK31* was observed in 47 – 86% cancer samples and cell lines from various tissues (Chapter 2). Does this means that *STK31* negative cancer cells do not retain CSCs “stemness” properties? According to the “clonal evolution” model, genetic alterations accumulate during divisions. Cells that acquire beneficial alteration have growing advantages against the selection pressures. In this sense, tumors might acquire several but not all “stemness” properties. Since *STK31* regulates the “stemness” properties, *STK31* positive cells represents a more primitive “stem cell” state while *STK31* negative cells might be at the mid-way of “stemness” acquisition from terminal differentiated cells to cancer stem cells. In cell lines model, only tumors cells with certain CSCs properties such as immortality are able to survive the cell line establishment protocol. Therefore, a numbers of cell lines should represent the CSCs. However, from our previous studies, significant populations of cell lines (15 – 30% of nasopharyngeal and liver cell lines) were *STK31* negative. A

reason for this might be due to activation of other “stemness” regulators from other stem cell systems. *Stk31*, the mouse homolog, has been demonstrated to regulate stem cell fate in germline stem cell system (Chapter 3). It is likely that *STK31* positive cancer cells adapted the regulating system from germline stem cell. *STK31* negative cancer cells might adopt other tissue specific “stemness” regulator from other stem cells system such as hematopoietic stem cell and neural stem cells system.

4.4.4 Cell fate specification in CSCs

In the “cancer stem cell” model, the heterogeneity of cancer comes from the self-renewal and differentiation of CSCs. How is the homeostasis between self-renewal and differentiation controlled in CSCs? In normal stem cells, this homeostasis was maintained through asymmetric division. The asymmetric division was regulated by the niche, extrinsic factors and intrinsic factors. Mis-regulation of asymmetric division has been demonstrated to cause tumorigenesis in *Drosophila* neuroblast¹¹⁴⁻¹¹⁶. In our previous studies, we have demonstrated that besides the asymmetry in germline stem cells, *STK31*-GFP fusion protein also divided asymmetrically in HEK293 cells. This led to the speculation that mis-regulation of *STK31* asymmetry caused tumorigenesis. However, *STK31* asymmetry was unlikely to occur in normal colon crypt stem cells since *STK31* is not expressed in normal colon (Chapter 2). Moreover, overexpression of *Stk31* in STO and GC1-spg cell line did not cause transformation in these cells (data not shown). Therefore, it is unlikely that *STK31* asymmetry caused tumorigenesis. On top of causing tumorigenesis, cell fate specifications by asymmetric division resembling the normal stem cell could also occur in CSCs, however, this area has not been considered. We hypothesize that *STK31* was reactivated in CSCs acting as a “stemness” regulator. Mitotic asymmetry in CSCs retains the “stemness” in CSCs while loss of *STK31* in

differentiated progeny lead to loss of “stemness” properties such as tumorigenicity. In support of this hypothesis, *Stk31* was only expressed in differentiating germline stem cells but not more differentiated germ cells (Chapter 2). However, mitotic asymmetry was not observed in Caco2 cell under standard culture condition (data not shown). This might due to the fact that normal culture condition favored the self-renewal of CSCs instead of differentiation. Further studies were required to demonstrate the *STK31* asymmetry in CSCs in culture condition that favors differentiation.

4.4.5 *STK31* as a novel diagnostic and therapeutic target

The discovery of CSCs has opened up new possibilities in cancer diagnosis and therapy. Here, we reported that *STK31* regulates “stemness” properties in cancer cells and that it could be a candidate for cancer diagnosis and therapy. *STK31* could be an excellent diagnostic marker for cancer occurrence because: first, the promoter hypomethylation cause abnormality in expression. This allows simple diagnosis by expression screening; second, reactivation of *STK31* is observed in multiple cancer tissues with a high hitting rate in gastrointestinal cancer (32% - 46.7%)²⁷ but not their normal tissue counterpart. This allows diagnosis for multiple cancers with one marker and high confidences in gastrointestinal cancer and possibly other cancers; and third, *STK31* regulates “stemness” in cancer cells. This allows the diagnosis for the presence of potential cancer stem cells which would in turn provide valuable information in therapeutic design.

In cancer therapy, targeting the right population of cells is the main challenge. Cancer would be curable if one can target the tumor initiating cells and eliminate them. Along with this idea, *STK31* would be an excellent candidate for cancer therapy because: first, *STK31* is expressed in cancer cells, but not normal tissue

counterparts. This allows therapeutic agents target to specifically target cancer cells without affecting normal cells; second, *STK31* regulates “stemness” properties. This provides a higher chance of targeting cancer stem cells; third, *STK31* belongs to a kinase family where inhibitors are often available. The use of inhibitor confers advantage in drug designs and delivery when compared to other agents such as antibodies and gene therapy; and fourth, knock down of *STK31* results in significant increase in differentiation and decrease in tumorigenicity. This type of differentiation therapy is a new direction to target specifically cancer stem cells. Since differentiation normally occur in normal stem cell system, this therapeutic approach is unlikely to cause side effects.

Together, using *STK31* as diagnostic marker might allow the diagnosis of cancer stem cells in multiple cancers. Meanwhile, using *STK31* as therapeutic marker might allow cancer cell specific treatment with readily available inhibitors and minimal side effects.

4.5 Conclusion

In conclusion, knock-down of *STK31* in Caco2 cells results in G1 phase arrest and decrease in proliferation in confluent culture. It also enhances the cell attachment to several ECM proteins and decrease cell migration. Moreover, it enhances enterocytic differentiation and inhibits tumorigenicity. *STK31* regulates these “stemness” properties through altering the expression of key players in various pathways including KIT, SMAD1 and Cycline D2. *STK31* appears to be an excellent candidate for cancer diagnosis and therapy. Further studies are needed to elucidate the detailed underlying mechanisms of “stemness” and investigate the clinical application of *STK31*.

Chapter 5

General discussion

5.1 *STK31*, presence and future

Functional genomics in spermatogenesis is a difficult task due to the lack of *in vitro* model. Although knock-out (KO) technology has been advanced throughout the years, knocking out essential genes in spermatogenesis often results in sterility even in the heterozygous animals. This has limited the breeding of KO mice and increases the difficulties for obtaining a sufficient number of mice for studies. The development of GSC cultures and transplantation techniques has significantly shortened the experimental period. A sufficient number of mice could be obtained by expanding the GSCs *in vitro* followed by transplanting them back into recipient mice. Since no breeding was required the bottleneck from KO mice sterility could be bypassed.

GSCs have been considered truly immortal since their progenies are able to form zygotes and ES cells in the beginning of the next generation of life. Research on GSCs has focused in their self-renewal where the differentiation has attracted less attention. Since asymmetric division is usually involved in differentiation, asymmetric division in GSCs has been poorly studied. We have demonstrated asymmetric division of GSCs where *Stk31* acts as a cell fate determinant. However, several lines of questions have to be answered in order to draw a clear picture of the functions of *Stk31* in spermatogenesis. First, is *Stk31* required for differentiation of GSCs *in vivo*? To answer this question, we can first stably introduce RNAi against *Stk31* in GSCs and study the regeneration of spermatogenesis where *Stk31* was knocked down upon transplantation. Second, since *Stk31* is specifically expressed in transition state of differentiating GSCs, is the absence of *Stk31* in more differentiated progeny also due to asymmetric division? What would happen if *Stk31* expression is

sustained in these progeny? To answer these questions, we can make use of “state-of-the-art” Imagestream Cytometry System (Amnis Corp.). In this system, we could use cell surface markers such as c-kit to identify the dividing population of differentiated spermatogonia. Imaging of *Stk31* in these populations would tell whether mitotic asymmetry is present in these populations. The use of transplantation models with a stage specific expression of *Stk31* would allow us to study the presence of *Stk31* in more differentiated progeny. Third, what is the mechanism for *Stk31* asymmetry? To answer this question, we can first determine whether this asymmetry is dependent on Par3/6-aPKC complex by co-immunoprecipitation analysis. If asymmetry is set up independent of the Par3/6-aPKC polarity complex, novel interacting partners could be identified by TAP tag protein interaction system. Fourth, what is the underlying mechanism of *Stk31* in GSCs differentiation? Although signaling pathways from cancer cell line was available, the expressions of downstream signaling players such as SMAD1, KIT and CyclinD2 have to be determined in GSCs system.

It has been postulated that certain types of tumors are initiated and maintained by a population of cells known as cancer stem cells. The identification of CSCs has great impact on the field of cancer biology but it is just the beginning of the functional genomics studies in CSCs. We have demonstrated that CSC “stemness” properties are regulated by *STK31* in a human colon adenocarcinoma cell line, Caco2. However, several lines of questions have to be answered in order to define the functions of *STK31* in CSCs. First, we have observed the expression of *STK31* in various cancer samples and cell lines. Among these cell lines, Caco2 expressed two common colon CSCs markers CD133 and CD44. However, direct evidence on expression of *STK31* in CSCs remains to be elucidated. To study this, CSC populations could be isolated from clinical samples using a combination of CSCs

markers. Expression of *STK31* in these populations could then be determined by flow cytometry. Second, we have demonstrated the function of *STK31* in enterocytic differentiation. However, its role in multi-lineage differentiation including goblet and enteroendocrine lineage have not been evaluated. To study this, a Caco2 model with multi-lineage capacity could be used³¹⁸. Besides, colon cell line with other lineage potential such as HT-29 and T84 could be used³¹⁹. On top of the cell line models, differentiation could be studied in CSCs isolated from patient. Third, we have demonstrated the change in expression of various players in signaling pathways. However, how do these signaling pathways work alone or in combination to regulate the “stemness” has not been delineated. To study this, individual players could be inhibited or knocked down and subsequent “stemness” phenotype could be analyzed. Fourth, we have demonstrated that *STK31* shows mitotic asymmetry in HEK293 cells, does this asymmetry occur in CSCs and regulates the homeostasis between self-renewal and differentiation? To study this, cell line model or CSCs could placed in differentiation condition where the distribution of *STK31* in dividing cells could be studied.

5.2 Differentiation in GSCs versus de-differentiation in CSCs

We have demonstrated that expression of *Stk31* in GSCs promote differentiation. On the other hand, reactivation of *STK31* in cancer cells may result in de-differentiation of terminally differentiated cells to cancer stem cells state. Two explanations for these controversial observations could be offered. First, although *STK31* is involved in these two processes, the underlying mechanisms may be different. There is no co-relation between these two events. Second, *STK31* is expressed in transit amplifying (TA) stage. In germline, expression of *Stk31* may marks the differentiation from GSCs to TA stage (Figure 5.1). In tumor, expression of

A: Mouse male germline stem cell

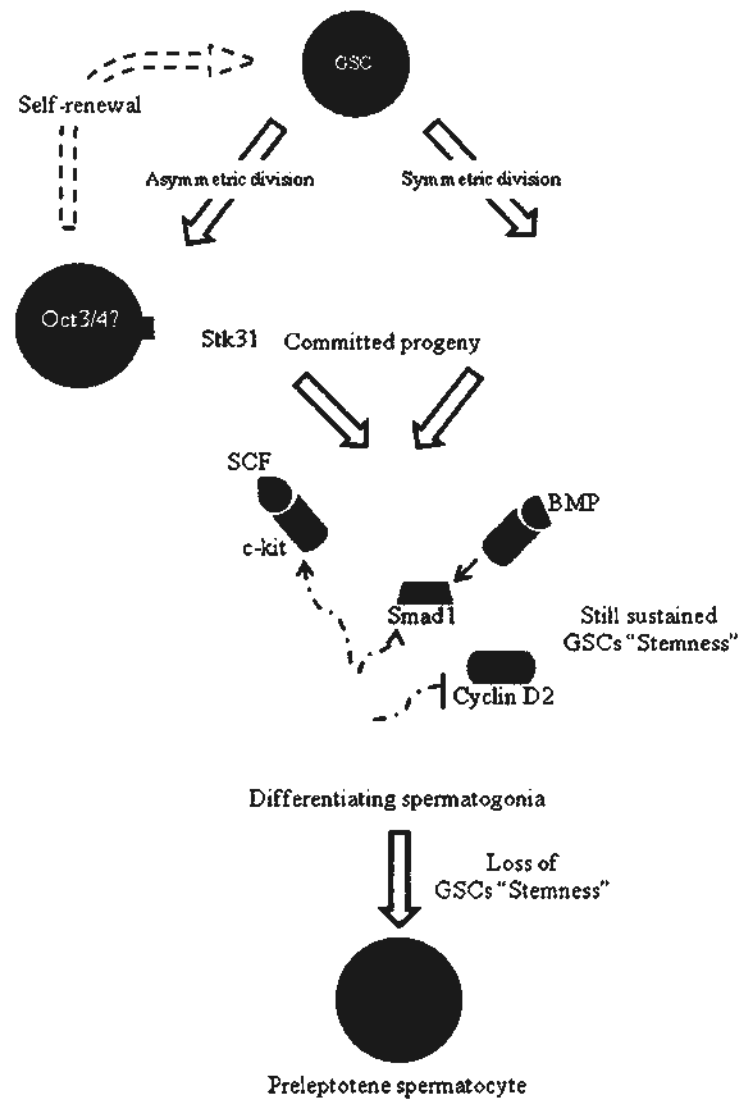
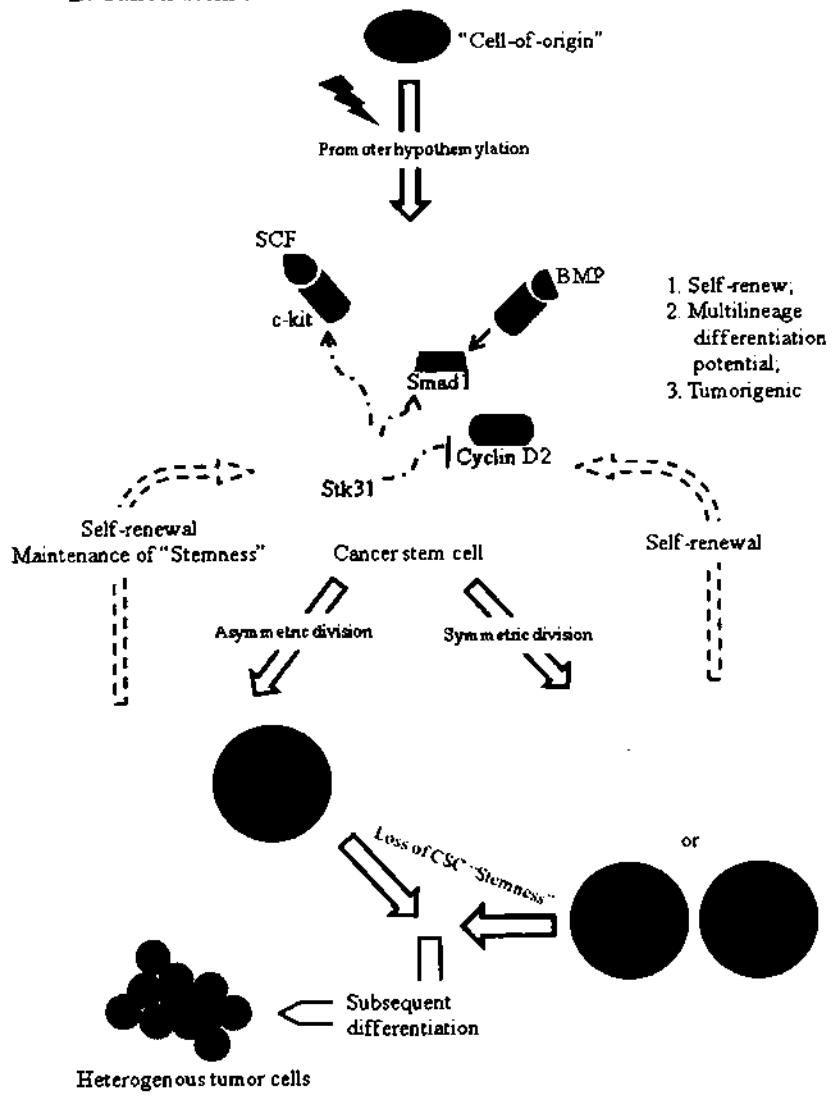


Figure 5.1| Schematic diagram of the role of *STK31* in germline stem cells and cancer stem cells. Involvement of *Stk31* in mouse male germline stem cell system was shown on A. Upon asymmetric division of GSC, *Stk31* distribute in committed progeny, but not self-renewing stem cells. *Stk31* act as a cell-fate determinant and trigger the expression of *c-kit*, *Smad1*, which take part in differentiation and suppress the expression of *Cyclin D2*, which take part in self-renewal of GSCs. In cancer stem cells (B), the “cell-of-origin” de-differentiate to a more stem-cell-like state. Reactivation of *STK31* by promoter hypomethylation may initiate the de-differentiation or it is reactivated during the proces. *STK31* acts as “stemness” regulator through regulating the expression of *KIT*, *SMAD1* and *Cyclin D2* which take part in tumor growth, differentiation, migration and tumorigenicity.

B: Cancer stem cell



STK31 remarked the de-differentiation from terminal differentiated cells to TA stage (Figure 5.1). The question is whether these TA stage cells confer “stemness” properties. Indeed, in mouse testis, the differentiating spermatogonia (TA stage) has been demonstrated to be able to generate stem cell populations *in vitro* and *in vivo* ⁵⁹. These suggest that “stemness” could be acquired or sustained in the TA stage of GSCs. In cancer, it has been postulated that CSCs could be derived from stem cells, TA population and differentiated cells ⁷. Are these “stemness” properties necessarily characteristics of the stem cells state of tumor cells? Is it possible that CSCs are in TA state instead of stem cells state? From our results, there are hints that the “cell-of-origin” in colon cancer uses the GSCs machinery to reprogram to CSCs. The CSCs state appears to be the same as the TA state in GSCs where “stemness” is sustained. Interestingly, the active proliferating properties of the TA state mimic more of the cancer state when compared to the quiescent stem cell state. This notion would be important in stem cell-based therapy since tumorigenicity is one of the biggest problems in the therapy. Take induced pluripotent stem cells (iPS) cells as an example. Since the first demonstration of reprogramming mouse fibroblast to iPS cells ³²⁰, the identity of iPS cells in the cell hierarchy has not been determined ³²¹. Although similar to ES cells, they have discrete molecular signatures ³²². Strikingly, the tumorigenicity of iPS cells derived neurosphere was significantly higher than that derived from ES cells. The authors explained the observation by the presence of higher number of pluripotent cells ³²³. However, according to our proposal that cancer stem cell is at the TA stage, it is possible that iPS cells may be at the TA stage, where the reprogramming is not all the way to the ES state, thus leading to a stronger tumorigenicity.

5.3 Concluding remarks

Genes involved in spermatogenesis and cancer stem cells are largely unknown. Due to the close relation between spermatogenesis and carcinogenesis, as exemplified by the CT antigens, functional studies of novel genes in these two processes could open up new opportunities in both reproductive biology and cancer biology, giving rise to novel therapeutic methods for sterility and cancer. The present study has demonstrated that *STK31* is one of these CT antigens playing a crucial role in GSC differentiation and cancer “stemness” regulation. Further studies on this gene may lead to promising new methods for treatment of cancer. On the other hand, novel *STK31*-mediated mechanisms regulating mammalian stem cell asymmetric division during spermatogenesis may unravel one of puzzling mysteries in reproductive biology.

Reference List

1. de Rooij, D. G. Rapid expansion of the spermatogonial stem cell tool box. *Proc. Natl. Acad. Sci. U. S. A* **103**, 7939-7940 (2006).
2. Zou, K. *et al.* Production of offspring from a germline stem cell line derived from neonatal ovaries. *Nat. Cell Biol.* **11**, 631-636 (2009).
3. Scanlan, M. J., Simpson, A. J. & Old, L. J. The cancer/testis genes: review, standardization, and commentary. *Cancer Immun.* **4**, 1 (2004).
4. Scanlan, M. J., Gure, A. O., Jungbluth, A. A., Old, L. J. & Chen, Y. T. Cancer/testis antigens: an expanding family of targets for cancer immunotherapy. *Immunol. Rev.* **188**, 22-32 (2002).
5. Wicha, M. S., Liu, S. & Dontu, G. Cancer stem cells: an old idea--a paradigm shift. *Cancer Res.* **66**, 1883-1890 (2006).
6. Visvader, J. E. & Lindeman, G. J. Cancer stem cells in solid tumours: accumulating evidence and unresolved questions. *Nat. Rev. Cancer* **8**, 755-768 (2008).
7. Marotta, L. L. & Polyak, K. Cancer stem cells: a model in the making. *Curr. Opin. Genet. Dev.* **19**, 44-50 (2009).
8. Gnnessi, L., Fabbri, A. & Spera, G. Gonadal peptides as mediators of development and functional control of the testis: an integrated system with hormones and local environment. *Endocr. Rev.* **18**, 541-609 (1997).
9. *The Physiology of Reproduction.*, pp. 933-974 (Raven Press, New York, 2009).
10. Skinner, M. K. Cell-cell interactions in the testis. *Endocr. Rev.* **12**, 45-77 (1991).
11. Cooke, H. J. & Saunders, P. T. Mouse models of male infertility. *Nat. Rev. Genet.* **3**, 790-801 (2002).
12. Oatley, J. M. & Brinster, R. L. Regulation of spermatogonial stem cell self-renewal in mammals. *Annu. Rev. Cell Dev. Biol.* **24**, 263-286 (2008).
13. de Rooij, D. G. Proliferation and differentiation of spermatogonial stem cells.

- Reproduction*. **121**, 347-354 (2001).
14. de Kretser, D. M. & Kerr, J. *The physiology of Reproduction*.1994).
 15. Russell LD, Ettlín RA, Sinha Hikim AP & Clegg ED, pp. 36-37 (Cache River Press, Clearwater,1990).
 16. Reddel, R. R. The role of senescence and immortalization in carcinogenesis. *Carcinogenesis* **21**, 477-484 (2000).
 17. Abercrombie, M. Contact inhibition in tissue culture. *In Vitro* **6**, 128-142 (1970).
 18. ABERCROMBIE, M. & AMBROSE, E. J. The surface properties of cancer cells: a review. *Cancer Res.* **22**, 525-548 (1962).
 19. Ridley, A. J. *et al.* Cell migration: integrating signals from front to back. *Science* **302**, 1704-1709 (2003).
 20. Thiery, J. P. Epithelial-mesenchymal transitions in tumour progression. *Nat. Rev. Cancer* **2**, 442-454 (2002).
 21. Thiery, J. P. & Sleeman, J. P. Complex networks orchestrate epithelial-mesenchymal transitions. *Nat. Rev. Mol. Cell Biol.* **7**, 131-142 (2006).
 22. Simpson, A. J., Caballero, O. L., Jungbluth, A., Chen, Y. T. & Old, L. J. Cancer/testis antigens, gametogenesis and cancer. *Nat. Rev. Cancer* **5**, 615-625 (2005).
 23. Sha, J. *et al.* Identification of testis development and spermatogenesis-related genes in human and mouse testes using cDNA arrays. *Mol. Hum. Reprod.* **8**, 511-517 (2002).
 24. Wang, P. J., McCarrey, J. R., Yang, F. & Page, D. C. An abundance of X-linked genes expressed in spermatogonia. *Nat. Genet.* **27**, 422-426 (2001).
 25. Wang, P. J., Page, D. C. & McCarrey, J. R. Differential expression of sex-linked and autosomal germ-cell-specific genes during spermatogenesis in the mouse. *Hum. Mol. Genet.* **14**, 2911-2918 (2005).
 26. Bellve, A. R., Millette, C. F., Bhatnagar, Y. M. & O'Brien, D. A. Dissociation of the mouse testis and characterization of isolated spermatogenic cells. *J.*

- Histochem. Cytochem.* **25**, 480-494 (1977).
27. Yokoe, T. *et al.* Efficient identification of a novel cancer/testis antigen for immunotherapy using three-step microarray analysis. *Cancer Res.* **68**, 1074-1082 (2008).
 28. Selenko, P. *et al.* SMN tudor domain structure and its interaction with the Sm proteins. *Nat. Struct. Biol.* **8**, 27-31 (2001).
 29. Ponting, C. P. Tudor domains in proteins that interact with RNA. *Trends Biochem. Sci.* **22**, 51-52 (1997).
 30. Talbot, K., Miguel-Aliaga, I., Mohaghegh, P., Ponting, C. P. & Davies, K. E. Characterization of a gene encoding survival motor neuron (SMN)-related protein, a constituent of the spliceosome complex. *Hum. Mol. Genet.* **7**, 2149-2156 (1998).
 31. Neubauer, G. *et al.* Mass spectrometry and EST-database searching allows characterization of the multi-protein spliceosome complex. *Nat. Genet.* **20**, 46-50 (1998).
 32. Rogne, M. *et al.* The KH-Tudor domain of a-kinase anchoring protein 149 mediates RNA-dependent self-association. *Biochemistry* **45**, 14980-14989 (2006).
 33. Huang, Y., Fang, J., Bedford, M. T., Zhang, Y. & Xu, R. M. Recognition of histone H3 lysine-4 methylation by the double tudor domain of JMJD2A. *Science* **312**, 748-751 (2006).
 34. Kachirskaia, I. *et al.* Role for 53BP1 Tudor domain recognition of p53 dimethylated at lysine 382 in DNA damage signaling. *J. Biol. Chem.* **283**, 34660-34666 (2008).
 35. Cote, J. & Richard, S. Tudor domains bind symmetrical dimethylated arginines. *J. Biol. Chem.* **280**, 28476-28483 (2005).
 36. Chuma, S. *et al.* Tdrd1/Mtr-1, a tudor-related gene, is essential for male germ-cell differentiation and nuage/germinal granule formation in mice. *Proc. Natl. Acad. Sci. U. S. A* **103**, 15894-15899 (2006).
 37. Hosokawa, M. *et al.* Tudor-related proteins TDRD1/MTR-1, TDRD6 and TDRD7/TRAP: domain composition, intracellular localization, and function

- in male germ cells in mice. *Dev. Biol.* **301**, 38-52 (2007).
38. Pan, J. *et al.* RNF17, a component of the mammalian germ cell nuage, is essential for spermiogenesis. *Development* **132**, 4029-4039 (2005).
 39. Goulet, I., Boisvenue, S., Mokas, S., Mazroui, R. & Cote, J. TDRD3, a novel Tudor domain-containing protein, localizes to cytoplasmic stress granules. *Hum. Mol. Genet.* **17**, 3055-3074 (2008).
 40. Wang, J., Saxe, J. P., Tanaka, T., Chuma, S. & Lin, H. Mili interacts with tudor domain-containing protein 1 in regulating spermatogenesis. *Curr. Biol.* **19**, 640-644 (2009).
 41. Manning, G., Whyte, D. B., Martinez, R., Hunter, T. & Sudarsanam, S. The protein kinase complement of the human genome. *Science* **298**, 1912-1934 (2002).
 42. Edelman, A. M., Blumenthal, D. K. & Krebs, E. G. Protein serine/threonine kinases. *Annu. Rev. Biochem.* **56**, 567-613 (1987).
 43. Capra, M. *et al.* Frequent alterations in the expression of serine/threonine kinases in human cancers. *Cancer Res.* **66**, 8147-8154 (2006).
 44. Boutros, T., Chevet, E. & Metrakos, P. Mitogen-activated protein (MAP) kinase/MAP kinase phosphatase regulation: roles in cell growth, death, and cancer. *Pharmacol. Rev.* **60**, 261-310 (2008).
 45. Katayama, H., Brinkley, W. R. & Sen, S. The Aurora kinases: role in cell transformation and tumorigenesis. *Cancer Metastasis Rev.* **22**, 451-464 (2003).
 46. Carmena, M. & Earnshaw, W. C. The cellular geography of aurora kinases. *Nat. Rev. Mol. Cell Biol.* **4**, 842-854 (2003).
 47. Dym, M., Kokkinaki, M. & He, Z. Spermatogonial stem cells: mouse and human comparisons. *Birth Defects Res. C. Embryo. Today* **87**, 27-34 (2009).
 48. CLERMONT, Y. The cycle of the seminiferous epithelium in man. *Am. J. Anat.* **112**, 35-51 (1963).
 49. Clermont, Y. Renewal of spermatogonia in man. *Am. J. Anat.* **118**, 509-524 (1966).

50. Clermont, Y. Spermatogenesis in man. A study of the spermatogonial population. *Fertil. Steril.* **17**, 705-721 (1966).
51. Clermont, Y. Kinetics of spermatogenesis in mammals: seminiferous epithelium cycle and spermatogonial renewal. *Physiol Rev.* **52**, 198-236 (1972).
52. Yoshida, S. Casting back to stem cells. *Nat. Cell Biol.* **11**, 118-120 (2009).
53. Clermont, Y. & Bustos-Obregon, E. Re-examination of spermatogonial renewal in the rat by means of seminiferous tubules mounted "in toto". *Am. J. Anat.* **122**, 237-247 (1968).
54. Dym, M. & Clermont, Y. Role of spermatogonia in the repair of the seminiferous epithelium following x-irradiation of the rat testis. *Am. J. Anat.* **128**, 265-282 (1970).
55. de Rooij, D. G. & Grootegoed, J. A. Spermatogonial stem cells. *Curr. Opin. Cell Biol.* **10**, 694-701 (1998).
56. Oakberg, E. F. Spermatogonial stem-cell renewal in the mouse. *Anat. Rec.* **169**, 515-531 (1971).
57. de Rooij, D. G. Stem cells in the testis. *Int. J. Exp. Pathol.* **79**, 67-80 (1998).
58. Oatley, J. M. & Brinster, R. L. Spermatogonial stem cells. *Methods Enzymol.* **419**, 259-282 (2006).
59. Barroca, V. *et al.* Mouse differentiating spermatogonia can generate germinal stem cells in vivo. *Nat. Cell Biol.* **11**, 190-196 (2009).
60. Chiarini-Garcia, H. & Russell, L. D. High-resolution light microscopic characterization of mouse spermatogonia. *Biol. Reprod.* **65**, 1170-1178 (2001).
61. Shinohara, T., Avarbock, M. R. & Brinster, R. L. beta1- and alpha6-integrin are surface markers on mouse spermatogonial stem cells. *Proc. Natl. Acad. Sci. U. S. A* **96**, 5504-5509 (1999).
62. Kanatsu-Shinohara, M., Toyokuni, S. & Shinohara, T. CD9 is a surface marker on mouse and rat male germline stem cells. *Biol. Reprod.* **70**, 70-75 (2004).

63. Tokuda, M., Kadokawa, Y., Kurahashi, H. & Marunouchi, T. CDH1 is a specific marker for undifferentiated spermatogonia in mouse testes. *Biol. Reprod.* **76**, 130-141 (2007).
64. Meng, X. *et al.* Regulation of cell fate decision of undifferentiated spermatogonia by GDNF. *Science* **287**, 1489-1493 (2000).
65. Conrad, S. *et al.* Generation of pluripotent stem cells from adult human testis. *Nature* **456**, 344-349 (2008).
66. Costoya, J. A. *et al.* Essential role of Plzf in maintenance of spermatogonial stem cells. *Nat. Genet.* **36**, 653-659 (2004).
67. Ohbo, K. *et al.* Identification and characterization of stem cells in prepubertal spermatogenesis in mice small star, filled. *Dev. Biol.* **258**, 209-225 (2003).
68. Dann, C. T. *et al.* Spermatogonial stem cell self-renewal requires OCT4, a factor downregulated during retinoic acid-induced differentiation. *Stem Cells* **26**, 2928-2937 (2008).
69. Nayernia, K. *et al.* In vitro-differentiated embryonic stem cells give rise to male gametes that can generate offspring mice. *Dev. Cell* **11**, 125-132 (2006).
70. Kubota, H., Avarbock, M. R. & Brinster, R. L. Spermatogonial stem cells share some, but not all, phenotypic and functional characteristics with other stem cells. *Proc. Natl. Acad. Sci. U. S. A* **100**, 6487-6492 (2003).
71. Schrans-Stassen, B. H., Saunders, P. T., Cooke, H. J. & de Rooij, D. G. Nature of the spermatogenic arrest in Dazl *-/-* mice. *Biol. Reprod.* **65**, 771-776 (2001).
72. Saunders, P. T. *et al.* Absence of mDazl produces a final block on germ cell development at meiosis. *Reproduction.* **126**, 589-597 (2003).
73. Tanaka, S. S. *et al.* The mouse homolog of Drosophila Vasa is required for the development of male germ cells. *Genes Dev.* **14**, 841-853 (2000).
74. Castrillon, D. H., Quade, B. J., Wang, T. Y., Quigley, C. & Crum, C. P. The human VASA gene is specifically expressed in the germ cell lineage. *Proc. Natl. Acad. Sci. U. S. A* **97**, 9585-9590 (2000).
75. Ohta, H., Yomogida, K., Dohmae, K. & Nishimune, Y. Regulation of

- proliferation and differentiation in spermatogonial stem cells: the role of c-kit and its ligand SCF. *Development* **127**, 2125-2131 (2000).
76. Vincent, S. *et al.* Stage-specific expression of the Kit receptor and its ligand (KL) during male gametogenesis in the mouse: a Kit-KL interaction critical for meiosis. *Development* **125**, 4585-4593 (1998).
 77. Rajpert-De, M. E. *et al.* The immunohistochemical expression pattern of Chk2, p53, p19INK4d, MAGE-A4 and other selected antigens provides new evidence for the premeiotic origin of spermatocytic seminoma. *Histopathology* **42**, 217-226 (2003).
 78. Kellogg, D. R., Moritz, M. & Alberts, B. M. The centrosome and cellular organization. *Annu. Rev. Biochem.* **63**, 639-674 (1994).
 79. Bruce Alberts, D. B. J. L. M. R. K. R. K. D. W. *Molecular Biology of The Cell.* (Garland Publishing,2009).
 80. Knoblich, J. A. Mechanisms of asymmetric stem cell division. *Cell* **132**, 583-597 (2008).
 81. Gonzalez, C. Spindle orientation, asymmetric division and tumour suppression in *Drosophila* stem cells. *Nat. Rev. Genet.* **8**, 462-472 (2007).
 82. Gonczy, P. Mechanisms of asymmetric cell division: flies and worms pave the way. *Nat. Rev. Mol. Cell Biol.* **9**, 355-366 (2008).
 83. Schwamborn, J. C., Berezikov, E. & Knoblich, J. A. The TRIM-NHL protein TRIM32 activates microRNAs and prevents self-renewal in mouse neural progenitors. *Cell* **136**, 913-925 (2009).
 84. Beckmann, J., Scheitza, S., Wernet, P., Fischer, J. C. & Giebel, B. Asymmetric cell division within the human hematopoietic stem and progenitor cell compartment: identification of asymmetrically segregating proteins. *Blood* **109**, 5494-5501 (2007).
 85. Kuang, S., Gillespie, M. A. & Rudnicki, M. A. Niche regulation of muscle satellite cell self-renewal and differentiation. *Cell Stem Cell* **2**, 22-31 (2008).
 86. Chang, J. T. *et al.* Asymmetric T lymphocyte division in the initiation of adaptive immune responses. *Science* **315**, 1687-1691 (2007).

87. Cairns, J. Mutation selection and the natural history of cancer. *Nature* **255**, 197-200 (1975).
88. Lark, K. G., Consigli, R. A. & Minocha, H. C. Segregation of sister chromatids in mammalian cells. *Science* **154**, 1202-1205 (1966).
89. Karpowicz, P. *et al.* Support for the immortal strand hypothesis: neural stem cells partition DNA asymmetrically in vitro. *J. Cell Biol.* **170**, 721-732 (2005).
90. Potten, C. S., Owen, G. & Booth, D. Intestinal stem cells protect their genome by selective segregation of template DNA strands. *J. Cell Sci.* **115**, 2381-2388 (2002).
91. Smith, G. H. Label-retaining epithelial cells in mouse mammary gland divide asymmetrically and retain their template DNA strands. *Development* **132**, 681-687 (2005).
92. Shinin, V., Gayraud-Morel, B., Gomes, D. & Tajbakhsh, S. Asymmetric division and cosegregation of template DNA strands in adult muscle satellite cells. *Nat. Cell Biol.* **8**, 677-687 (2006).
93. Kiel, M. J. *et al.* Haematopoietic stem cells do not asymmetrically segregate chromosomes or retain BrdU. *Nature* **449**, 238-242 (2007).
94. Boutros, R. & Ducommun, B. Asymmetric localization of the CDC25B phosphatase to the mother centrosome during interphase. *Cell Cycle* **7**, 401-406 (2008).
95. Rujano, M. A. *et al.* Polarised asymmetric inheritance of accumulated protein damage in higher eukaryotes. *PLoS. Biol.* **4**, e417 (2006).
96. Zendman, A. J., Ruiter, D. J. & Van Muijen, G. N. Cancer/testis-associated genes: identification, expression profile, and putative function. *J. Cell Physiol* **194**, 272-288 (2003).
97. Kalejs, M. & Erenpreisa, J. Cancer/testis antigens and gametogenesis: a review and "brain-storming" session. *Cancer Cell Int.* **5**, 4 (2005).
98. 2009).
99. McLean, D. J., Russell, L. D. & Griswold, M. D. Biological activity and

enrichment of spermatogonial stem cells in vitamin A-deficient and hyperthermia-exposed testes from mice based on colonization following germ cell transplantation. *Biol. Reprod.* **66**, 1374-1379 (2002).

100. Rockett, J. C. *et al.* Effects of hyperthermia on spermatogenesis, apoptosis, gene expression, and fertility in adult male mice. *Biol. Reprod.* **65**, 229-239 (2001).
101. Lin, H. The tao of stem cells in the germline. *Annu. Rev. Genet.* **31**, 455-491 (1997).
102. Lin, H. The self-renewing mechanism of stem cells in the germline. *Curr. Opin. Cell Biol.* **10**, 687-693 (1998).
103. Sabeur, K., Ball, B. A., Corbin, C. J. & Conley, A. Characterization of a novel, testis-specific equine serine/threonine kinase. *Mol. Reprod. Dev.* **75**, 867-873 (2008).
104. Shinohara, T., Orwig, K. E., Avarbock, M. R. & Brinster, R. L. Spermatogonial stem cell enrichment by multiparameter selection of mouse testis cells. *Proc. Natl. Acad. Sci. U. S. A* **97**, 8346-8351 (2000).
105. Schrans-Stassen, B. H., van de Kant, H. J., de Rooij, D. G. & van Pelt, A. M. Differential expression of c-kit in mouse undifferentiated and differentiating type A spermatogonia. *Endocrinology* **140**, 5894-5900 (1999).
106. Anderson, P. & Kedersha, N. Stress granules: the Tao of RNA triage. *Trends Biochem. Sci.* **33**, 141-150 (2008).
107. Kotaja, N. & Sassone-Corsi, P. The chromatoid body: a germ-cell-specific RNA-processing centre. *Nat. Rev. Mol. Cell Biol.* **8**, 85-90 (2007).
108. Parvinen, M. The chromatoid body in spermatogenesis. *Int. J. Androl* **28**, 189-201 (2005).
109. Saffman, E. E. & Lasko, P. Germline development in vertebrates and invertebrates. *Cell Mol. Life Sci.* **55**, 1141-1163 (1999).
110. Fuentealba, L. C., Eivers, E., Geissert, D., Taelman, V. & De Robertis, E. M. Asymmetric mitosis: Unequal segregation of proteins destined for degradation. *Proc. Natl. Acad. Sci. U. S. A* **105**, 7732-7737 (2008).

111. Yamashita, Y. M. & Fuller, M. T. Asymmetric centrosome behavior and the mechanisms of stem cell division. *J. Cell Biol.* **180**, 261-266 (2008).
112. Jordan, C. T. Cancer stem cells: controversial or just misunderstood? *Cell Stem Cell* **4**, 203-205 (2009).
113. Kim, C. F. & Dirks, P. B. Cancer and stem cell biology: how tightly intertwined? *Cell Stem Cell* **3**, 147-150 (2008).
114. Clevers, H. Stem cells, asymmetric division and cancer. *Nat. Genet.* **37**, 1027-1028 (2005).
115. Wodarz, A. & Gonzalez, C. Connecting cancer to the asymmetric division of stem cells. *Cell* **124**, 1121-1123 (2006).
116. Morrison, S. J. & Kimble, J. Asymmetric and symmetric stem-cell divisions in development and cancer. *Nature* **441**, 1068-1074 (2006).
117. Tegelenbosch, R. A. & de Rooij, D. G. A quantitative study of spermatogonial multiplication and stem cell renewal in the C3H/101 F1 hybrid mouse. *Mutat. Res.* **290**, 193-200 (1993).
118. Brinster, R. L. Germline stem cell transplantation and transgenesis. *Science* **296**, 2174-2176 (2002).
119. de Rooij, D. G. & Russell, L. D. All you wanted to know about spermatogonia but were afraid to ask. *J. Androl* **21**, 776-798 (2000).
120. McLean, D. J., Friel, P. J., Johnston, D. S. & Griswold, M. D. Characterization of spermatogonial stem cell maturation and differentiation in neonatal mice. *Biol. Reprod.* **69**, 2085-2091 (2003).
121. Yoshida, S. *et al.* The first round of mouse spermatogenesis is a distinctive program that lacks the self-renewing spermatogonia stage. *Development* **133**, 1495-1505 (2006).
122. Scadden, D. T. The stem-cell niche as an entity of action. *Nature* **441**, 1075-1079 (2006).
123. Spradling, A., Drummond-Barbosa, D. & Kai, T. Stem cells find their niche. *Nature* **414**, 98-104 (2001).
124. Tulina, N. & Matunis, E. Control of stem cell self-renewal in *Drosophila*

- spermatogenesis by JAK-STAT signaling. *Science* **294**, 2546-2549 (2001).
125. Yamashita, Y. M., Fuller, M. T. & Jones, D. L. Signaling in stem cell niches: lessons from the *Drosophila* germline. *J. Cell Sci.* **118**, 665-672 (2005).
 126. Yamashita, Y. M., Jones, D. L. & Fuller, M. T. Orientation of asymmetric stem cell division by the APC tumor suppressor and centrosome. *Science* **301**, 1547-1550 (2003).
 127. Wong, M. D., Jin, Z. & Xie, T. Molecular mechanisms of germline stem cell regulation. *Annu. Rev. Genet.* **39**, 173-195 (2005).
 128. Gonczy, P. & DiNardo, S. The germ line regulates somatic cyst cell proliferation and fate during *Drosophila* spermatogenesis. *Development* **122**, 2437-2447 (1996).
 129. Kiger AA, F. MT. *Stem Cell Biology.*, pp. 149-188 (Cold Spring Harbor Lab. Press,2001).
 130. Oatley, J. M., Avarbock, M. R. & Brinster, R. L. Glial cell line-derived neurotrophic factor regulation of genes essential for self-renewal of mouse spermatogonial stem cells is dependent on Src family kinase signaling. *J. Biol. Chem.* **282**, 25842-25851 (2007).
 131. Naughton, C. K., Jain, S., Strickland, A. M., Gupta, A. & Milbrandt, J. Glial cell-line derived neurotrophic factor-mediated RET signaling regulates spermatogonial stem cell fate. *Biol. Reprod.* **74**, 314-321 (2006).
 132. Kubota, H., Avarbock, M. R. & Brinster, R. L. Growth factors essential for self-renewal and expansion of mouse spermatogonial stem cells. *Proc. Natl. Acad. Sci. U. S. A* **101**, 16489-16494 (2004).
 133. Tadokoro, Y., Yomogida, K., Ohta, H., Tohda, A. & Nishimune, Y. Homeostatic regulation of germinal stem cell proliferation by the GDNF/FSH pathway. *Mech. Dev.* **113**, 29-39 (2002).
 134. de Rooij, D. G., Repping, S. & van Pelt, A. M. Role for adhesion molecules in the spermatogonial stem cell niche. *Cell Stem Cell* **3**, 467-468 (2008).
 135. Kanatsu-Shinohara, M. *et al.* Homing of mouse spermatogonial stem cells to germline niche depends on beta1-integrin. *Cell Stem Cell* **3**, 533-542 (2008).

136. Kanatsu-Shinohara, M., Morimoto, T., Toyokuni, S. & Shinohara, T. Regulation of mouse spermatogonial stem cell self-renewing division by the pituitary gland. *Biol. Reprod.* **70**, 1731-1737 (2004).
137. Yoshida, S., Sukeno, M. & Nabeshima, Y. A vasculature-associated niche for undifferentiated spermatogonia in the mouse testis. *Science* **317**, 1722-1726 (2007).
138. Oatley, J. M., Oatley, M. J., Avarbock, M. R., Tobias, J. W. & Brinster, R. L. Colony stimulating factor 1 is an extrinsic stimulator of mouse spermatogonial stem cell self-renewal. *Development* **136**, 1191-1199 (2009).
139. Xie, T. & Spradling, A. C. A niche maintaining germ line stem cells in the *Drosophila* ovary. *Science* **290**, 328-330 (2000).
140. Wirtz-Peitz, F. & Knoblich, J. A. Lethal giant larvae take on a life of their own. *Trends Cell Biol.* **16**, 234-241 (2006).
141. Betschinger, J., Eisenhaber, F. & Knoblich, J. A. Phosphorylation-induced autoinhibition regulates the cytoskeletal protein Lethal (2) giant larvae. *Curr. Biol.* **15**, 276-282 (2005).
142. Barros, C. S., Phelps, C. B. & Brand, A. H. *Drosophila* nonmuscle myosin II promotes the asymmetric segregation of cell fate determinants by cortical exclusion rather than active transport. *Dev. Cell* **5**, 829-840 (2003).
143. Wirtz-Peitz, F., Nishimura, T. & Knoblich, J. A. Linking cell cycle to asymmetric division: Aurora-A phosphorylates the Par complex to regulate Numb localization. *Cell* **135**, 161-173 (2008).
144. Smith, C. A. *et al.* aPKC-mediated phosphorylation regulates asymmetric membrane localization of the cell fate determinant Numb. *EMBO J.* **26**, 468-480 (2007).
145. Luo, J., Megee, S. & Dobrinski, I. Asymmetric distribution of UCH-L1 in spermatogonia is associated with maintenance and differentiation of spermatogonial stem cells. *J. Cell Physiol* **220**, 460-468 (2009).
146. Wang, Y. L. *et al.* Overexpression of ubiquitin carboxyl-terminal hydrolase L1 arrests spermatogenesis in transgenic mice. *Mol. Reprod. Dev.* **73**, 40-49 (2006).

147. Klezovitch, O., Fernandez, T. E., Tapscott, S. J. & Vasioukhin, V. Loss of cell polarity causes severe brain dysplasia in Lgl1 knockout mice. *Genes Dev.* **18**, 559-571 (2004).
148. Costa, M. R., Wen, G., Lepier, A., Schroeder, T. & Gotz, M. Par-complex proteins promote proliferative progenitor divisions in the developing mouse cerebral cortex. *Development* **135**, 11-22 (2008).
149. Konno, D. *et al.* Neuroepithelial progenitors undergo LGN-dependent planar divisions to maintain self-renewability during mammalian neurogenesis. *Nat. Cell Biol.* **10**, 93-101 (2008).
150. Noctor, S. C., Martinez-Cerdeno, V. & Kriegstein, A. R. Distinct behaviors of neural stem and progenitor cells underlie cortical neurogenesis. *J. Comp Neurol.* **508**, 28-44 (2008).
151. Kawase, E., Wong, M. D., Ding, B. C. & Xie, T. Gbb/Bmp signaling is essential for maintaining germline stem cells and for repressing bam transcription in the Drosophila testis. *Development* **131**, 1365-1375 (2004).
152. Brawley, C. & Matunis, E. Regeneration of male germline stem cells by spermatogonial dedifferentiation in vivo. *Science* **304**, 1331-1334 (2004).
153. Kiger, A. A., Jones, D. L., Schulz, C., Rogers, M. B. & Fuller, M. T. Stem cell self-renewal specified by JAK-STAT activation in response to a support cell cue. *Science* **294**, 2542-2545 (2001).
154. Shivdasani, A. A. & Ingham, P. W. Regulation of stem cell maintenance and transit amplifying cell proliferation by *tgf-beta* signaling in Drosophila spermatogenesis. *Curr. Biol.* **13**, 2065-2072 (2003).
155. Cox, D. N. *et al.* A novel class of evolutionarily conserved genes defined by piwi are essential for stem cell self-renewal. *Genes Dev.* **12**, 3715-3727 (1998).
156. Tazuke, S. I. *et al.* A germline-specific gap junction protein required for survival of differentiating early germ cells. *Development* **129**, 2529-2539 (2002).
157. Lee, J. *et al.* Akt mediates self-renewal division of mouse spermatogonial stem cells. *Development* **134**, 1853-1859 (2007).

158. Oatley, J. M., Avarbock, M. R., Telaranta, A. I., Fearon, D. T. & Brinster, R. L. Identifying genes important for spermatogonial stem cell self-renewal and survival. *Proc. Natl. Acad. Sci. U. S. A* **103**, 9524-9529 (2006).
159. Puglisi, R., Montanari, M., Chiarella, P., Stefanini, M. & Boitani, C. Regulatory role of BMP2 and BMP7 in spermatogonia and Sertoli cell proliferation in the immature mouse. *Eur. J. Endocrinol.* **151**, 511-520 (2004).
160. Zhao, G. Q., Chen, Y. X., Liu, X. M., Xu, Z. & Qi, X. Mutation in Bmp7 exacerbates the phenotype of Bmp8a mutants in spermatogenesis and epididymis. *Dev. Biol.* **240**, 212-222 (2001).
161. Kanatsu-Shinohara, M. *et al.* Long-term proliferation in culture and germline transmission of mouse male germline stem cells. *Biol. Reprod.* **69**, 612-616 (2003).
162. Kanatsu-Shinohara, M. *et al.* Long-term culture of mouse male germline stem cells under serum-or feeder-free conditions. *Biol. Reprod.* **72**, 985-991 (2005).
163. Kanatsu-Shinohara, M. *et al.* Clonal origin of germ cell colonies after spermatogonial transplantation in mice. *Biol. Reprod.* **75**, 68-74 (2006).
164. Tsuda, M. *et al.* Conserved role of nanos proteins in germ cell development. *Science* **301**, 1239-1241 (2003).
165. Falender, A. E. *et al.* Maintenance of spermatogenesis requires TAF4b, a gonad-specific subunit of TFIID. *Genes Dev.* **19**, 794-803 (2005).
166. Buaas, F. W. *et al.* Plzf is required in adult male germ cells for stem cell self-renewal. *Nat. Genet.* **36**, 647-652 (2004).
167. Schulz, C. *et al.* A misexpression screen reveals effects of bag-of-marbles and TGF beta class signaling on the Drosophila male germ-line stem cell lineage. *Genetics* **167**, 707-723 (2004).
168. Gilboa, L., Forbes, A., Tazuke, S. I., Fuller, M. T. & Lehmann, R. Germ line stem cell differentiation in Drosophila requires gap junctions and proceeds via an intermediate state. *Development* **130**, 6625-6634 (2003).
169. Tazuke, S. I. *et al.* A germline-specific gap junction protein required for survival of differentiating early germ cells. *Development* **129**, 2529-2539

(2002).

170. Matunis, E., Tran, J., Gonczy, P., Caldwell, K. & DiNardo, S. *punt* and *schnurri* regulate a somatically derived signal that restricts proliferation of committed progenitors in the germline. *Development* **124**, 4383-4391 (1997).
171. Kiger, A. A., White-Cooper, H. & Fuller, M. T. Somatic support cells restrict germline stem cell self-renewal and promote differentiation. *Nature* **407**, 750-754 (2000).
172. Tran, J., Brenner, T. J. & DiNardo, S. Somatic control over the germline stem cell lineage during *Drosophila* spermatogenesis. *Nature* **407**, 754-757 (2000).
173. Schulz, C., Wood, C. G., Jones, D. L., Tazuke, S. I. & Fuller, M. T. Signaling from germ cells mediated by the rhomboid homolog *stet* organizes encapsulation by somatic support cells. *Development* **129**, 4523-4534 (2002).
174. Yoshinaga, K. *et al.* Role of *c-kit* in mouse spermatogenesis: identification of spermatogonia as a specific site of *c-kit* expression and function. *Development* **113**, 689-699 (1991).
175. de Rooij, D. G., Okabe, M. & Nishimune, Y. Arrest of spermatogonial differentiation in *jsd/jsd*, *Sl17H/Sl17H*, and cryptorchid mice. *Biol. Reprod.* **61**, 842-847 (1999).
176. Feng, L. X. *et al.* Generation and in vitro differentiation of a spermatogonial cell line. *Science* **297**, 392-395 (2002).
177. Nagano, M., Ryu, B. Y., Brinster, C. J., Avarbock, M. R. & Brinster, R. L. Maintenance of mouse male germ line stem cells in vitro. *Biol. Reprod.* **68**, 2207-2214 (2003).
178. Pellegrini, M., Grimaldi, P., Rossi, P., Geremia, R. & Dolci, S. Developmental expression of BMP4/ALK3/SMAD5 signaling pathway in the mouse testis: a potential role of BMP4 in spermatogonia differentiation. *J. Cell Sci.* **116**, 3363-3372 (2003).
179. Yoshida, S. *et al.* Neurogenin3 delineates the earliest stages of spermatogenesis in the mouse testis. *Dev. Biol.* **269**, 447-458 (2004).
180. Kanatsu-Shinohara, M. & Shinohara, T. Culture and genetic modification of mouse germline stem cells. *Ann. N. Y. Acad. Sci.* **1120**, 59-71 (2007).

181. Ogawa, T. *et al.* Derivation and morphological characterization of mouse spermatogonial stem cell lines. *Arch. Histol. Cytol.* **67**, 297-306 (2004).
182. Sariola, H. & Immonen, T. GDNF maintains mouse spermatogonial stem cells in vivo and in vitro. *Methods Mol. Biol.* **450**, 127-135 (2008).
183. Ogawa, T., Arechaga, J. M., Avarbock, M. R. & Brinster, R. L. Transplantation of testis germinal cells into mouse seminiferous tubules. *Int. J. Dev. Biol.* **41**, 111-122 (1997).
184. Oatley, J. M., Avarbock, M. R., Telaranta, A. I., Fearon, D. T. & Brinster, R. L. Identifying genes important for spermatogonial stem cell self-renewal and survival. *Proc. Natl. Acad. Sci. U. S. A* **103**, 9524-9529 (2006).
185. Kanatsu-Shinohara, M. *et al.* Allogeneic offspring produced by male germ line stem cell transplantation into infertile mouse testis. *Biol. Reprod.* **68**, 167-173 (2003).
186. Nagano, M. *et al.* Transgenic mice produced by retroviral transduction of male germ-line stem cells. *Proc. Natl. Acad. Sci. U. S. A* **98**, 13090-13095 (2001).
187. Brinster, R. L. & Zimmermann, J. W. Spermatogenesis following male germ-cell transplantation. *Proc. Natl. Acad. Sci. U. S. A* **91**, 11298-11302 (1994).
188. Brinster, R. L. & Avarbock, M. R. Germline transmission of donor haplotype following spermatogonial transplantation. *Proc. Natl. Acad. Sci. U. S. A* **91**, 11303-11307 (1994).
189. Kanatsu-Shinohara, M., Toyokuni, S. & Shinohara, T. Genetic selection of mouse male germline stem cells in vitro: offspring from single stem cells. *Biol. Reprod.* **72**, 236-240 (2005).
190. Kanatsu-Shinohara, M. *et al.* Leukemia inhibitory factor enhances formation of germ cell colonies in neonatal mouse testis culture. *Biol. Reprod.* **76**, 55-62 (2007).
191. Yomogida, K., Yagura, Y., Tadokoro, Y. & Nishimune, Y. Dramatic expansion of germinal stem cells by ectopically expressed human glial cell line-derived neurotrophic factor in mouse Sertoli cells. *Biol. Reprod.* **69**, 1303-1307 (2003).

192. Kubota, H., Avarbock, M. R. & Brinster, R. L. Culture conditions and single growth factors affect fate determination of mouse spermatogonial stem cells. *Biol. Reprod.* **71**, 722-731 (2004).
193. Kanatsu-Shinohara, M. *et al.* Anchorage-independent growth of mouse male germline stem cells in vitro. *Biol. Reprod.* **74**, 522-529 (2006).
194. Wang, Z. F., Sirotkin, A. M., Buchold, G. M., Skoultchi, A. I. & Marzluff, W. F. The mouse histone H1 genes: gene organization and differential regulation. *J. Mol. Biol.* **271**, 124-138 (1997).
195. Sarg, B., Chwatal, S., Talasz, H. & Lindner, H. H. Testis-specific linker histone H1t is multiply phosphorylated during spermatogenesis. Identification of phosphorylation sites. *J. Biol. Chem.* **284**, 3610-3618 (2009).
196. Resnick, J. L., Bixler, L. S., Cheng, L. & Donovan, P. J. Long-term proliferation of mouse primordial germ cells in culture. *Nature* **359**, 550-551 (1992).
197. Matsui, Y., Zsebo, K. & Hogan, B. L. Derivation of pluripotential embryonic stem cells from murine primordial germ cells in culture. *Cell* **70**, 841-847 (1992).
198. Pesce, M. & Scholer, H. R. Oct-4: gatekeeper in the beginnings of mammalian development. *Stem Cells* **19**, 271-278 (2001).
199. Anderson, R., Schaible, K., Heasman, J. & Wylie, C. Expression of the homophilic adhesion molecule, Ep-CAM, in the mammalian germ line. *J. Reprod. Fertil.* **116**, 379-384 (1999).
200. Lele, K. M. & Wolgemuth, D. J. Distinct regions of the mouse cyclin A1 gene, *Ccn1*, confer male germ-cell specific expression and enhancer function. *Biol. Reprod.* **71**, 1340-1347 (2004).
201. Nayernia, K. *et al.* Derivation of male germ cells from bone marrow stem cells. *Lab Invest* **86**, 654-663 (2006).
202. Johannesson, M. *et al.* FGF4 and retinoic acid direct differentiation of hESCs into PDX1-expressing foregut endoderm in a time- and concentration-dependent manner. *PLoS. One.* **4**, e4794 (2009).
203. Kim, M. *et al.* Regulation of mouse embryonic stem cell neural

- differentiation by retinoic acid. *Dev. Biol.* **328**, 456-471 (2009).
204. Ostrom, M. *et al.* Retinoic acid promotes the generation of pancreatic endocrine progenitor cells and their further differentiation into beta-cells. *PLoS. One.* **3**, e2841 (2008).
 205. Yoshida, S., Nabeshima, Y. & Nakagawa, T. Stem cell heterogeneity: actual and potential stem cell compartments in mouse spermatogenesis. *Ann. N. Y. Acad. Sci.* **1120**, 47-58 (2007).
 206. Yamashita, Y. M., Mahowald, A. P., Perlin, J. R. & Fuller, M. T. Asymmetric inheritance of mother versus daughter centrosome in stem cell division. *Science* **315**, 518-521 (2007).
 207. Betschinger, J., Mechtler, K. & Knoblich, J. A. Asymmetric segregation of the tumor suppressor brat regulates self-renewal in Drosophila neural stem cells. *Cell* **124**, 1241-1253 (2006).
 208. Lee, C. Y., Wilkinson, B. D., Siegrist, S. E., Wharton, R. P. & Doe, C. Q. Brat is a Miranda cargo protein that promotes neuronal differentiation and inhibits neuroblast self-renewal. *Dev. Cell* **10**, 441-449 (2006).
 209. Nagano, M., Avarbock, M. R., Leonida, E. B., Brinster, C. J. & Brinster, R. L. Culture of mouse spermatogonial stem cells. *Tissue Cell* **30**, 389-397 (1998).
 210. Tadokoro, Y., Yomogida, K., Ohta, H., Tohda, A. & Nishimune, Y. Homeostatic regulation of germinal stem cell proliferation by the GDNF/FSH pathway. *Mech. Dev.* **113**, 29-39 (2002).
 211. Kanatsu-Shinohara, M. *et al.* Production of knockout mice by random or targeted mutagenesis in spermatogonial stem cells. *Proc. Natl. Acad. Sci. U. S. A* **103**, 8018-8023 (2006).
 212. Takehashi, M. *et al.* Adenovirus-mediated gene delivery into mouse spermatogonial stem cells. *Proc. Natl. Acad. Sci. U. S. A* **104**, 2596-2601 (2007).
 213. Conner DA. *Current Protocols in Molecular Biology*. (John Wiley & Sons, Inc.,2001).
 214. He, Z., Jiang, J., Hofmann, M. C. & Dym, M. Gfra1 silencing in mouse spermatogonial stem cells results in their differentiation via the inactivation

- of RET tyrosine kinase. *Biol. Reprod.* **77**, 723-733 (2007).
215. Hofmann, M. C., Braydich-Stolle, L. & Dym, M. Isolation of male germ-line stem cells; influence of GDNF. *Dev. Biol.* **279**, 114-124 (2005).
 216. von, S., V, Wistuba, J. & Schlatt, S. Notch-1, c-kit and GFRalpha-1 are developmentally regulated markers for premeiotic germ cells. *Cytogenet. Genome Res.* **105**, 235-239 (2004).
 217. Filipponi, D. *et al.* Repression of kit expression by Plzf in germ cells. *Mol. Cell Biol.* **27**, 6770-6781 (2007).
 218. Cunto, F. D. *et al.* Essential role of citron kinase in cytokinesis of spermatogenic precursors. *J. Cell Sci.* **115**, 4819-4826 (2002).
 219. Lee, J. *et al.* Genetic reconstruction of mouse spermatogonial stem cell self-renewal in vitro by Ras-cyclin D2 activation. *Cell Stem Cell* **5**, 76-86 (2009).
 220. Ichim, C. V. & Wells, R. A. First among equals: the cancer cell hierarchy. *Leuk. Lymphoma* **47**, 2017-2027 (2006).
 221. Heppner, G. H. Tumor heterogeneity. *Cancer Res.* **44**, 2259-2265 (1984).
 222. Heppner, G. H. & Miller, B. E. Tumor heterogeneity: biological implications and therapeutic consequences. *Cancer Metastasis Rev.* **2**, 5-23 (1983).
 223. Campbell, L. L. & Polyak, K. Breast tumor heterogeneity: cancer stem cells or clonal evolution? *Cell Cycle* **6**, 2332-2338 (2007).
 224. Merlo, L. M., Pepper, J. W., Reid, B. J. & Maley, C. C. Cancer as an evolutionary and ecological process. *Nat. Rev. Cancer* **6**, 924-935 (2006).
 225. Nowell, P. C. The clonal evolution of tumor cell populations. *Science* **194**, 23-28 (1976).
 226. Crespi, B. & Summers, K. Evolutionary biology of cancer. *Trends Ecol. Evol.* **20**, 545-552 (2005).
 227. Reya, T., Morrison, S. J., Clarke, M. F. & Weissman, I. L. Stem cells, cancer, and cancer stem cells. *Nature* **414**, 105-111 (2001).
 228. Pardal, R., Clarke, M. F. & Morrison, S. J. Applying the principles of

- stem-cell biology to cancer. *Nat. Rev. Cancer* **3**, 895-902 (2003).
229. Bjerkvig, R., Tysnes, B. B., Aboody, K. S., Najbauer, J. & Terzis, A. J. Opinion: the origin of the cancer stem cell: current controversies and new insights. *Nat. Rev. Cancer* **5**, 899-904 (2005).
 230. Polyak, K. & Hahn, W. C. Roots and stems: stem cells in cancer. *Nat. Med.* **12**, 296-300 (2006).
 231. Barabe, F., Kennedy, J. A., Hope, K. J. & Dick, J. E. Modeling the initiation and progression of human acute leukemia in mice. *Science* **316**, 600-604 (2007).
 232. Krivtsov, A. V. *et al.* Transformation from committed progenitor to leukaemia stem cell initiated by MLL-AF9. *Nature* **442**, 818-822 (2006).
 233. Jordan, C. T. Cancer stem cells: controversial or just misunderstood? *Cell Stem Cell* **4**, 203-205 (2009).
 234. Singh, S. K. *et al.* Identification of human brain tumour initiating cells. *Nature* **432**, 396-401 (2004).
 235. Bao, S. *et al.* Glioma stem cells promote radioresistance by preferential activation of the DNA damage response. *Nature* **444**, 756-760 (2006).
 236. Eramo, A. *et al.* Identification and expansion of the tumorigenic lung cancer stem cell population. *Cell Death. Differ.* **15**, 504-514 (2008).
 237. Yang, Z. F. *et al.* Significance of CD90+ cancer stem cells in human liver cancer. *Cancer Cell* **13**, 153-166 (2008).
 238. O'Brien, C. A., Pollett, A., Gallinger, S. & Dick, J. E. A human colon cancer cell capable of initiating tumour growth in immunodeficient mice. *Nature* **445**, 106-110 (2007).
 239. Ricci-Vitiani, L. *et al.* Identification and expansion of human colon-cancer-initiating cells. *Nature* **445**, 111-115 (2007).
 240. Dalerba, P. *et al.* Phenotypic characterization of human colorectal cancer stem cells. *Proc. Natl. Acad. Sci. U. S. A* **104**, 10158-10163 (2007).
 241. Hermann, P. C. *et al.* Distinct populations of cancer stem cells determine tumor growth and metastatic activity in human pancreatic cancer. *Cell Stem*

- Cell* **1**, 313-323 (2007).
242. Li, C. *et al.* Identification of pancreatic cancer stem cells. *Cancer Res.* **67**, 1030-1037 (2007).
 243. Al-Hajj, M., Wicha, M. S., Ito-Hernandez, A., Morrison, S. J. & Clarke, M. F. Prospective identification of tumorigenic breast cancer cells. *Proc. Natl. Acad. Sci. U. S. A* **100**, 3983-3988 (2003).
 244. Yu, F. *et al.* let-7 regulates self renewal and tumorigenicity of breast cancer cells. *Cell* **131**, 1109-1123 (2007).
 245. Cho, R. W. & Clarke, M. F. Recent advances in cancer stem cells. *Curr. Opin. Genet. Dev.* **18**, 48-53 (2008).
 246. Quintana, E. *et al.* Efficient tumour formation by single human melanoma cells. *Nature* **456**, 593-598 (2008).
 247. Glinsky, G. V., Berezovska, O. & Glinskii, A. B. Microarray analysis identifies a death-from-cancer signature predicting therapy failure in patients with multiple types of cancer. *J. Clin. Invest* **115**, 1503-1521 (2005).
 248. Lahad, J. P., Mills, G. B. & Coombes, K. R. Stem cell-ness: a "magic marker" for cancer. *J. Clin. Invest* **115**, 1463-1467 (2005).
 249. Ishikawa, F. *et al.* Chemotherapy-resistant human AML stem cells home to and engraft within the bone-marrow endosteal region. *Nat. Biotechnol.* **25**, 1315-1321 (2007).
 250. Venezia, T. A. *et al.* Molecular signatures of proliferation and quiescence in hematopoietic stem cells. *PLoS Biol.* **2**, e301 (2004).
 251. Park, Y. & Gerson, S. L. DNA repair defects in stem cell function and aging. *Annu. Rev. Med.* **56**, 495-508 (2005).
 252. Wang, S., Yang, D. & Lippman, M. E. Targeting Bcl-2 and Bcl-XL with nonpeptidic small-molecule antagonists. *Semin. Oncol.* **30**, 133-142 (2003).
 253. Ricci-Vitiani, L., Pagliuca, A., Palio, E., Zeuner, A. & De, M. R. Colon cancer stem cells. *Gut* **57**, 538-548 (2008).
 254. Muller-Sieburg, C. E., Cho, R. H., Thoman, M., Adkins, B. & Sieburg, H. B. Deterministic regulation of hematopoietic stem cell self-renewal and

- differentiation. *Blood* **100**, 1302-1309 (2002).
255. van Staveren, W. C. *et al.* Human cancer cell lines: Experimental models for cancer cells in situ? For cancer stem cells? *Biochim. Biophys. Acta* **1795**, 92-103 (2009).
 256. Kondo, T. Stem cell-like cancer cells in cancer cell lines. *Cancer Biomark.* **3**, 245-250 (2007).
 257. Zucchi, I. *et al.* The properties of a mammary gland cancer stem cell. *Proc. Natl. Acad. Sci. U. S. A* **104**, 10476-10481 (2007).
 258. Wang, J., Guo, L. P., Chen, L. Z., Zeng, Y. X. & Lu, S. H. Identification of cancer stem cell-like side population cells in human nasopharyngeal carcinoma cell line. *Cancer Res.* **67**, 3716-3724 (2007).
 259. Yu, F. *et al.* let-7 regulates self renewal and tumorigenicity of breast cancer cells. *Cell* **131**, 1109-1123 (2007).
 260. Chiba, T. *et al.* Side population purified from hepatocellular carcinoma cells harbors cancer stem cell-like properties. *Hepatology* **44**, 240-251 (2006).
 261. Pardal, R., Molofsky, A. V., He, S. & Morrison, S. J. Stem cell self-renewal and cancer cell proliferation are regulated by common networks that balance the activation of proto-oncogenes and tumor suppressors. *Cold Spring Harb. Symp. Quant. Biol.* **70**, 177-185 (2005).
 262. Lobo, N. A., Shimono, Y., Qian, D. & Clarke, M. F. The biology of cancer stem cells. *Annu. Rev. Cell Dev. Biol.* **23**, 675-699 (2007).
 263. Taipale, J. & Beachy, P. A. The Hedgehog and Wnt signalling pathways in cancer. *Nature* **411**, 349-354 (2001).
 264. Jiang, J. & Hui, C. C. Hedgehog signaling in development and cancer. *Dev. Cell* **15**, 801-812 (2008).
 265. Wang, Z., Li, Y., Banerjee, S. & Sarkar, F. H. Emerging role of Notch in stem cells and cancer. *Cancer Lett.* **279**, 8-12 (2009).
 266. Sneddon, J. B. & Werb, Z. Location, location, location: the cancer stem cell niche. *Cell Stem Cell* **1**, 607-611 (2007).
 267. Arkenau, H. T., Chua, Y. J. & Cunningham, D. Current treatment strategies in

- elderly patients with metastatic colorectal cancer. *Clin. Colorectal Cancer* **6**, 508-515 (2007).
268. Liotta, L. A. & Kohn, E. C. The microenvironment of the tumour-host interface. *Nature* **411**, 375-379 (2001).
269. Fong, Y., Kemeny, N., Paty, P., Blumgart, L. H. & Cohen, A. M. Treatment of colorectal cancer: hepatic metastasis. *Semin. Surg. Oncol.* **12**, 219-252 (1996).
270. Shmelkov, S. V. *et al.* CD133 expression is not restricted to stem cells, and both CD133+ and C. *J. Clin. Invest* **118**, 2111-2120 (2008).
271. Du, L. *et al.* CD44 is of functional importance for colorectal cancer stem cells. *Clin. Cancer Res.* **14**, 6751-6760 (2008).
272. Haraguchi, N. *et al.* CD133+CD44+ population efficiently enriches colon cancer initiating cells. *Ann. Surg. Oncol.* **15**, 2927-2933 (2008).
273. Boman, B. M. & Huang, E. Human colon cancer stem cells: a new paradigm in gastrointestinal oncology. *J. Clin. Oncol.* **26**, 2828-2838 (2008).
274. Vermeulen, L. *et al.* Single-cell cloning of colon cancer stem cells reveals a multi-lineage differentiation capacity. *Proc. Natl. Acad. Sci. U. S. A* **105**, 13427-13432 (2008).
275. Humphries, A. & Wright, N. A. Colonic crypt organization and tumorigenesis. *Nat. Rev. Cancer* **8**, 415-424 (2008).
276. Barker, N. *et al.* Crypt stem cells as the cells-of-origin of intestinal cancer. *Nature* **457**, 608-611 (2009).
277. Gregorieff, A. & Clevers, H. Wnt signaling in the intestinal epithelium: from endoderm to cancer. *Genes Dev.* **19**, 877-890 (2005).
278. He, T. C. *et al.* Identification of c-MYC as a target of the APC pathway. *Science* **281**, 1509-1512 (1998).
279. Shtutman, M. *et al.* The cyclin D1 gene is a target of the beta-catenin/LEF-1 pathway. *Proc. Natl. Acad. Sci. U. S. A* **96**, 5522-5527 (1999).
280. Tetsu, O. & McCormick, F. Beta-catenin regulates expression of cyclin D1 in colon carcinoma cells. *Nature* **398**, 422-426 (1999).

281. Hult, J. *et al.* Cyclin D1 genetic heterozygosity regulates colonic epithelial cell differentiation and tumor number in ApcMin mice. *Mol. Cell Biol.* **24**, 7598-7611 (2004).
282. Sancho, E., Batlle, E. & Clevers, H. Signaling pathways in intestinal development and cancer. *Annu. Rev. Cell Dev. Biol.* **20**, 695-723 (2004).
283. He, X. C. *et al.* BMP signaling inhibits intestinal stem cell self-renewal through suppression of Wnt-beta-catenin signaling. *Nat. Genet.* **36**, 1117-1121 (2004).
284. Cui, W., Taub, D. D. & Gardner, K. qPrimerDepot: a primer database for quantitative real time PCR. *Nucleic Acids Res.* **35**, D805-D809 (2007).
285. Burkert, J., Otto, W. R. & Wright, N. A. Side populations of gastrointestinal cancers are not enriched in stem cells. *J. Pathol.* **214**, 564-573 (2008).
286. Stoker, M. G. & Rubin, H. Density dependent inhibition of cell growth in culture. *Nature* **215**, 171-172 (1967).
287. Fisher, H. W. & Yeh, J. Contact inhibition in colony formation. *Science* **155**, 581-582 (1967).
288. Takai, Y., Miyoshi, J., Ikeda, W. & Ogita, H. Nectins and nectin-like molecules: roles in contact inhibition of cell movement and proliferation. *Nat. Rev. Mol. Cell Biol.* **9**, 603-615 (2008).
289. Bell, P. B., Jr. Contact inhibition of movements in transformed and nontransformed cells. *Birth Defects Orig. Artic. Ser.* **14**, 177-194 (1978).
290. Marasanapalle, V., Li, X., Polin, L. & Jasti, B. R. Novel in vitro model barriers for evaluation of the permeability of antitumor compounds, thioxanthenes. *Invest New Drugs* **24**, 111-116 (2006).
291. Evan, G. I. & Vousden, K. H. Proliferation, cell cycle and apoptosis in cancer. *Nature* **411**, 342-348 (2001).
292. Ding, Q. M., Ko, T. C. & Evers, B. M. Caco-2 intestinal cell differentiation is associated with G1 arrest and suppression of CDK2 and CDK4. *Am. J. Physiol* **275**, C1193-C1200 (1998).
293. Polyak, K. & Weinberg, R. A. Transitions between epithelial and

mesenchymal states: acquisition of malignant and stem cell traits. *Nat. Rev. Cancer* **9**, 265-273 (2009).

294. Yin, L. L. *et al.* A suppressor of multiple extracellular matrix-degrading proteases and cancer metastasis. *J. Cell Mol. Med.* (2008).
295. Odoux, C. *et al.* A stochastic model for cancer stem cell origin in metastatic colon cancer. *Cancer Res.* **68**, 6932-6941 (2008).
296. Markowitz, A. J. *et al.* Regulation of lineage-specific transcription of the sucrase-isomaltase gene in transgenic mice and cell lines. *Am. J. Physiol* **269**, G925-G939 (1995).
297. Jumarie, C. & Malo, C. Caco-2 cells cultured in serum-free medium as a model for the study of enterocytic differentiation in vitro. *J. Cell Physiol* **149**, 24-33 (1991).
298. O'Brien, C. A., Pollett, A., Gallinger, S. & Dick, J. E. A human colon cancer cell capable of initiating tumour growth in immunodeficient mice. *Nature* **445**, 106-110 (2007).
299. Gattoni-Celli, S. *et al.* Partial suppression of anchorage-independent growth and tumorigenicity in immunodeficient mice by transfection of the H-2 class I gene H-2Ld into a human colon cancer cell line (HCT). *Proc. Natl. Acad. Sci. U. S. A* **85**, 8543-8547 (1988).
300. Yasuda, A. *et al.* The stem cell factor/c-kit receptor pathway enhances proliferation and invasion of pancreatic cancer cells. *Mol. Cancer* **5**, 46 (2006).
301. Bashamboo, A. *et al.* The survival of differentiating embryonic stem cells is dependent on the SCF-KIT pathway. *J. Cell Sci.* **119**, 3039-3046 (2006).
302. Yasuda, A. *et al.* Stem cell factor/c-kit receptor signaling enhances the proliferation and invasion of colorectal cancer cells through the PI3K/Akt pathway. *Dig. Dis. Sci.* **52**, 2292-2300 (2007).
303. Ronnstrand, L. Signal transduction via the stem cell factor receptor/c-Kit. *Cell Mol. Life Sci.* **61**, 2535-2548 (2004).
304. Tamir, A. *et al.* Stem cell factor inhibits erythroid differentiation by modulating the activity of G1-cyclin-dependent kinase complexes: a role for

- p27 in erythroid differentiation coupled G1 arrest. *Cell Growth Differ.* **11**, 269-277 (2000).
305. Evers, B. M., Ko, T. C., Li, J. & Thompson, E. A. Cell cycle protein suppression and p21 induction in differentiating Caco-2 cells. *Am. J. Physiol* **271**, G722-G727 (1996).
 306. Daly, A. C., Randall, R. A. & Hill, C. S. Transforming growth factor beta-induced Smad1/5 phosphorylation in epithelial cells is mediated by novel receptor complexes and is essential for anchorage-independent growth. *Mol. Cell Biol.* **28**, 6889-6902 (2008).
 307. Freudenberg, J. A. & Chen, W. T. Induction of Smad1 by MT1-MMP contributes to tumor growth. *Int. J. Cancer* **121**, 966-977 (2007).
 308. Korchynskiy, O. *et al.* Expression of Smad proteins in human colorectal cancer. *Int. J. Cancer* **82**, 197-202 (1999).
 309. Gordon, K. J., Kirkbride, K. C., How, T. & Blobe, G. C. Bone morphogenetic proteins induce pancreatic cancer cell invasiveness through a Smad1-dependent mechanism that involves matrix metalloproteinase-2. *Carcinogenesis* **30**, 238-248 (2009).
 310. Hamel, P. A. & Hanley-Hyde, J. G1 cyclins and control of the cell division cycle in normal and transformed cells. *Cancer Invest* **15**, 143-152 (1997).
 311. Sherr, C. J. D-type cyclins. *Trends Biochem. Sci.* **20**, 187-190 (1995).
 312. Kobayashi, T. *et al.* Restoration of cyclin D2 has an inhibitory potential on the proliferation of LNCaP cells. *Biochem. Biophys. Res. Commun.* (2009).
 313. Roy, M. K. *et al.* Inhibition of colon cancer (HT-29) cell proliferation by a triterpenoid isolated from *Azadirachta indica* is accompanied by cell cycle arrest and up-regulation of p21. *Planta Med.* **72**, 917-923 (2006).
 314. Dey, A. & Li, W. Cell cycle-independent induction of D1 and D2 cyclin expression, but not cyclin-Cdk complex formation or Rb phosphorylation, by IFN γ in macrophages. *Biochim. Biophys. Acta* **1497**, 135-147 (2000).
 315. Mermelshtein, A. *et al.* Expression of D-type cyclins in colon cancer and in cell lines from colon carcinomas. *Br. J. Cancer* **93**, 338-345 (2005).

316. Matsui, J., Wakabayashi, T., Asada, M., Yoshimatsu, K. & Okada, M. Stem cell factor/c-kit signaling promotes the survival, migration, and capillary tube formation of human umbilical vein endothelial cells. *J. Biol. Chem.* **279**, 18600-18607 (2004).
317. Shen, H. *et al.* Transforming growth factor-beta1 downregulation of Smad1 gene expression in rat hepatic stellate cells. *Am. J. Physiol Gastrointest. Liver Physiol* **285**, G539-G546 (2003).
318. de Bruine, A. P. *et al.* Human Caco-2 cells transfected with c-Ha-Ras as a model for endocrine differentiation in the large intestine. *Differentiation* **53**, 51-60 (1993).
319. Schroy, P. C. *et al.* Growth and intestinal differentiation are independently regulated in HT29 colon cancer cells. *J. Cell Physiol* **161**, 111-123 (1994).
320. Takahashi, K. & Yamanaka, S. Induction of pluripotent stem cells from mouse embryonic and adult fibroblast cultures by defined factors. *Cell* **126**, 663-676 (2006).
321. Baker, M. Stem cells: Fast and furious. *Nature* **458**, 962-965 (2009).
322. Chin, M. H. *et al.* Induced pluripotent stem cells and embryonic stem cells are distinguished by gene expression signatures. *Cell Stem Cell* **5**, 111-123 (2009).
323. Miura, K. *et al.* Variation in the safety of induced pluripotent stem cell lines. *Nat. Biotechnol.* (2009).

Appendix

I. Primer list

Primer name	Sequence	Annealing temp.
AR F	5' - AGT CAA TGG GCA AAA CAT GG - 3'	60°C
AR R	5' - TTG TGT CAA AAG CGA AAT GG - 3'	60°C
ARL11 F	5' - ATT CAC AGA ACC CAT GGT GG - 3'	60°C
ARL11 R	5' - CTT CCT TCC CAT CTC GCT CT - 3'	60°C
Ccna1 F	5' - GCT GTG GCT TAC TAG GCA AT - 3'	55°C
Ccna1 R	5' - GCT GTG GCT TAC TAG GCA AT - 3'	55°C
CCND2 F	5' - ACG TTG GTC CTG ACG GTA CT - 3'	60°C
CCND2 R	5' - TGA GCT GCT GGC TAA GAT CA - 3'	60°C
Cd9 F	5' - TGA TGC TGG TTG GTT TCC - 3'	55°C
Cd9 R	5' - CCC ACT GCT CCA ATG ATG - 3'	55°C
c-kit F	5' - CTG CCG AAA TGT ATG ACG - 3'	55°C
c-kit R	5' - TCG TAA AGG CGG AAT CAC - 3'	55°C
E-cadherin F	5' - GAC AAC GCT CCC ATC CCA - 3'	55°C
E-cadherin R	5' - CCA CCT CCT TCT TCA TCA TAG - 3'	55°C
EpCAM F	5' - AGA ACC GAC AAG GAC ACG - 3'	55°C
EpCAM R	5' - ACC ACA ATG ACA GCG ATG - 3'	55°C
FGF12 F	5' - GGT ACC ATC TGG GTG CAT CT - 3'	62°C
FGF12 R	5' - ATT GAA CTT CCC AGC ACT CG - 3'	62°C
GAPDH F	5' - TCC CAT CAC CAT CTT CCA G - 3'	52°C
GAPDH R	5' - TCC ACC ACT GAC ACG TTG - 3'	52°C
Gapdh F	5' - GAC CAC AGT CCA TGC CAT CAC TGC - 3'	60°C
Gapdh R	5' - GCT GTT GAA GTC GCA GGA GAC AAC - 3'	60°C
GAPDH Realtime F	5' - AGG GTC ATC ATC TCT GCC - 3'	60°C
GAPDH Realtime R	5' - CCA TCA CGC CAC AGT TTC - 3'	60°C
HDGFRP3 F	5' - GGA AAA AGG TCT TTG GGA CC - 3'	60°C
HDGFRP3 R	5' - CAA GAT GAA GGG CTA CCC G - 3'	60°C
HIF3 F	5' - TCT TGA CCA TGT CGG AAA CG - 3'	60°C
HIF3 R	5' - CTT TGG CGG GGC TTT TAC GT - 3'	60°C
KIT F	5' - GTT CTG CTC CTA CTG CTT CGC - 3'	60°C
KIT R	5' - TAA CAG CCT AAT CTC GTC GCC - 3'	60°C
LUM F	5' - AGT AGG ATA ATG GCC CCA GG - 3'	62°C
LUM R	5' - GGT TGA GCT GGA TCT GTC CT - 3'	62°C

Primer name	Sequence	Annealing temp.
Oct3/4 F	5' - TGG CAT ACT GTG GAC CTC - 3'	62°C
Oct3/4 R	5' - ATT GTT GTC GGC TTC CTC - 3'	62°C
PTPN13 F	5' - GCC CAT ATT TCT TCC TCC TGA - 3'	60°C
PTPN13 R	5' - GCG CTC CAG TAG CAG GAC - 3'	60°C
SMAD-1 F	5' - TTG AAG TCC AGA AGA GTA GAA ATT ACC - 3'	60°C
SMAD-1 R	5' - CCA CTC GTG CTC CCA CA - 3'	60°C
SSEA-1 F	5' - ATT CCA GTG CCT TGA GCC - 3'	60°C
SSEA-1 R	5' - ACC CAA GGA AGC CAA AGG - 3'	60°C
STK31 F	5' - GCA TAG ATC AAA CCA GTC AAC C - 3'	55°C
STK31 R	5' - AGT AGT AAA GCA CCC TTC ATC C - 3'	55°C
Stk31 F	5' - ACT TAG CAG CAA GCG TCC - 3'	55°C
Stk31 R	5' - GAG AGC AAA CTC AAT CCA CC - 3'	55°C
Stk31 FL F	5' - ATA GCG GCC GCA AGC TGG AGG GCT GAG G - 3'	62°C
Stk31 FL R	5' - GGG GGA TCC AAG GGA CAT ATA CAG CAA CAA - 3'	62°C
STK31 miR 1F	5' - TGC TGT AAA GTC ACC AAC AGC CAA ACG TTT TGG CCA CTG ACT GAC GTT TGG CTT GGT GAC TTT A - 3'	N/A
STK31 miR 1R	5' - CCT GTA AAG TCA CCA AGC CAA ACG TCA GTC AGT GGC CAA AAC GTT TGG CTG TTG GTG ACT TTA C - 3'	N/A
STK31 miR 2F	5' - TGC TGA TAA GTC TGA ACC TGG AGA AGG TTT TGG CCA CTG ACT GAC CTT CTC CAT TCA GAC TTA T - 3'	N/A
STK31 miR 2R	5' - CCT GAT AAG TCT GAA TGG AGA AGG TCA GTC AGT GGC CAA AAC CTT CTC CAG GTT CAG ACT TAT C - 3'	N/A
STK31 miR 453 F	5' - TGC TGT GAG CAA CCA ATC TTC ATG ATG TTT TGG CCA CTG ACT GAC ATC ATG AAT TGG TTG CTC A - 3'	N/A
STK31 miR 453 R	5' - CCT GTG AGC AAC CAA TTC ATG ATG TCA GTC AGT GGC CAA AAC ATC ATG AAG ATT GGT TGC TCA C - 3'	N/A
β 1-integrin F	5' - ACC AAT CGC AGC AAA GGG - 3'	60°C
β 1-integrin R	5' - TGA AAC CCA GCA TCC GTG - 3'	60°C

II. PCR reaction

Template	1 ul
Primer F (2.5 uM)	2.5 ul
Primer R (2.5 uM)	2.5 ul
dNTPs (10 uM)	0.5 ul
<i>Go Taq</i>	0.2 ul
10X PCR buffer	2.5 ul
ddH ₂ O	15.8 ul

III. Cloning PCR reaction

Template	2 ul
Primer F (2.5 uM)	2.5 ul
Primer R (2.5 uM)	2.5 ul
dNTPs (10 uM)	1 ul
<i>FideliTaq</i>	0.2 ul
10X <i>FideliTaq</i> buffer	2.5 ul
MgCl ₂ (25 mM)	0.25 ul
ddH ₂ O	14.05 ul

IV. Real-time PCR reaction

Template	2.5 ul
Primer F (2.5 uM)	2.5 ul
Primer R (2.5 uM)	2.5 ul
2X SYBR green master mix	12.5 ul
ddH ₂ O	5 ul

V. Buffer recipe

Sample buffer

Tris-Cl, pH 6.8	0.35M
Glycerol	30%
SDS	10.3%
DTT	0.6M
Bromophenol Blue	0.05% - 0.1%

RIPA buffer

NaCl	150mM
Tris-Cl, pH 8.0	50mM
NP-40	1%

Deoxycholic acid	0.5%
SDS	0.1%
PI mix	1X
PMSF	0.5mM

Protein transfer buffer

Tris base	25mM
Glycine	0.192M
SDS	0.1%
Methanol	20%

Running buffer

Tris base	25mM
Glycine	0.192M
SDS	0.1%

TBST

Tris-Cl, pH 8.0	10mM
NaCl	150mM
Tween 20	0.5%

PBS

NaCl	137mM
KCl	2.7mM
Na ₂ HPO ₄	4.3mM
KH ₂ PO ₄	1.4mM

PBST

PBS	1X
Tween 20	0.5%